Moisture Effects on Short Term Durability and Mechanical Properties of Two Puerto Rico Crushed Limestone Aggregates

By:

Alesandra Cristina Morales Vélez

A thesis submitted in partial fulfillment of the requirements for the degree of

MASTER OF SCIENCE
in
CIVIL ENGINEERING

UNIVERSITY OF PUERTO RICO
MAYAGÜEZ CAMPUS

December 2009

Approved by:

__________________________ ____________
Miguel A. Pando López, Ph.D. Date
President, Graduate Committee

__________________________ ____________
Felipe J. Acosta Costa, Ph.D. Date
Member, Graduate Committee

__________________________ ____________
Ricardo Ramos Cabeza, Ph.D. Date
Member, Graduate Committee

__________________________ ____________
Mario Rivera Borrero, Ph.D. Date
Representative of Graduate School

__________________________ ____________
Ismael Pagán Trinidad, M.S.C.E. Date
Chairperson of the Department of
Civil Engineering and Surveying

Abstract

This Master of Science thesis includes an experimental characterization of the mechanical properties of two Puerto Rico crushed limestone aggregates (CLA). Specifically, the crushed limestone was obtained from two quarries from the North and South Puerto Rico Karst Landforms. The main objective was to evaluate the short term durability and possible degradation of mechanical properties under different levels of exposure to moist environments (fresh and salt water baths). The experimental program included: Index testing, XRD and TGA Mineralogy, Slake Durability Tests, Los Angeles Abrasion Tests, Point Load Tests, 1-D Compression Tests and a series of Triaxial Compression Tests. The two crushed limestone types had high contents of calcium carbonate (both above 94%). The main differences of the CLA types were observed in their porosity and water absorption. The CLA from northern PR (Aymamon Formation) had a porosity and water absorption of 7.93% and 3.88%, respectively. In contrast the CLA from the southern PR (Cuevas Formation) has a porosity and water absorption of 1.95% and 1.29%, respectively. The two CLA types were tested after different tries of submergence in fresh and salt water with a maximum submergence time of 150 days. No degradation in terms of slake durability and point load index was observed at a submergence time of 150 days in fresh and salt water. Moisture conditions produced greater deformations on the CLA materials tested in Los Angeles abrasion and 1-D Compression tests. No variability was observed in the internal friction angles when subjected to moisture changes and time conditions.

Resumen

Esta tesis de Maestría en Ciencias incluye una caracterización experimental de las propiedades mecánicas de dos agregados de roca caliza triturada de Puerto Rico. Este agregado de roca caliza fue obtenido específicamente de dos canteras en las formaciones del carso del Norte y del Sur de Puerto Rico. El objetivo principal fue evaluar las propiedades de durabilidad a corto plazo y la posible degradación de las propiedades mecánicas bajo diferentes niveles de exposición a ambientes húmedos (baños de agua fresca y salada). El programa experimental incluyó: Pruebas Índices, Mineralogía del suelo mediante XRD y TGA, Ensayos de Durabilidad de *"Slake"*, Ensayos de Abrasión Los Ángeles, Ensayos de Carga Puntual, Compresión en 1-D y una serie de ensayos triaxiales de compresión. Los dos agregados de roca caliza presentaron altos contenidos de carbonatos de calcio (ambos mayor al 94%). La diferencia mayor de estos agregados de roca caliza fue observada en la porosidad y adsorción de agua. El agregado de roca caliza del norte de P.R. (Formación Aymamón) obtuvo un valor de porosidad y adsorción de agua igual a 7.93% y 3.88%, respectivamente. En contraste el agregado de roca caliza del sur de P.R. (Formación Cuevas) obtuvo un valor de porosidad y absorción de agua igual a 1.95% y 1.29%, respectivamente. Los dos tipos de agregados de roca caliza fueron ensayados luego de diferentes intentos de sumersión en agua fresca y salada con un tiempo de sumergido máximo de 150 días. No se observó ninguna degradación en términos del índice de durabilidad de "slake" y carga puntual a un tiempo de 150 días de sumersión en agua potable y salada. Los cambios en humedad produjeron deformaciones mayores para las muestras de agregados de roca caliza ensayada en abrasión de Los Ángeles y Compresión en 1-D. Los ángulos de fricción interna no mostraron variabilidad antes presencia de humedad y condiciones de tiempo.

Acknowledgments

First of all I would like to thank my family for their unconditional love and support. Especially my parents Edwin and Nilsa for being my North, my guide and support through out this journey and for making me the person who I am today. To my grandparents, especially Mamá. I have no words to express my gratitude and love towards you. To my sister Paola, just for those late night talks and laughs that kept me through this.

I would also like to thank the members of my committee: Dr. Felipe Acosta and Dr. Ricardo Ramos for their help and commitment. Special thanks to my advisor Dr. Miguel Pando. For his guidance, advice, and motivation since we started this challenge.

I can not forget to thank Mr. Jaime Ramirez. Without him this could have never been completed. You are more than a laboratory technician, you are a friend!

Finally, I want to thank my best friend and my other half Yaurel Guadalupe Torres. For being there right when I needed him the most, for believing in me, and for giving me the gift of true and unconditional love every day. I can not wait to start our new life together.

Table of Contents

List of Figures

List of Tables

Chapter 1. Introduction

1.1. Introduction

This MS thesis involved a detailed experimental evaluation of the short term durability and possible degradation of the mechanical properties of two crushed limestone aggregates (CLA) produced from two quarries in Puerto Rico (PR). CLA are a common construction material used for road and backfill civil engineering projects. In PR constructions materials are exposed to heavy rainfall, UV rays, and cycles of wetting and drying. The long term durability of CLA materials are not well characterized. This thesis hopes to contribute on this regard by evaluating the influence that exposure to fresh and salt water environments will have on the durability and mechanical properties of CLA materials. The extent of time of exposure was constrained by the typical duration of a Master of Science (MS) degree. This MS research thesis involved a comprehensive geotechnical test program that tracked possible changes in the behavior and mechanical properties of two different types of CLA after different periods of submergence in fresh and salt water, which included evaluation periods of up to 150 days. This chapter provides background information on this CLA soils, a justification for this project, the main research objectives, and a description of the thesis organization.

1.2. Background and research

The island of (PR) has a potentially serious environmental concern related to the extensive mining of mineral resources to produce aggregates for construction purposes. One of the most commonly mined rock formations in Puerto Rico are limestone formations. This type of rock is mined to produce crushed limestone aggregate (CLA) which are extensively used in civil engineering construction. Crushed limestone aggregates are commonly used in North America as fill material for road construction and embankments. They are traditionally considered as a good quality mineral aggregate with adequate durability performance. However, little information regarding the durability of CLA was found in the literature review carried out for this thesis. In some areas of PR, limestone formations show severe signs of weathering and meteorization. The quality of CLA will depend greatly on the conditions of the limestone formation used during mining. However, this level of degradation could be product of very long periods of environmental deformation which is not possible replicating or evaluating at a laboratory. Despite the lack of long term performance data, CLA are extensively used in civil and military engineering projects. For example, the United States Army Corps of Engineers (USACOE) every year uses millions of tons of limestone and dolomitic limestone aggregate for civil and military constructions like dams, spillways, highways, tunnels, and, airfields (Brewer, 1996). Limestone and dolostone are carbonate rocks with at least 54% of calcium carbonate content ($CaCO_3$) (http://www.geology.arkansas.gov). The term limestone refers to sedimentary rocks in which the carbonate fraction ($CaCO_3$) exceeds the non-carbonate. Crushed limestone and dolomitic limestones correspond to 75% of the aggregate used by the USACOE (Brewer, 1996). In PR the crushed limestone production is approximately 16 metric tons/year (AIPA, 2004) and is used extensively in civil engineering projects within the island.

The engineering and mechanical properties of the crushed limestone aggregate will greatly depend on the geological genesis and limestone type used for processing the aggregate, e.g.,rock quality, age, degree of weathering, geologic genesis, geologic composition and formation type. Depending on the degree of crushing used during mining and processing, this type of aggregate can be obtained in size ranging from boulders and gravels all the way to fine sand. Puerto Rico has several limestone formations which have important differences in composition, geology, and even degree of weathering. Some formations are very weak and/or porous, i.e., chalk type limestone and some are strong and very dense such as dolomitic limestone. Chalk type limestone is usually soft and has high content of calcium carbonate, whereas dolomitic limestone is usually harder and more durable. Another important consideration is the wide range of limestone geologic formations in PR which not only will have important differences in composition but also in geologic genesis, age, and degree of weathering. All these factors and variability result in a wide range CLA properties and characteristics. The scope of this thesis is to assess possible differences in two CLA materials obtained from two different geologic formations and to focus on their durability characteristics.

1.3. Objectives

The main objective of this research is to evaluate durability and possible short term degradation of the mechanical properties of two PR crushed limestone aggregates under sustained exposure to fresh and salt water environments. The two crushed limestone aggregates selected for this study are from two currently functioning quarries located in two distinct geologic limestone formations. Other more specific objectives of this MS research included to:

1) Perform a geotechnical characterization of the two selected PR crushed limestone aggregates. Geotechnical characterization includes determination of the baseline mechanical properties, 1-D compression tests, and triaxial compression tests.

2) Conduct mineralogical analyses for the selected crushed limestone aggregates. This involves mineralogical composition and calcium carbonate content.

3) Evaluate the mechanical and durability properties of submerged crushed limestone aggregate samples. This evaluation will be performed on CLA samples submerged in fresh and salt water for duration of submergence of 90 and 150 days.

4) Evaluate the grain crushing potential of the two selected crushed limestone aggregates. This evaluation will be performed by comparing the gradation curves before and after modified proctor compaction tests and before and after triaxial compression tests. This will be done for fresh and aged conditions.

5) Evaluate the possible changes in stress-strain behavior of the selected crushed limestone aggregates after different levels of submergence to fresh and salt water

1.4. Thesis organization

This thesis is organized into six chapters and three appendices. Besides this chapter, Chapter 2 presents background information such as definitions and *limestone* terminology, typical properties chemical and physical properties of limestone formations, and a review of the PR Karst Landforms and formations. Chapter 2 also provides a literature review and previous investigations related to the main focus of this research project which is CLA properties and durability of these materials when exposed to weak environments.

Chapter 3 presents a detailed description of the experimental plan and methodology in this research project. Chapter 4 describes the quarries from where the two CLA materials were obtained. Specifically, this chapter provides a detailed geological description of the two quarries including aerial photos, land registry maps, geological formations and soil taxonomy.

Chapter 5 presents the results of the experimental study proposed for this MS thesis. The chapter first presents the soil classification of the two CLA materials including mineralogy evaluations and the baseline properties that will be the basis for the durability or degradation assessment. The chapter ends with a presentation and detailed discussion of the variation of the different mechanical properties and index properties as a function of submergence time in fresh and salt water. The test results presented include: slake durability, point load tests, los Angeles abrasion tests, 1-D compression tests, and triaxial compression tests.

The final chapter of this thesis is chapter 6 which includes a summary of the findings, conclusions, and also recommendations for future work.

This thesis also includes 3 appendices. Appendice A describes and presents the results from the porosity test performed in the selected crushed limestone soils. Appendice B presents additional results and details obtained from the slake durability tests, and Appendice C includes additional results obtained from the point load tests.

Chapter 2. Background and Literature Review

2.1. Introduction

This chapter has two main sections, namely: a general background and the literature review. The background section provides general limestone related terminology and definitions, some general physical and chemical properties of limestone, and a general description of the different limestone formations in PR. The literature review section presents a general literature review related to the engineering and mechanical properties of CLA materials with a particular focus on durability studies. This section also presents a summary of the few studies found available for CLA materials of PR.

2.2. Background

2.2.1. Definitions and limestone terminology

Limestone is a calcareous sedimentary rock composed primarily of the mineral calcite ($CaCO_3$) which has been deposited by organic or inorganic chemical processes (Leet and Judson, 1971). Limestones formed organically respond to the action of plants and animals that extract the calcium carbonate from water. Limestones formed inorganically respond to precipitated calcite from fresh water, caverns and/or springs. Limestone rocks are carbonate rocks that have at least of 80% of carbonates of calcium or magnesium (http://www.geology.com).

A karst landform or topography is typically formed in limestone, dolomite, and gypsum formations. A karts landform is characterized by depressions, sinkholes, caverns, and underground drainage formed by the dissolution of the most soluble rocks. The northwestern portion of Puerto Rico is rich in limestone deposits and karstic features.

Dolimite is also a sedimentary carbonate rock where the rock is primarily composed of calcium magnesium carbonate $CaMg(CO_3)_2$ formed by diagenesis or hydrothermal metasomatism of limestone (Mineral Data Publishing 2001-2005 Version 1). Limestone rocks can vary greatly in composition and physical and engineering properties. Important factors that influence their physical and chemical properties include geologic genesis, geologic composition, rock quality, age, degree of weathering, and limestone type. Table 2.1 illustrates the range of physical and chemical properties from two Canadian limestone rocks with different composition. The rocks listed in this table include a high calcium limestone and a dolomitic limestone. The high calcium carbonate limestone has 98% of calcium carbonate content, while the dolomitic limestone has only 55.35% of $CaCO_3$. In contrast, the dolomitic limestone has 42.25% of magnesium carbonate compared to only 0.73% for the high calcium carbonate limestone. This table shows that the high calcium limestone has higher values for the abrasion and soundness tests compared to the dolomitic limestone. Unfortunately this study does not report the porosity of the two rocks compared in this table.

Table 2.1. Chemical and physical properties of two Canadian limestones (Adapted from Atlantic Minerals Limited, 2008).

Chemical Composition		
	High Calcium Limestone	Dolomitic Limestone
Calcium Carbonate ($CaCO_3$)	98.00%	55.35%
Calcium Oxide (CaO)	54.80%	31.00%
Magnesium Carbonate ($MgCO_3$)	0.73%	42.25%
Magnesium Oxide (MgO)	0.35%	20.20%
Silica (SiO_2)	0.66%	1.65%
Iron Oxide ($Fe2O_3$)	0.10%	0.23%
Alumina ($Al2O_3$)	0.22%	0.21%
Lost on Ignition	43.30%	46.40%
Physical Properties		
Specific Gravity	2.71	2.77
Water Absorption	0.25%	0.75%
L.A. Abrasion	27.60%	20.20%
Soundness	1.04%	0.34%

For engineering purposes porosity and degree of weathering will also be important considerations when evaluating the physical and engineering properties of CLA materials obtained from limestone rocks.

Therefore, CLA yield good aggregates because they are commonly the most indurated (hard) members of the sedimentary rocks. Sedimentary rocks, including limestone, in general are fine-grained, hard, durable rocks. They have a dense crystalline or cemented fabric and are not weakened by the existence of cavities or porosity (Dukatz, 1995). Although they are soluble in water, they are easily re-deposited. This condition may result in characteristics that are significantly changed after compared to those after original deposition. In general, rocks are more durable and useful for aggregate when they are indurated, crystalline, fine-grained in texture and best if the matrix which holds the grains together is itself crystalline (Barksdale, 1991). Aggregate durability may be defined as the ability of the individual particles to retain their integrity and not to suffer physical, mechanical or chemical changes to an extent which could adversely affect their properties (Rusell, 1976). For this research, the aggregate durability will be assessed for two crushed limestone aggregates from local quarries in PR.

For background purposes and comparison, Table 2.2 presents typical values of physical properties for three commonly used aggregates. Limestone aggregate, the focus of this thesis, is compared with granite and sandstone aggregates. Information provided in this table includes: unit weight, compressive strength, tensile strength, shear strength, flexural strength, modulus of elasticity, water absorption, porosity, thermal coefficient of expansion, and specific gravity. This table highlights the greater variability of tensile strength, shear strength, water absorption, average porosity, and specific gravity of the CLA compared to the other two aggregates. The previous table showed typical property values for CLA and two other aggregates. It is also important to include information regarding the parent rock used to obtained CLA materials. Table 2.3 shows general properties of the limestone rock. From this table we can see that 2.3 limestone rocks have a wide range of tensile strength values from 7,400 to 35,000 psi. Similarly, shear strength values range from 3,000 to 30,000 psi and the Young Modulus varies from 2 to 97 GPa. This table, coupled with Table 2.2 (for CLA), illustrates the variability of this limestone material which, as discussed before, depend of many factors such as geological genesis, geological composition, age, and degree of weathering.

Table 2.2. Physical properties of granite, limestone, and sandstone aggregates (Source: Barksdale, 1991).

Property	Limestone Aggregate	Granite Aggregate	Sandstone Aggregate
Unit weight (lb/ft^3)	117-175	162-172	119-168
Tensile Strength (psi)	427-853	427-711	142-427
Shear Strength (x 10^3 psi)	0.8-3.6	3.7-4.8	0.3-3.0
Modulus of Rupture (psi)	500-2000	1380-5550	700-2300
Modulus of Elasticity (x 10^3 psi)	4.3-8.7	4.5-8.7	2.3-10.8
Water Absorption (% by wt)	0.50-24.0	0.07-0.30	2.0-12.0
Average Porosity (%)	1.1-31.0	0.4-3.8	1.9-27.3
Linear Expansion (x 10^{-6} in./in.C)	0.9-12.2	1.8-11.9	4.3-13.9
Specific Gravity	1.88-2.81	2.60-2.76	2.44-2.61

Table 2.3. Typical values of physical properties for limestone rock.

Property	Range	Units	Reference
Unit Weight	117-168	lb/ft^3	Winchell (1942) & Barksdale (1991)
Specific Gravity	1.88-2.7		Winchell (1942) & Barksdale (1991)
Hardness	2.5-3	%	Mitchell & Soga (2005)
Wave Velocity	6000-6500	m/s	Fourmaintraux (1976)
Point Load Index Value	0.03-1.16	kip/ft^2	Broch and Franklin (1972)
Tensile Strength	7400-35000	psi	Goodman (1989)
Shear Strength	3,000-30,000	psi	Hendron Jr. (1969)
Cohesion	500-5,000	psi	Hendron Jr. (1969)
Angle of Internal Friction	37-58	°	Hendron Jr. (1969)
Young Modulus	2-97	GPa	Mitchell & Soga (2005)
Shear Modulus	1.6-3.8	GPa	Mitchell & Soga (2005)
Poisson's Ratio	0.01-0.32		Mitchell & Soga (2005)
Permeability @ Lab	10^{-5} to 10^{-13}	cm/s	Brace et al. (1968)
Permeability @ Field	10^{-3} to 10^{-7}	cm/s	Brace et al. (1968)

2.2.2. *Limestone formations in Puerto Rico*

The karsts landforms of Puerto Rico cover approximately 27.5% of the area of the island and are subdivided into three principal zones: North Karst Landform, South Karst Landform, and Disperse Karst Landform (Guisti, 1978; Lugo, 2004). The main karst landforms of Puerto Rico are shown in Figure 2.1.

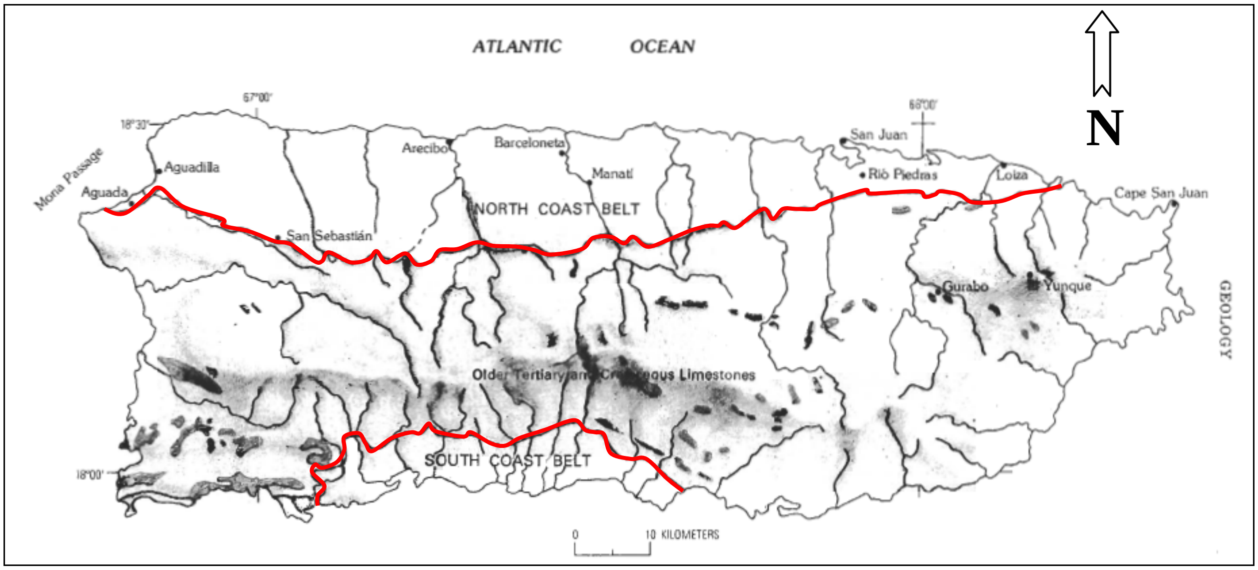

Figure 2.1. Main karst landforms in Puerto Rico (adapted from Guisti, 1978).

Limestone formations of Puerto Rico are from marine origin and have suffered low postdepositional changes (Lugo, 2004). The most common rocks in the Puerto Rico karst landforms are principally limestone, and to a lesser extent chalk and dolomite (Monroe, 1980). The following subsections describe the three principal zones of the PR Karst Landform.

2.2.2.1 North karst landform

The North karst landform is subdivided into the following six mayor formations: Lares Limestone, Cibao Formation, Aguada Limestone, Aymamon Limestone, Camuy Formation, and Mucarabones Sands (Monroe, 1973). These six formations are shown in Figure 2.2.

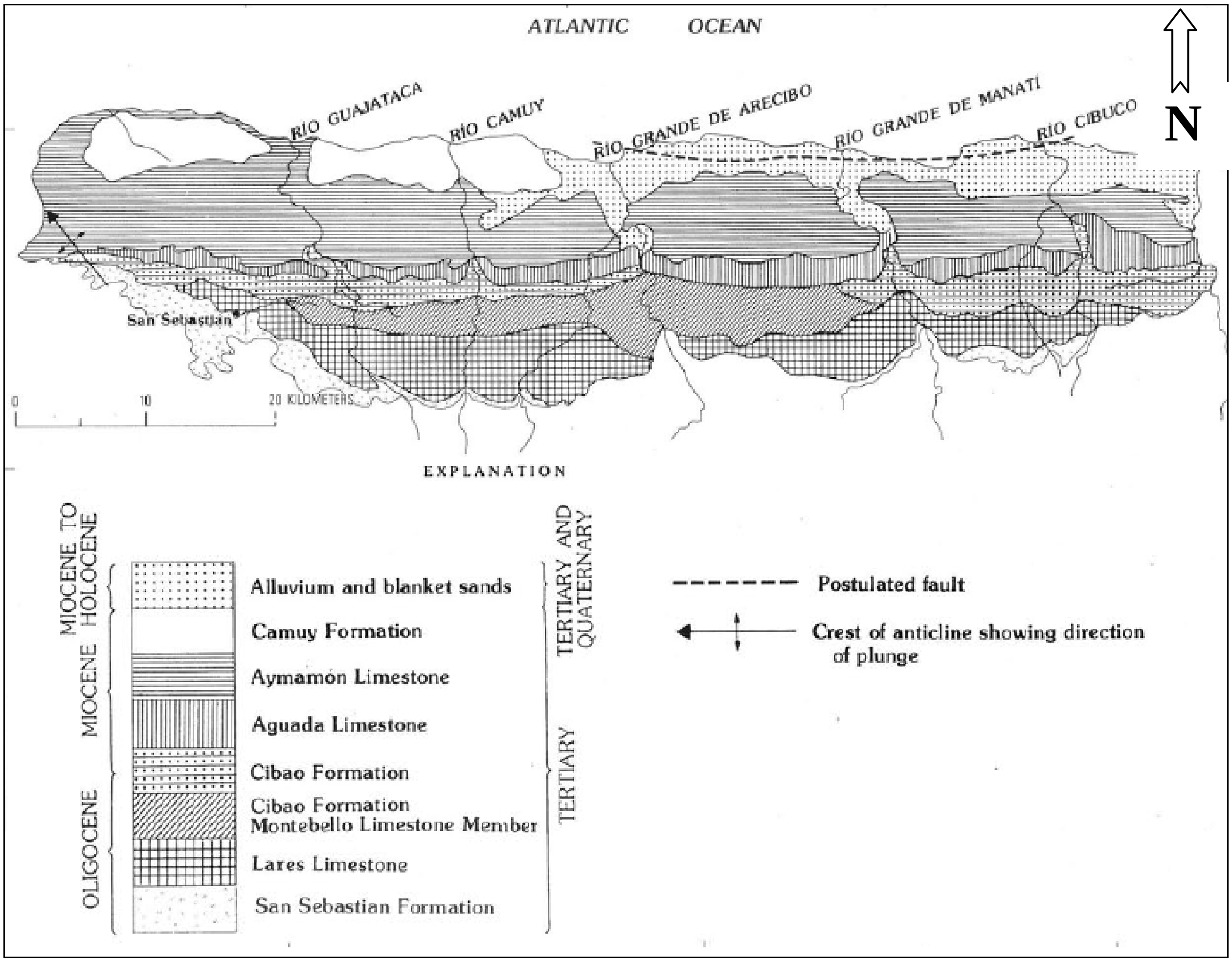

Figure 2.2. Geologic formation of the north coast limestone area (adapted from Guisti, 1978).

The North karst landform of PR is a band that extends a distance of about 140 km from the Río Grande of Loiza to Aguadilla. As shown in Figure 2.2 the band is about 22 kilometers wide in the Arecibo area and covers an area of approximately 218,692 hectares, which represents 90% of the karst landforms of Puerto Rico (Lugo, 2004). This North Karst Landform presents ample manifestations of karst phenomena such as dissolution, sinkholes, and caves. A general description for the mayor limestone formations of the North Karst landform of Puerto Rico are presented in Table 2.4.

Table 2.4. General description of the mayor limestone formation in the North karst landform of Puerto Rico. (adapted from Monroe, 1976 and Lugo, 2004)

Formation	Average Thickness	Description
Lares	Varies along its extension in between 270-310 meters	Extends from Corozal to Moca and rests over the San Sebastian Formation. Consist of limestone, mainly pure calcium carbonate, calcarenite, and fossils. Chemical analyses of this limestone show a 85-99% of $CaCO_3$.
Cibao	Ranges from 250-280 meters	Most heterogeneous formation in the North Region. It is a lenticular formation composed of calcareous clay, clayey chalk, quartz sand, sand and gravel. Chemical analyses show a 76-85% of CaCO3, and of the various limestone members from 91-98% $CaCO_3$.
Aguada	Most uniform formation in thickeness from the North Region. From the Rio Grande de Arecibo to Aguadilla it is 90 meters in thickness. Near the valley of the Rio Grande de Arecibo it is approximately 150 meters and less than 50 meters in the San Juan area.	It is a transition between the Cibao Formation and the Aymamon Limestone. Extends from the Rio Grande de Loiza to Aguadilla and consists primarily of limestone but with many chalky layers at the base (resembling the Cibao) and hardened limestone at the top (resembling the Aymamon). Chemical analyses show that the limestone ranges from 89-96% of $CaCO_3$.
Aymamon	Ranges from 190-200 meters	Extends from Loiza Aldea to the west coast north of Aguadilla. It is uniform in lithology consisting mainly of thick bedded very pure quarzt free limestone. It contains abundant fossils, calcareous algae, corals, and mollusks. Chemical analyses show 98-99% $CaCO_3$. Near the coast,dolomite (18.6% MgO) has replaced some of the limestone.
Camuy	Maximum thickness of 170 meters	Forms a discontinuos belt from the Rio de la Plata to west Isabela. It is predominantly calcareous, containing appreciable quantities of quartz sand, and in the upper part contains thin bedded quarzt sandstone. Chemical analyses show that the limestone parts of the formation contains as much as 95% $CaCO_3$.

2.2.2.2 South karst landform

The deposition of the limestone rocks in the South of Puerto Rico started and ended before the deposition of the limestone landforms in the North of Puerto Rico. Limestone rocks in the South of PR are full of fissures and discontinuities (Monroe, 1980). These dips towards the south with dip angles between 10° to 30° (Monroe, 1976). A large area of the south karst landform is buried deep down under thick alluvial deposits that reach depths up to 900 meters near the town of Santa Isabel.

The South karst landform is subdived into four mayor formations: Juana Diaz Formation, Ponce Limestone, Parguera Limestone, and Guanajibo Formation. The middle tertiary rocks in the South of PR consist primarily of the Juana Diaz Formation of Oligocene and Miocene age and the Ponce Limestone of Miocene age (adapted from Lugo,2004). The Juana Diaz Formation consists of lenticular end interlonguing beds of sand, gravel, clay, mudstone, chalk, and limestone. Most of the limestone in this formation is very chalky except for a thick organic reef complex 8-14 kilometers west-northwest of Ponce (Monroe, 1976). Analyses show that the Juana Diaz Formation contains 97-98% of calcium carbonate (Monroe, 1976). This reef complex is the only area of this formation that shows karst phenomena, which includes several long caves and depressions. The Juana Diaz Formation is overlain by the Ponce Limestone, which is of very hard, generally light grayish-orange calcarenite containing abundant molds of mollusks, solitary corals, echinoids, and foraminifera. Ponce Limestone was deposited as a fringing reef of pure limestone containing about 96% of calcium carbonate. Ponce Limestone is a karstifiable limestone and would have many karst features if it were in a more humid climate. Lithologically it resembles both the Aymamon and the Aguada Limestones from the North karst landform.

A secondary karst feature in the South, which is dependent on the climate, is the large amount of *caliche* that has formed on the surface of southern PR. The presence of *caliche* is especially notorious in areas underlain by limestone of Ponce and Juana Diaz (Monroe, 1976). The *caliche* consists of as much as 4 meters of soft chalk to indurate chalky limestone, formed in the soil and above the soil overlying limestone beds, presumably by evaporation of water containing calcium bicarbonate that has been drawn to the surface by capillary action. *Caliche* contains neither plant nor animal remains and analyses show that it can contain up to 95% of calcium carbonate. The main limestone formations of the South karst landform are described in Table 2.5.

Table 2.5. General description of the mayor limestone formation in the southern area of Puerto Rico (adapted from Monroe, 1976 and Lugo, 2004).

Formation	Description
Juana Diaz	Consists of lenticular beds of sands, gravel, mudstone, chalk, and limestone. Most of the limestone is chalky except for an organic reef, rich in corals and algae, located from 8-14 kilometers to the west-northwest of Ponce. Chemical analyses show that it contains 97-98% $CaCO_3$. The formation also contains lenses of less pure limestone and chalk that are 75-91% $CaCO_3$.
Ponce	Consists of a very hard, light gray/orange calcarenite rich in mollusks, corals, and floramines. It was deposited as a reef of primarily calcium carbonate containing 96% $CaCO_3$ but in some places near the coast it has been slightly dolomitized and contains as much as 7% MgO.

2.2.2.3 Disperse karst landform

The Disperse karst landform is located in several disperse and localized areas throughout PR. This landform is not as significant in size as the North and South Landforms, and is not subdivided into limestone formations. As its name indicates, this landform represents isolated cases of karst along the island.

2.3. Literature review

This subsection presents a summary of the literature review carried out for this research project. This literature review is presented in two subsections. The first subsection includes a more general literature review related to crushed limestone aggregate research in the topics of mechanical properties and durability studies (if any). The second subsection presents a summary of the literature review related to studies on crushed limestone aggregates in Puerto Rico.

2.3.1. General literature review on CLA materials

As mentioned earlier, crushed limestone aggregates are commonly used in civil and military projects (Brewer, 1996). There are several studies related to mechanical and engineering properties of crushed limestone aggregates. Table 2.6 presents a summary of some of the most relevant studies of this type.

Table 2.6. Summary of previous studies related to crushed aggregate.

Reference	Country	Crushed Aggregate Size	Description of the study	Main Findings
Gupta (2009)	India	$D_{50(1)}$=4mm $D_{50(2)}$=8mm $D_{50(3)}$=10.5mm	The author carried out a series of consolidated drained triaxial tests on two different rockfill materials (Ranjit Sagar and Purulia rockfill). Tests were carried out on samples with Dr=87% and confining pressures ranging from 0.3 to 1.2 MPa. Tests were carried out to study and compare the stress-strain-volume behavior of the rockfill materials.	Stress-strain volume change behavior in general is non-linear for both the rockfill materials. Ranjit Sagar rockfill material undergoes volume compression throughout the test while Perulia rockfill material shows compression initially and dilatation on further shearing of the sample. Both rockfill materials show increase in axial strain with increase in confining pressure for all particle sizes. Both rockfill materials show decrease in the Poisson's Ratio value with increase in particle size.
Gupta (b) (2009)	India	$D_{50(1)}$=4mm $D_{50(2)}$=8mm $D_{50(3)}$=10.5mm	This research investigates the effect of maximum particle size on breakage and strength parameters of two rockfill materials (Ranjit Sagar - riverbed material and Purulia - blasted material). Drained triaxial tests were conducted on different size of rockfill materials and effect of size and confining pressure on breakage and strength parameters were studied. A dry density corresponding to 87% of relative density was adopted for testing. Specimens were tested at different confining pressures ranging from 0.2 to 1.4 MPa. Tests were carried out to investigate the effect of size and confining pressure on breakage and strength parameters of alluvial and blasted rockfill materials.	Both the materials show increase breakage factor (3.96-11.87% and 1.3-15.3% corresponding to the Ranjit Sagar and Purulia rockfills, respectively) with the increase in confining pressure for all particle sizes. The values of the internal angle of friction increase with the size of the particles for the Ranjit Sagar rockfill (31.5-35.4°) while this value decrease for the Purulia rockfill (32.5-30.6°). Thus, the nature of particles (rounded/angular) appears to influence certain behavior of the rockfill material.
Nazzal (2007)	USA	D_{10}=0.18mm D_{60}=6mm D_{max}=19mm	A series of triaxial compression tests and cyclic triaxial tests were conducted on unreinforced and geogrid reinforced crushed limestone aggregate samples. The main objective of this study was to investigate the effects of the geogrid type, location, and number of layers on the strength, stiffness, and cyclic deformability of these samples.	The tested CLA has a maximum dry unit weight of 17.2 kN/m^3 and an optimum moisture content of 7% (Standar Proctor Test). The CLA material has an internal friction angles of 48° and a specific gravity value of 2.72. This study did not investigate durability effects.

Table 2.6. Summary of previuos studies related to crushed aggregate.

Table 2.6. (cont.) Summary of previous studies related to crushed aggregate.

Reference	***Country***	***Crushed Aggregate Size***	***Description of the study***	***Main Findings***
Thom and Brown (1985)	UK	D_{50}=0.8-9mm	This research involves a series of cyclic triaxial compression test and permeability tests of dry crushed dolomitic limestone of different gradings carried out in order to determine the characteristics necessary for use in pavement design. Three specimens were made at each grading, using different compaction efforts, to investigate the influence of density in the mechanical properties.	For the compaction levels investigated, the authors found only a slight increase in stiffness with relative density increase. Similarly, gradation has only a slight response. Shear strength parameters ranged from 54 to 46°. In terms of shear strength, this study found that compaction density did have a great influence. Compaction moisture content influence on elastic and permanent deformation under cyclic loading.
Attewell (1970)	Great Britain	-	The author investigated the mechanical properties of the Great Limestone in northern England. Two types of limestone (blue limestone and brown limestone) were compared via specific gravity, moisture absorption, unconfined compressive strength, and aggregate crushing tests. Unconfined compressive strength tests were carried out in mixed aggregates of blue and brown limestone.	The specific gravity values from the two limestones evaluated range from 2.72 to 2.82 and the water absorption values varied from 1.38 to 3.42% for the blue and brown limestone, respectively. Is was observed that due to the higher porosity and moisture absorption that the brown limestone experienced, it was less favorable than the blue one as a construction aggregate material. Aggregate crushing values were in the range of 22-25 and 16-23 for the brown and blue limestone, respectively. Shear strength test confirmed that in a mixed aggregate of blue and brown limestone, the brown in more likely to break up under stress than the blue one.
Bolton, Frgaszy, and Lee (1991)	UK	5.6 mm	The authors carried out a series of triaxial test on unconventional fills. Triaxial test specimens were 70mm in diameters and all tests were conducted with a cell pressure of 60 kPa.The shear strength of gap graded fills, with 15 and 30% of large particles in a fine matrix of sand were compared with the matrix alone at a range of relative densities. Specific gravity tests were also carried out on the two different selected limestones for the study.	Specific gravity values range from 2.71 to 2.73. Dry density values varied from 1.74 to 2.017 gm/cm^3 and the values for the maximum internal angle of friction were in the range of 38.8 to 45.6°. The authors found that some variation occurred in the angle of shearing resistance (Φ') when the various soils were compacted to target relative densities. A well compacted mixture with 15% or large particles could lose 1.5° in Φ', whereas with 30% of large particles a gain of about 3° was available.

2.3.2. *Previous studies on CLA in Puerto Rico*

Very little information about crushed limestone aggregates (CLA) and limestone derived soils is available for Puerto Rico. Romero and Bernal (1998) studied the shear strength and compressibility characteristics of several limestone soils obtained from PR quarries located in three different limestone formations. Specifically these authors studied limestone soils manufactured with limestone from Ponce, Aymamon, and Camuy formations. This study was a research funded by the Puerto Rico Department of Transportation and Public Works and the Highway and Transportation Authority. The project involved gathering different limestone soil samples from different ongoing highway projects of the Puerto Rico Highway Authority. The principal objective of the investigation was to study geotechnical characteristics such as shear strength and compressibility parameters for these soils. Table 2.7 presents a summary of the location of the samples and its corresponding geologic formation.

Table 2.7. Location of samples (adapted from Bernal and Romero, 1998)

Sample	Location	Geologic Formation
1	Project AC-525269 (Ponce By-Pass)	Ponce Limestone
2	Quarry in Arecibo Along PR-129	Aymamon Limestone
3	Quarry in Aguadilla	Camuy Formation
4	Project AC-001091 Sta 120+00	Aymamon Limestone

The average particle size (D_{50}) of the limestone soils studied by Romero and Bernal (1998) ranged from 0.5 to 7mm. The average grain size curves for the limestone soils of these four highway projects are shown in Figure 2.3. It can be observed in this figure that the four limestone soils studied had a wide range of particle sizes, but all were relatively well graded and with a relatively high percentage of fine particles.

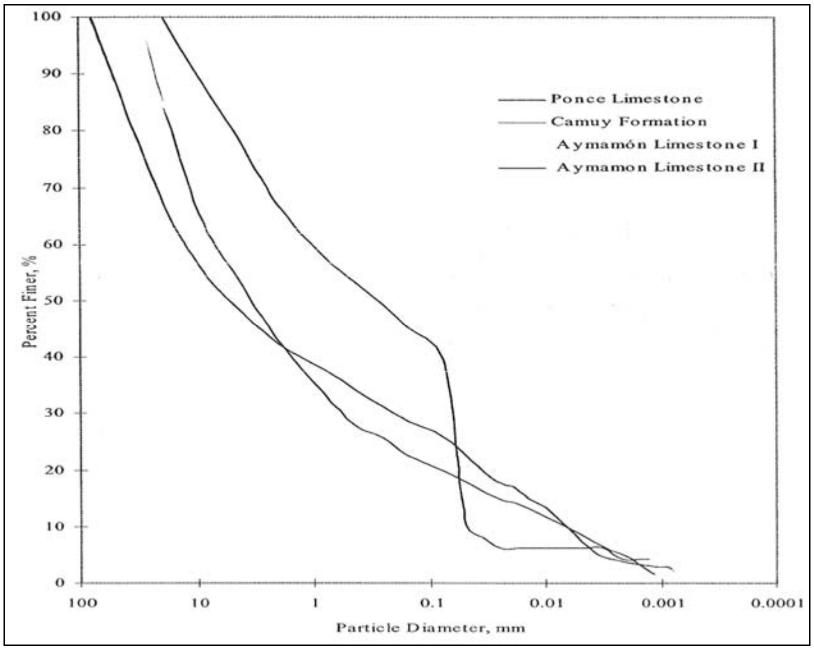

Figure 2.3. Average grain size curves for the four limestone soils studied by Romero (1998) and Bernal.

The results of the index tests are summarized in Table 2.8. The limestone soils from the Ponce Limestone, Camuy Formation, and Aymamon Limestone I all classified as silty gravels (GM). The Aymamon Limestone II soil was classified as silty sand (SM). Specific gravity values for these four limestone soils varied from 2.69 to 2.76.

Table 2.8. Summary of the results from index tests (adapted from Romero and Bernal, 1998).

Laboratory Tests		Units	Limestone Soils Resource Formation			
			Ponce Limestone	Camuy Formation	Aymamon Limestone I	Aymamon Limestone II
Particle Size Distribution	gravel	%	50.5	45.3	37.6	20.2
	sand	%	23.3	35	23.3	40.4
	fines	%	26.2	19.7	39.1	39.4
	<0.002mm	%	3.6	4.7	7.3	8.4
	C_u	-	18.33	10	11.67	22.92
	C_c	-	0.6	7.3	0.1	0.1
Atterberg Limits	LL	%	21	-	20	19.5
	PL	%	18	18	18	-
	PI	%	3	-	2	-
Specific Gravity		-	2.71	2.69	2.72	2.76
Soil Classification		-	GM	GM	GM	SM

Romero and Bernal (1998)carried out unconsolidated-undrained and consolidated-drained triaxial compression tests and direct shear tests for soil samples compacted at relative compaction values of 95% and 100% and a compaction moisture content equal to the optimum moisture content , based on the Modified Proctor Test (ASTM D 1557). The unconsolidated-undrained (UU) and consolidated-drained (CD) triaxial compression tests were carried out on samples compacted at relative compaction values of 95 and 100%, based on the Modified Proctor. Triaxial tests were carried out at confining pressures of 5, 10, and 30 psi. Direct shear tests were performed on soil samples from the Aymamon Limestone II because the material was a non-cohesive, silty sand. The direct shear tests were carried out at normal stresses of 25, 50, and 75 psi. Table 2.9 summarizes the Mohr-Coulomb parameters obtained by Romero and Bernal (1998).

Table 2.9. Mohr-Coulomb parameters obtained by Romero and Bernal (1998).

		UU Tests		CD Tests		Direct Shear(2)	
Soil	**Relative Compaction(1) %**	**c (psi)**	**Φ (°)**	**c' (psi)**	**Φ' (°)**	**c (psi)**	**Φ (°)**
Ponce Limestone	100	5	45	5	39	-	-
	95	2	41	6	35	-	-
Camuy Formation	100	10	50	8	49	-	-
	95	1	41	0	42	-	-
Aymamon Limestone I	100	22	42	11	52	-	-
	95	3	40	7	39	-	-
Aymamon Limestone II	100	-	-	-	-	11.5	34
	95	-	-	-	-	6.7	31.4

Notes (1) Based on the Modified Proctor Test
(2) The authors did not stated if the direct shear parameters were drained or undrained.

This study also investigated the compressibility of limestone soils. One dimensional compression tests were carried out on each of the four limestone soils by means of collapse potential test evaluated according to the ASTM D 4546 Method B. For these tests, samples were compacted at a relative compaction value of 95%, based on the Modified Proctor. Table 2.10

shows a summary of the results from the collapse potential test carried out on the Ponce Limestone, Camuy Formation, and Aymamon Limestone I soils. As shown by the results in Table 2.10, the limestone soils show a low collapse potential.

Table 2.10. Summary of results from the collapse potential test obtained by Romero and Bernal (1998).

Soil	Stress (psi)	Collapse Potential (%)
Ponce Limestone	5.6	0.16
	14	1.19
	30.8	1.05
Camuy Formation	5.6	0.4
	14	0.13
	30.8	0.23
Aymamon Limestone I	5.6	0.15
	14	0.43
	30.8	0.42

Also, the constrained modulus and the coefficient of volume change were calculated for a vertical pressure range of 2.8 to 45.8 psi. Results are presented in Table 2.11.

Table 2.11. Coefficient of volume change and confined constrained modulus results obtained by Romero and Bernal (1998).

Soil	m_v (in^2/lb)	D(lb/in^2)
Ponce Limestone	0.0003	3,333
Camuy Formation	0.001	1,000
Aymamon Limestone I	0.0003	3,333
Aymamon Limestone II	0.001	1,000

In general, the authors concluded that the four limestone soils studied (3 GM's and 1 SM) had reasonably high effective shear strength parameters when compacted at relative compaction values 95% or higher with respect to the Modified Proctor Standard test. The authors also found these soils had adequate stiffness values for the purpose of conventional highway projects such as road fills and shallow embankments. This study did not investigate coarser CLA materials, nor did it investigate durability properties or characteristics.

The values of strength parameters found in this investigation were similar to those reported by Nedavia (1979) as quoted by Frydman (1982) (adapted from Romero and Bernal, 1998) and are shown in Table 2.12. The soils studied by Nedavia (1979) correspond to quarried calcareous sandstone from the Mediterranean coastal plain of Israel, locally termed *"kurkar"*.

Table 2.12. CU Triaxial compression test results values reported by Nedavia, 1979 (adapted from Romero and Bernal, 1998).

Parameter	Nedavia (1979)	Romero and Bernal (1998)
Maximum Unit Weight (lb/ft^3)[1]	115-127	112-122
Angle of Friction (°)	42-50	31-52
Cohesion (lb/in^2)	2-10.0	2-22.0

Notes: [1]Based on Modified Proctor Energy

The results of this investigation provided useful information for establishing strength and compressibility parameters for limestone soils typically used for highway embankment fills in Puerto Rico which can reach heights up to 40 to 50 feet. This investigation focused on short term shear strength parameters of the soil samples and no mineralogy/petrography tests were carried out.

Chapter 3. Methodology

3.1. Introduction

This chapter presents a description of the research methodology used to carry out the experimental program of this MS study. Specifically this chapter describes the methodology used for the selection of the crushed limestone soil samples, the procedure for submergence of the CLA in fresh and salt water, and describes the test procedures of the different experiments and tests carried out in this research project.

3.2. General research methodology

The general methodology carried out for this research project consisted on the following main tasks:

i. *Background and literature review* – This task involved gathering background information on crushed limestone aggregates and a literature review focused on summarizing the state of knowledge of CLA properties and durability. This information was presented in Chapter 2.

ii. *Selection of quarries* – This task involved reviewing the different limestone quarries registered in the Department of Natural Resources of PR (DNR-PR) and selecting two that were mining limestone of different geologic formations. This task was not trivial since DNR-PR records are not well organized and some quarries refused to participate in this research. Initially 30 candidate quarries, from all over PR, were evaluated and considered before selecting two final quarries. The two final quarries selected are described in Chapter 4.

iii. *Design of the test matrix and test program* – This task involved the selection of the different test types, and quantity to be carried out for this research project. Also, the maximum particle size for the two selected CLA materials was determined at this stage.

iv. *Characterization of parent limestone rock properties for the two selected quarries, and determination of the baseline properties of the CLA materials* – This task involved two components. For the evaluation of the parent limestone rock tests carried out included mineralogy, porosity, density, water absorption, and specific gravity. For the CLA baseline materials it involved tests such as grain size distribution, soil classification, maximum and minimum dry densities, and soil mineralogy which was carried out for the CLA selected.

v. *Submergence of the CLA samples* – This task involved the selection of the location from where the salt water was going to be collected, the design preparation, filling, and storage of the water tanks and the procedure for submergence of the CLA materials. This procedure is described later in this chapter.

vi. *Assessment of properties on aged CLA samples (fresh and salt water)* – This task involved slake durability tests, Los Angeles abrasion tests, point load tests, 1-D compression tests, and a series of triaxial compression tests to evaluate both the durability and mechanical properties of the CLA under different levels of moisture absorption or exposure (the baseline properties were based on as received conditions from the quarries, and the aged samples correspond of different times of submergence in fresh and salt water).

vii. *Thesis preparation* – This task involved writing this thesis document which describes and documents the different components of this research project including tests, tests results, analyses, discussions, and the summary and conclusions for this research project.

3.3. Experimental program

3.3.1. Test matrix

A summary of all the tests carried out for this investigation, divided into three main categories: (1) soil classification and baseline properties, (2) soil mineralogy, and (3) durability and mechanical properties is shown in the following table.

Table 3.1. Tests matrix for experimental program of CLA durability study.

	Test	Reference	Quantity of Tests for Each Quarry				
			@ t=0 days	**@ t=90 days Fresh Water**	**@ t=90 days Salt Water**	**@ t=150 days Fresh Water**	**@ t=150 days Salt Water**
Soil Classification and Baseline Properties	Soil Classification (USCS)	ASTM D 422 - Grain Size Analysis	2	1	1	1	1
	Visual Description	ASTM D 2488	1	-	-	-	-
	Specific Gravity	ASTM D 854	2	-	-	-	-
	Natural Water Content	ASTM D 2216	2	-	-	-	-
	Maximum Dry Density	ASTM D 1557	3	-	-	-	-
	Minimum Dry Density	ASTM D 4254	3	-	-	-	-
	Porosity	Alternative Method[1]	1	-	-	-	-
	Absorption	ASTM C 97	1	-	-	-	-
Mineralogy	X-Ray Diffraction		1	-	-	-	-
	Thermo-Gravimetric Analysis	Todor (1976)	1	-	-	-	-
Durability and Mechanical Properties	Slake Durability	ASTM D 4644	1	1	1	1	1
	Los Angeles Abrasion	ASTM C 131	1	1	1	1	1
	Point Load	ASTM D 5731					
	One-D Compression	Alternative Method[2]	1	-	-	1	1
	Triaxial Compression	ASTM D 2850	4	4	4	4	4
	Crushability	Lade et. al. (1996)	4	4	4	4	4

Note [1] – Alternative Method is described in Appendix A
Note [2] – Alternative Method is described later on this chapter.

3.3.2. Soil classification and baseline properties for CLA materials

As shown in Table 3.1 a series of tests were carried out to classify the selected CLA materials. To determine its baseline properties tests such as: grain size analysis, visual description, specific gravity, natural water content of the soils samples as received from the quarry and before each test to monitor moisture changes (if any) were carried out. Also, maximum and minimum dry densities relative density, void ratio, porosity, and water absorption were carried out on the CLA samples.

3.3.3. Soil mineralogy

The mineralogy of the crushed limestone soils was evaluated using two different methods: X-ray diffraction analyses and Thermo-gravimetric analyses. These tests are described below.

X-ray diffraction analyses – A qualitative mineralogical characterization of the two crushed limestone aggregates selected for the study were carried out using X-ray diffraction (XRD) analyses. Tests were carried out at the UPR-NSF Earth X-ray Analysis Center (EXACt) using an X-ray diffractometer model SIEMENS D5000. This diffractometer is shown in Figure 3.1.

Thermo gravimetric analysis – Thermo gravimetric analysis were used to determine the thermal stability of the different CLA materials by monitoring the weight change that occurs as the soil samples are heated. More specifically, thermo gravimetric analyses (TGA) were conducted to qualitatively determine the amount of calcium carbonate ($CaCO_3$) present in the two crushed limestone aggregates selected for this study. Calcium carbonate content was determined from the loss of mass expected to occur in a soil sample that contains calcium carbonate when subjected to temperatures up to 950°C. Todor (1976) indicates that calcium carbonate ($CaCO_3$) looses carbon dioxide (CO_2) at about 675°C and reaches complete outgassing at about 950°C.

The following chemical equation illustrates the reaction that occurs in calcium carbonate when subjected to high temperatures.

$$CaCO_3 \xrightarrow{heat} CaO + CO_2 \uparrow \ldots\ldots\ldots\ldots\ldots\ldots\ldots\ldots\ldots\ldots\ldots\ldots\ldots\ldots\ldots\ldots\ldots\ldots\ldots\ldots\ldots[3.1]$$

Based on these observations, the amount of calcium carbonate present in the two crushed limestone aggregates selected for this study were calculated using TGA tests. The TGA tests were conducted at the Materials Research Laboratory of the University of Puerto Rico at Mayagüez using a thermal analyzer system TGA/SDTA85. Figure 3.2 shows the thermal analyzer system used for this thesis. During each test this temperature was gradually increased from 24°C to 950°C in a period of 122 minutes. The rate of temperature increase was kept constant throughout each test.

Figure 3.1. X-Ray Diffractometer at the UPR-NSF Earth X-ray Analysis Center (EXACt).


Figure 3.2. TGA/SDTA85 equipment at the Materials Research Laboratory.

3.3.4. *Test procedure for aged CLA samples*

One of the main objectives of this investigation was to evaluate the short term mechanical properties of two crushed limestone aggregates under different levels of moisture conditions. Samples were submerged in water containers filled with (1) fresh water and (2) salt water for a maximum period of 150 days. Fresh water was collected from the Infrastructure Civil Laboratory at the University of Puerto Rico while salt water was collected from the ocean at Club Deportivo at Joyudas, Cabo Rojo Puerto Rico. Daily aeration of both types of water was applied to prevent decomposition of any organic matter especially for the salt water. Both the fresh and salt water were changed every 30 days. Figure 3.3 shows the sampling location of the salt water. The water containers used for aging CLA samples are shown in Figure 3.4. The water containers were stored at room temperature (~18°C) during the aging process of the CLA samples.

The *pH* is a measure of the acidity or basicity of a solution and the conductivity is the ability to conduct or transmit heat, electricity or sound. Conductivity and *pH* tests were carried out in the Environmental Laboratory at the University of Puerto Rico. The *pH* values reported were 6.72 and 8.18 for the fresh and salt water respectively. The conductivity values exhibited were 236 and 78767 μs/cm at 23.5°C for the fresh and salt water respectively.

Figure 3.3. Club Deportivo beach, Cabo Rojo, PR.

Figure 3.4. Water containers filled with salt water.

3.3.5. Durability and mechanical properties of the selected crushes limestone aggregates

Properties: A) Durability characteristics and durability properties of the two selected crushed limestone aggregated were evaluated by performing Slake Durability Tests, Point Load Tests, Los Angeles Abrasion Tests, and Porosity Tests. Additional to these tests durability of the CLA materials was assessed by tracking variation of selected mechanical properties discussed later in this chapter. Following is a detailed description of each durability test.

<u>Slake Durability Test (ASTM D 4644-87)</u> : The slake durability tests were carried out in general accordance with the procedure outlined in ASTM Standard D 4644-87. This test is used to estimate qualitatively the durability characteristics of rocks in the service environment and to assign a quantitative durability index value for the rocks. The slake durability index is defined as the percentage of dry mass retained from a collection of rock pieces on a 2.00mm (No. 10) sieve after two test cycles which includes oven drying and water soaking with a standard tumbling and abrasion action. Slake durability depends on many factors such as rock type, degree of weathering, grain size, mineralogical composition, and structural/textural properties (Kolay and Kayabali, 2006). Figure 3.5 shows a cross section of the Slake Durability Test Device and Figure 3.6 shows the Slake Durability Test device at the Graduate Soils Laboratory in the University of Puerto Rico at Mayagüez.

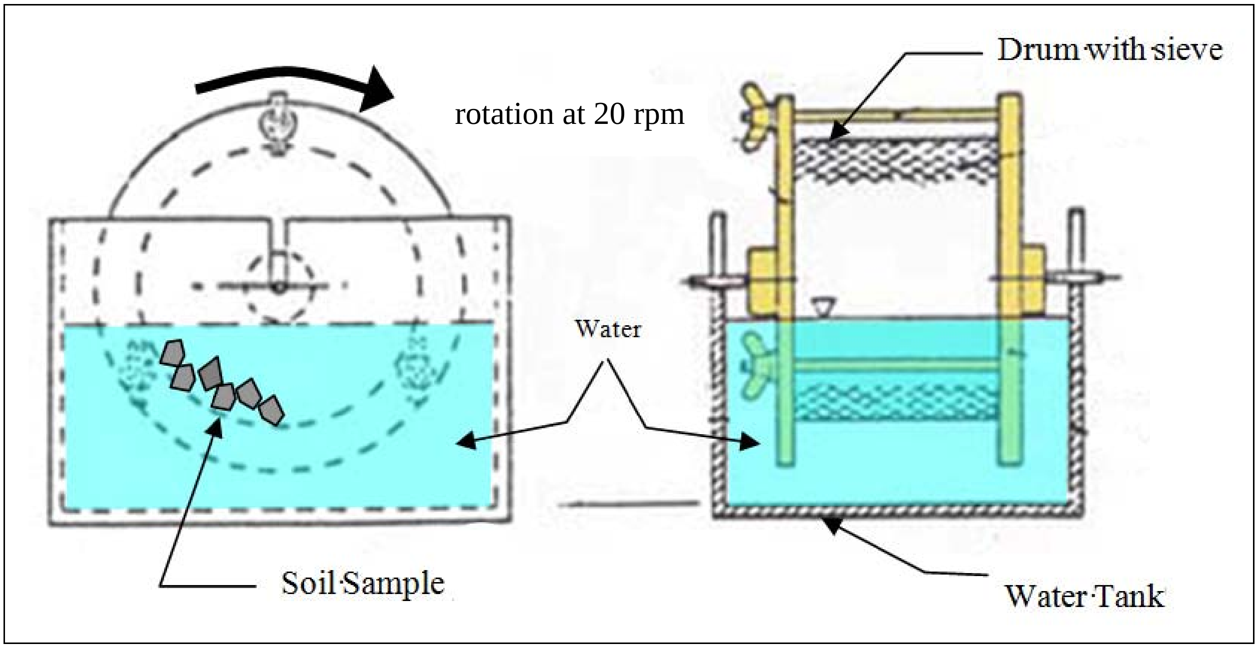

Figure 3.5. Schematic of slake durability device.

It has been reported that the results of the slake durability test are susceptible to the porosity and permeability of the rocks tested, nature of the testing fluid, resistance of rocks against swelling and disintegration, the shape of sample pieces places in the testing drum, properties of testing equipment, conditions of sample storing, and the number of wetting and drying cycles (Franklin and Chandra, 1971).

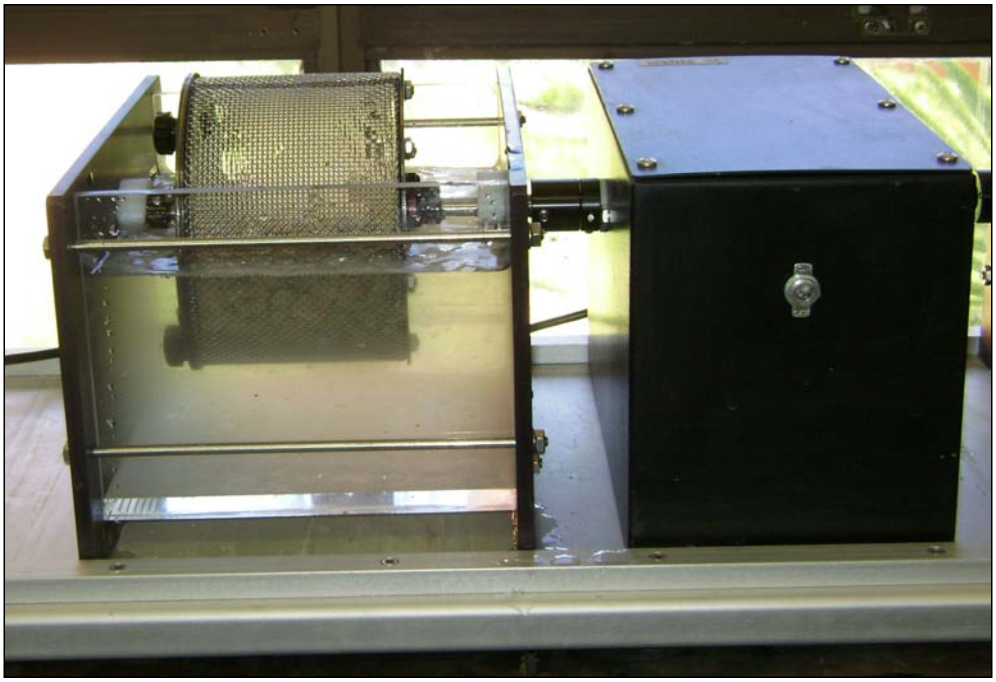

Figure 3.6. Photo of the slake durability test device used in this research.

Typically a slake test specimen consisted of approximately 450 to 500 grams of aggregate particles. The total sample is then placed inside the meshed drum, weighed, and dry in the oven for 24 hours or until a constant weight reading is reached. The rocks and the drum are then allowed to cool at room temperature for 20 minutes and weighed again. The natural water content was calculated as follows:

$$w(\%) = \frac{A - B}{B - C} * 100 \quad \ldots\ldots\ldots\ldots\ldots\ldots\ldots\ldots\ldots\ldots\ldots\ldots\ldots\ldots\ldots\ldots\ldots\ldots\ldots\ldots \text{[3.2]}$$

Where: w = water content (%)

A = mass of drum + sample @ natural moisture content (grams),

B = mass of drum + oven dried sample before first cycle (grams),and

C = mass of drum (grams)

After the initial moisture content was measured, the drum with aggregate particles inside is mounted in the trough and coupled to the motor. A water tank is then filled with fresh water at room temperature to an elevation of 20mm (0.8in) below the rotating drum axis (see Figure 3.5). The drum is then rotated at 20 rpm during 10 minutes. Immediately after the rotation period the drum is removed from the trough and placed in the oven for 24 hours or for a time period until a constant weight is reached. Then, the drum and aggregate sample is weighed to obtain the oven dried sample weight for cycle two. This procedure is then repeated one more time to obtain the oven dried mass sample of cycle three. Photographs before and after the slake durability test were taken to record the sample particle characteristics and mass loss. At the end of each test the Slake Durability Index was calculated as follows:

$$I_{d(2)} = \left(\frac{W_f - C}{B - C}\right) * 100 \quad \text{……………………………………………………. [3.2]}$$

Where: $I_{d(2)}$ = slake durability index (second cycle),
B = mass of drum + oven dried sample before the first cycle (grams),
W_f = mass of drum + oven dried sample retained after second cycle (grams), and
C = mass of drum (grams).

Slake durability tests were performed for both CLA materials at three distinct conditions: (1) natural, fresh or unaged condition, (2) specimens submerged in salt water at two time periods, and (3) specimens submerged in fresh water for two time periods.

Point Load Test (ASTM D 5731-95): The point load tests were carried out on large samples of the parent limestone rock mined at the two quarries that produce the selected CLA materials. The point load test is used as an index test for strength classification of rock specimens. In this test the rock specimens are subjected to an increasingly concentrated load until failure occurs, splitting the specimen. Load is applied through coaxial, truncated conical platens and the failure load is used to calculate the point load strength index and to estimate the uniaxial compressive strength. For this research the point load tests were carried out using a procedure in general accordance with ASTM Standard D 5731-95. According to this standard, the Uncorrected Point Load Strength Index is calculated as follows:

$$I_s = \frac{P}{De^2}, MPa \quad \text{...………………………………………………………. [3.3]}$$

Where: I_s = uncorrected point load strength index (MPa),
P = failure load (N), and
De = equivalent core diameter (mm)

For axial, block and lump test the equivalent core diameter is calculated as follows

$$De^2 = \frac{4A}{\pi} \quad \text{[3.4]}$$

$$A = W * D \quad \text{[3.5]}$$

Where: A = minimum cross-sectional area of a plane through the platen contact points.

A size correction factor must be applied because the point load strength index (I_s) varies as a function of the equivalent core diameter. The size corrected point load strength index $I_{s(50)}$ of a rock specimen is defined as the value of I_s that would have been measure in a diametral test with D=50mm. The size correction factor is calculated as follows:

$$I_{s_{50}} = F * I_s \quad \text{[3.6]}$$

$$F = \left(\frac{De}{50}\right)^{0.45} \quad \text{[3.7]}$$

Where: F = Size Correction Factor.

The estimated uniaxial compressive strength can be obtained from the corrected point load strength index $I_{s(50)}$ using the following formula:

$$q_u = CI_{s(50)} \quad \text{[3.8]}$$

Where : q_u = uniaxial compressive strength, and
C = factor that depends on site-specific correlation between q_u and $I_{s(50)}$.

Table 3.2 provides the generalized values of C if no exact site-specific correlation factor C is available.

Table 3.2. Generalized value of "C" (adapted from ISRM Suggested Methods).

Core size (mm)	Value of "C" (Generalized)
20	17.5
30	19
40	21
50	23
54	24
60	24.5

The Point Load Strength Index Apparatus used in this thesis is located at the Graduate Geotechnical Laboratory of the University of Puerto Rico at Mayagüez, and is shown in Figure 3.7.

Figure 3.7. Point load test apparatus, UPR-Mayagüez

The point load test results are often reported as an indirect measure of the compressive or tensile strength of the rock. The point load apparatus has been widely used in practice due to the ease of testing, the simplicity of specimen preparation and its field application (Kahraman and Gunayding, 2007). Broch and Franklin (1972) stated that advantages of the point load test include: (1) smaller forces are needed so that a small and portable testing machine can be used, (2) specimens in the form of core or irregular lumps are used and requires no machining, and, (3) fragile and broken materials can be tested.

Point load test were performed under three different conditions: (1) natural condition (fresh and unaged), (2) specimens submerged in salt water, and (3) specimens submerged in fresh water. Tests were performed at time zero, 90 days, and 150 days after received and cured.

<u>Los Angeles Abrasion Test (ASTM C 131-96)</u>: The demand for crushed stone aggregate has increased with the expansion of highways and other constructions (Kahraman and Gunaydin, 2007). Abrasion resistance is an important property of aggregate and is generally determined using the Los Angeles abrasion test which measures the resistance of aggregate to wear during the attrition of rock particles due to impact and crushing by steel spheres (Kahraman and Gunaydin, 2007). The Los Angeles Abrasion Test is a measure of degradation of mineral aggregates resulting from a combination of actions such as: (1) abrasion or attrition, (2) impact, and (3) grinding in a rotating steel drum containing a specified number of steel spheres. For this thesis, the Los Angeles abrasion tests were carried out in general accordance with ASTM Standard C 131-96. According to this standard, the number of steel spheres in the drum will depend on the grading of the sample tested. The sample and the corresponding number of steel spheres are placed inside the Los Angeles testing machine and rotated at a speed of 30 to 33 rpm until a total of 500 revolutions is reached. After this number of revolutions was completed, the sample is carefully discharged from the machine and sieved through a 1.71mm (No.12) sieve.

Figure 3.8 shows the Los Angeles Abrasion machine of the Materials Laboratory of the University of Puerto Rico, Mayagüez Campus.

Figure 3.8. Los Angeles abrasion machine at UPR-Mayagüez

The loss by abrasion and impact of the sample is calculated as follows:

$$\%Loss = \frac{OriginalMass - FinalMass}{OriginalMass} * 100 \quad \ldots\ldots\ldots\ldots\ldots\ldots\ldots\ldots\ldots\ldots\ldots\ldots \text{[3.9]}$$

Los Angeles abrasion test were performed under three different conditions: (1) natural condition (fresh and unaged), (2) specimens after submerged in salt water, and (3) specimens after submerged in fresh water. Tests were performed at time zero, 90 days, and 150 days after received and submerged in fresh and salt water.

B) Geotechnical Properties: The geotechnical properties of the two selected crushed limestone aggregates, from the two quarries representing the North and South Karst Formations, were evaluated by means of 1-D compression tests and triaxial compression tests. Following is a detailed description of each test type.

1-D Compression tests: 1-D compression tests were carried out on the two CLA materials. The 1-D compression tests carried out using a Bishop type consolidometer. CLA samples were prepared inside a standard consolidation oedometer ring in a dry condition. Samples were prepared in a loose state by tamping. Once the sample was prepared the sample was subjected to 8 load increments of 500, 1000, 2000, 4000, 6000, 8000, 16000 and 32000 psf. Each stress increment was maintained for 60 minutes. The test device used for these tests is shown in Figure 3.9.

Figure 3.9. Bishop consolidometer used for the 1-D compression tests.

For each 1-D compression tests a stress-strain curve was obtained which allowed evaluating compressibility properties of the dry CLA materials for a loose compaction state. These tests also allowed evaluating particle breakage and crushing by comparing grain size distribution curves before and after each test. This is discussed at the end of this chapter.

1-D compression tests were carried out for the two CLA materials selected for this study under the following conditions: (1) as received or unaged, (2) submerged in salt water for 90 and 150 days, and (3) submerged in fresh water for 90 and 150 days.

Triaxial compression test: Triaxial compression tests were performed on fresh and aged samples of the two CLA materials selected for this study. Tests were carried out in general accordance with ASTM Standard D 2850. However, it is important to explain that the CLA specimens subjected to triaxial testing were practically in dry condition ($w \approx 0\%$) therefore; strictly speaking neither consolidation nor pore pressure dissipation occurs. The stress-strain curves and associated shear strength parameters obtained from these tests are effective parameters. The samples were first subjected to a cell pressure and after a prudent waiting period deviatoric stresses were applied with the load piston. The triaxial test device used to carry out these tests is shown in Figure 3.10. This is a W-F triaxial 50 kN triaxial device with a constant speed of the load platen. For this thesis the triaxial tests were carried out at 1mm/min.

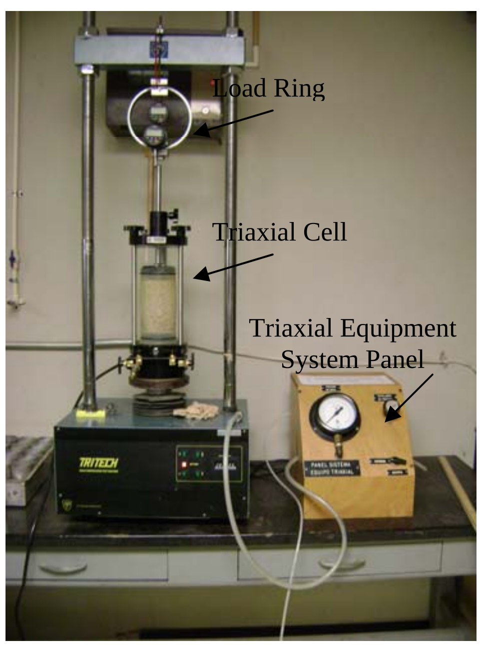

Figure 3.10. Triaxial compression test setup used in this research.

Triaxial samples of the two CLA materials were prepared using a split mold and by filling in layers with light tamping in each layer. Specifically, triaxial samples were prepared using 10 layers of about 15 mm in thickness. A round tamper of 33mm in base diameter was used to apply 10 blows per layer. The final sample dimensions were 150 mm (6 inches) in height by 75 mm (3 inches) in diameter. The dry density values of the CLA samples prepared using this procedure ranged between 92 and 103 pcf. All triaxial samples were prepared using this procedure. The objective was to try to keep a constant relative density through out the durability study. The final sample dimensions were based on a minimum of 4 diameter and height measurements. Samples were carefully assembled on the triaxial cell by applying a small vaccum which allowed assemblage of the triaxial cell system. The vaccum was removed once the triaxial cell was filled with water.

The triaxial compression tests had two main loading stages: (1) cell pressure application, and (2) deviatoric stress application. To evaluate possible curvature of the shear strength envelope of the CLA materials a series of triaxial tests were carried out with confining cell pressures of 7, 15, 30, and 73 psi. The cell pressure was applied gradually and once the target pressure was reached it was maintained constant for the CLA materials. Due to the angularity of the CLA materials some membranes were damaged during application of the high cell pressures levels (particularly 73 psi). Therefore for tests with a pressure levels of 73 psi samples were protected with a double latex membrane. After cell pressure application the CLA materials were sheared by means of deviatoric stress application. If possible, triaxial tests were carried out up to axial strain levels of about 20%.

Crushability analyses: As discussed in Chapter 2, susceptibility to crushing is a very important consideration for granular soils since it highly influences its geotechnical properties. A component of this investigation was to evaluate crushing potential for both crushed limestone aggregates. Crushing susceptibility was quantified using the particle brakeage factor (B_{10}) proposed by Lade et al. (1996). This particle brakeage factor can be calculated as follows:

$$B_{10} = 1 - \frac{D_{10f}}{D_{10i}} \quad \text{[3.10]}$$

where D_{10f} is the final grain diameter corresponding to the 10% of the material being smaller by weight after shearing and D_{10i} is the initial grain diameter corresponding to the 10% of the material being smaller by weight before the application of shearing stresses. This particle brakeage factor ranges from [0,1]. Zero when there is no particle brakeage and 1 for the hypothetical case where there is infinite particle brakeage.

Crushing of particles was measured by comparing the grain size distribution curves of the crushed limestone aggregates before and after: (1)Triaxial Compression Testing, (2) 1-D Compression Test, and (3) Modified Proctor Compaction Testing.

Chapter 4. Quarries Selected for Study

4.1. Introduction

This chapter describes the two limestone quarries selected for this MS study. The chapter describes the geology of each quarry and the characteristics of the parent limestone rock and limestone soils of each quarry, as they have a direct influence on the properties of the CLA materials they produce.

4.2. General location of the two limestone quarries

Two quarries were selected as sources of crushed limestone aggregate for this project. One quarry is located in the south of Puerto Rico (PR) and for this thesis it will identified as Quarry A. The second quarry is located in the northwest corner of PR and is labeled as Quarry B. The location of the two quarries is shown in Figure 4.1. This figure also shows the geology formation of both quarries. The following subsections describe in more detail each quarry.

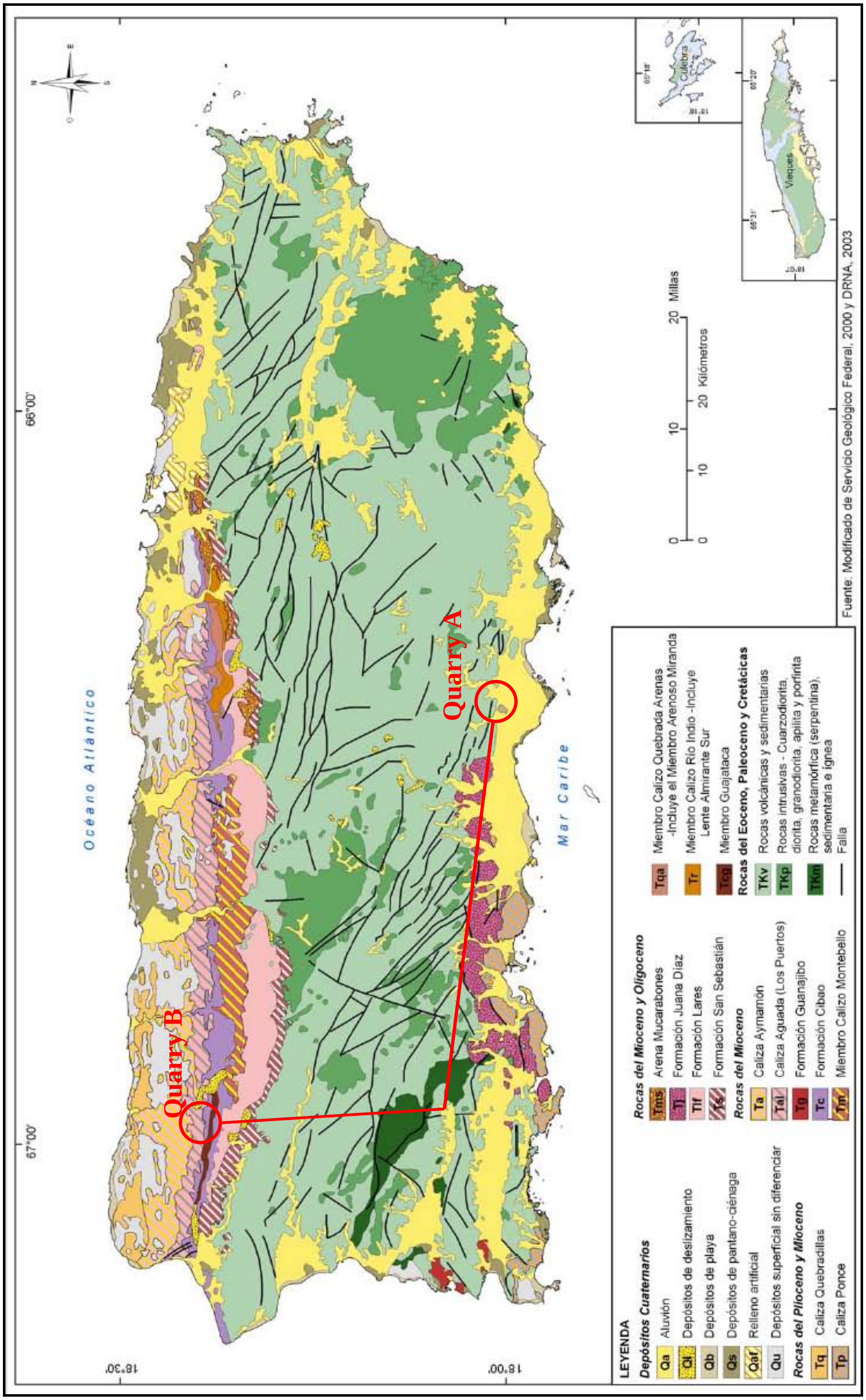

Figure 4.1. Map of Puerto Rico soils with the selected areas of study (USGS, 2000 and DRN, 2003).

4.3. Quarry A in the South of PR

As shown in Figure 4.1 Quarry A is located in the South of PR. Specifically this Quarry is located between Ponce and Santa Isabel as shown in Figure 4.2. An aerial photo of the localization of Quarry A is shown in Figure 4.3. A detailed geological description of the soils found in Quarry A is presented in the following subsection.

4.3.1. Quarry A: South karst landform - Cuevas limestone Tc – (Tertiary)

The geology map for the area of Quarry A shown in Figure 4.4 (adapted from Glover and Mattson, 1973) indicated that Quarry A is located on Cuevas Limestone. Cuevas Limestone was formed in the Tertiary period as an algal limestone. This limestone is nearly white with no visible pores. Fissures can be observed in the surface of the rocks. This limestone is nearly white but the bottom or “basal” impure facies may be grayish red. The Cuevas limestone consist of variables proportions of fossil skeletal debris and carbonate mud (biomicrite). The major organism that composes this limestone is calcareous red algae. The texture of the Cuevas limestone has an intact framework of coarse to fine fragments of this red algae. The structure of this formation is thick-bedded or massive in the major part and thin beds are less common. The approximate thickness of this formation is 35 meters.

4.3.2. Soil Taxonomy of the South karst landform

The selected quarry from the South karst landform, Quarry B, is a member of the Caguabo-Mucara-Quebrada Association that consists of moderately steep to very steep, well drained, medium acid to neutral, loamy and clayey soils over weathered and hard rock; on side slopes and ridges on the volcanic uplands. Caguabo-Mucara-Quebrada Association belongs to the Inceptisoils soil order. Caguabo are a family of loamy, mixed, active, isohyperthermic, and shallow soils. Muacara are a family of fine-loamy, mixed, superactive, and isohyperthermic soils. Quebrada are a family of fine, mixed, active, and isohyperthermic soils. Figure 4.2 shows the soil taxonomy map for the Juana Diaz, PR area.

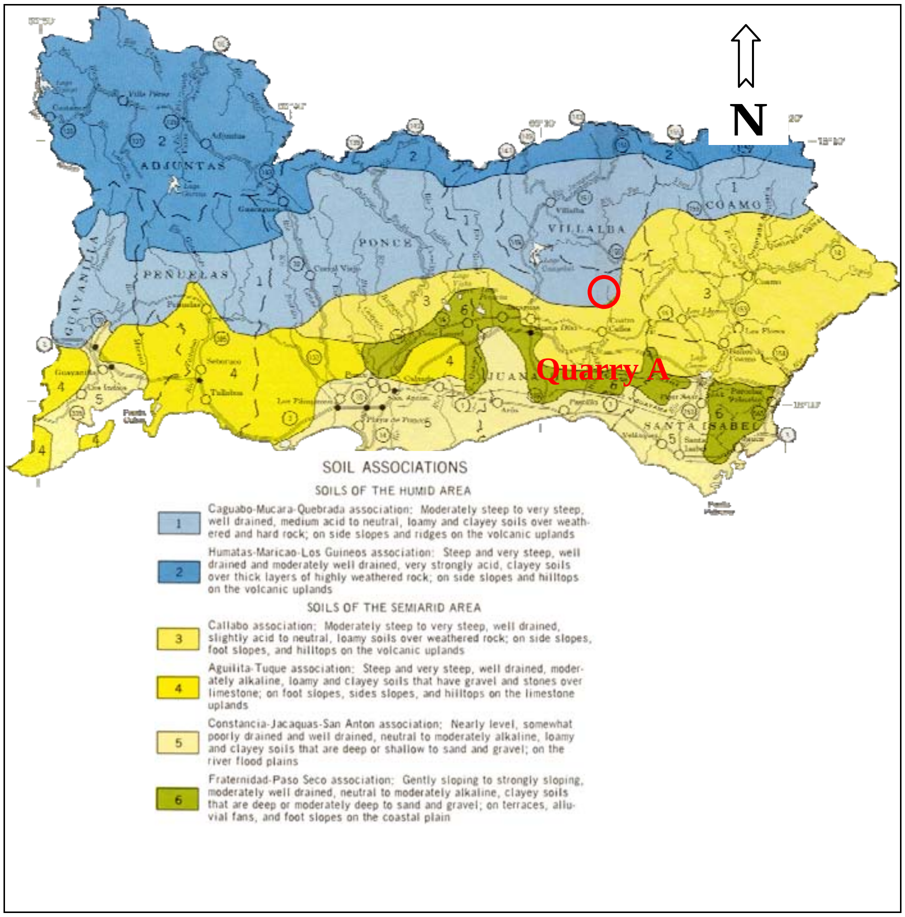

Figure 4.2. Soil taxonomy map of Juana Diáz, Puerto Rico and vicinity area of Quarry A (adapted from USGS, 1976).

Figure 4.3. Aerial photo of Quarry A - South karst landform (photo from Google Earth).

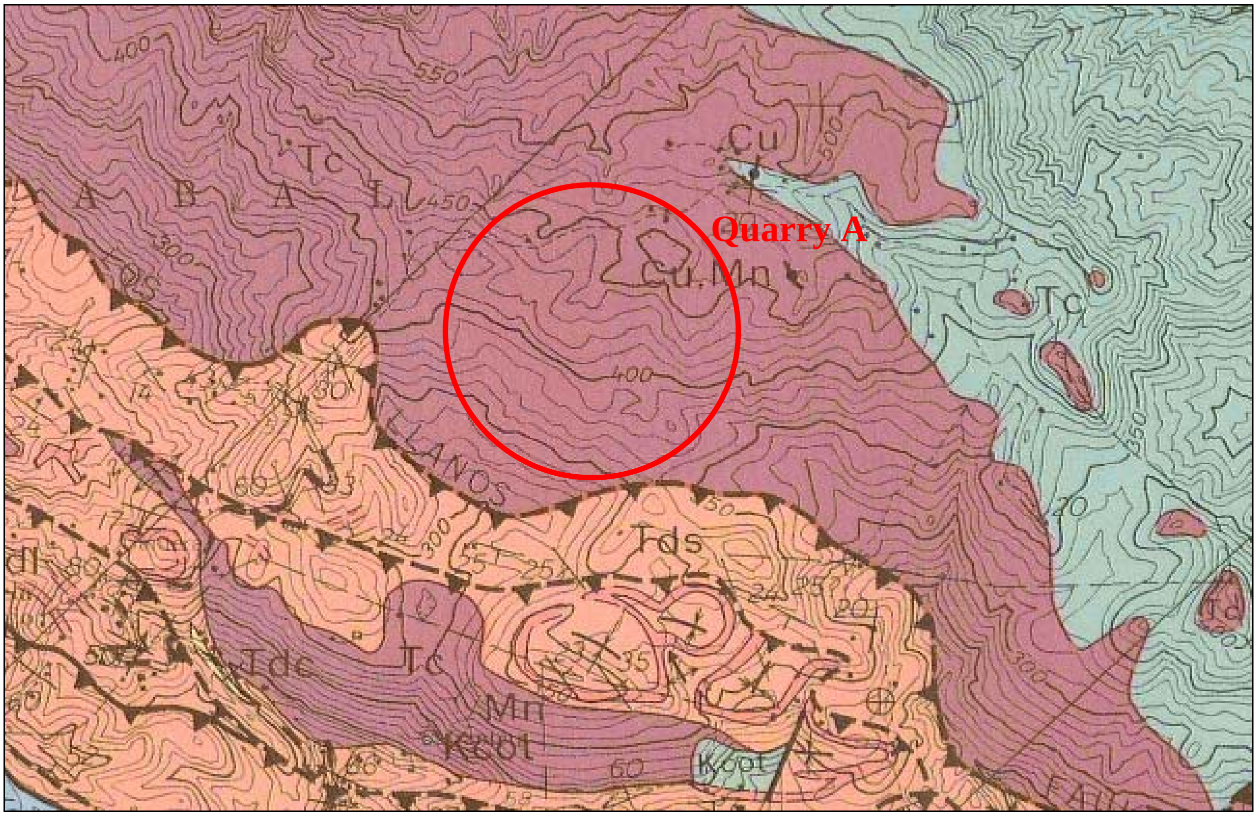

Figure 4.4. Geologic map of the Juana Díaz area near Quarry A. (adapted from Glover and Mattson, 1973)

4.4. Quarry B in the Northwest of PR

As shown in Figure 4.1, Quarry B is located in the northwestern corner of PR. Specifically this Quarry is located between Aguadilla and Quebradillas. An aerial photo of the localization of Quarry A is shown in Figure 4.5. A detailed geological description of the soils found in Quarry B is presented in the following subsection.

4.4.1. Quarry B: North karst landform - Aymamon limestone, upper member. – Taz .- (Tertiary)

From the geologic maps of the area, Quarry B is located in the North karst landform. Specifically it falls within the Aymamon limestone formation, as shown in Figure 4.7. Monroe (1969) described the Aymamon tertiary limestone. This limestone is divided into two different members, upper and lower. The upper member (Taz) is characterized by a very pale orange to bright-yellow chalk. This chalk contains many beds of large oysters as much as 15 cm long and other fossils. These chalk units of this formation are interbedded with solution–riddled very pale orange to white hard limestone and some of this limestone are fossiliferous. The upper part is commonly white, very pure and commonly re-crystallized hard limestone like the lower member (Tay) of the entire Formation. This upper member (Taz) intertongues towards the east with beds that are indistinguishable from upper beds of the lower member (Tay). The approximate thickness of this upper member is 50 to 80 meters. (adapted from Monroe, 1969). From the visual inspection of the aggregates, fossils were found in the aggregates from this quarry. This suggests that this limestone formation could be a result from a deposition of an organic chemical process.

4.4.2. Soil Taxonomy of the Northwest karst landform

The selected quarry from the northwest karst landform, Quarry A, is a member of the Coto-Aceitunas Association composed of slightly leached and strongly porous soils that are dominantly clayey throughout. Coto belongs to the soil order of the oxisols which are a family of very fine, kaolinitic, and isohyperthermic soils. Aceitunas belong to the Udults soil order which is a family of fine, kaolinitic, and isohyperthermic soils. Figure 4.5 shows the soil taxonomy map from the Isabela,PR area.

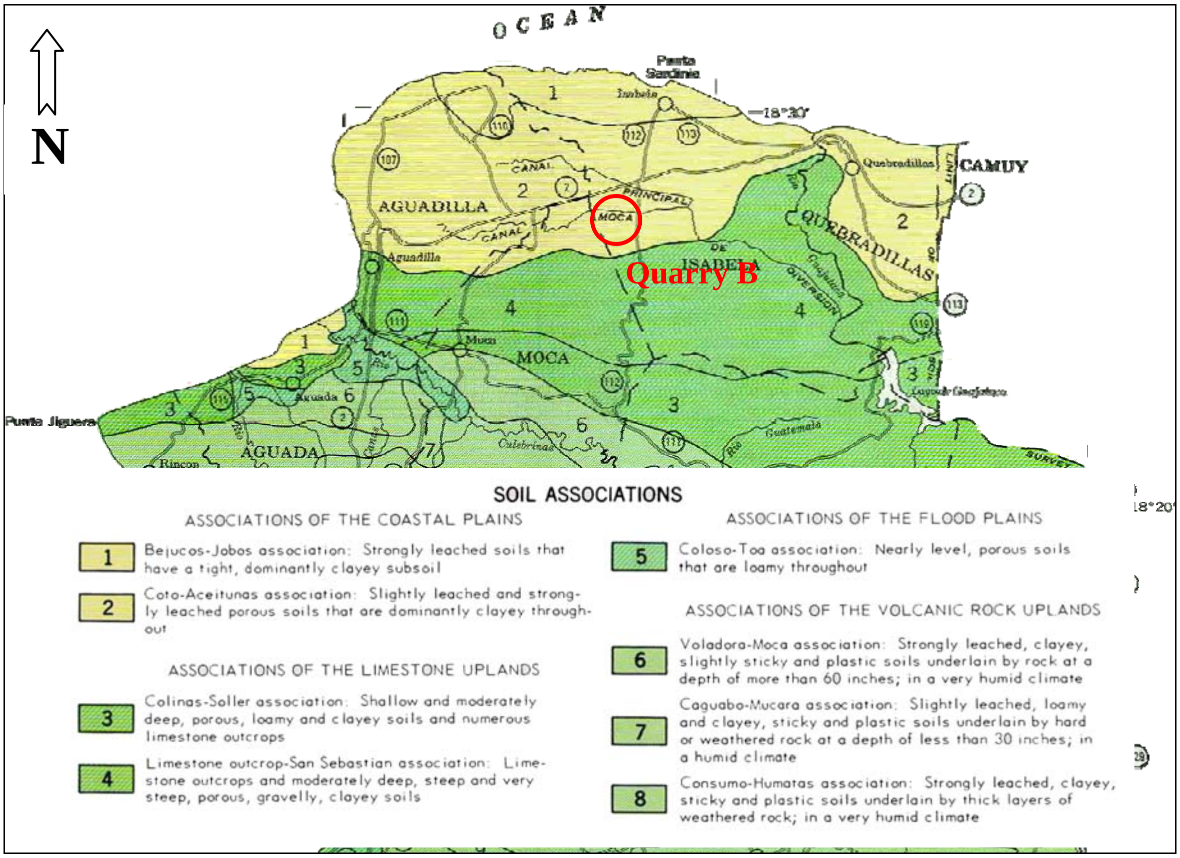

Figure 4.5. Soil taxonomy map for Isabela, Puerto Rico and vecinity area (adapted from Monroe,1969).

Figure 4.6. Aerial photo of Quarry B - North karst landform (photo from Google Earth).

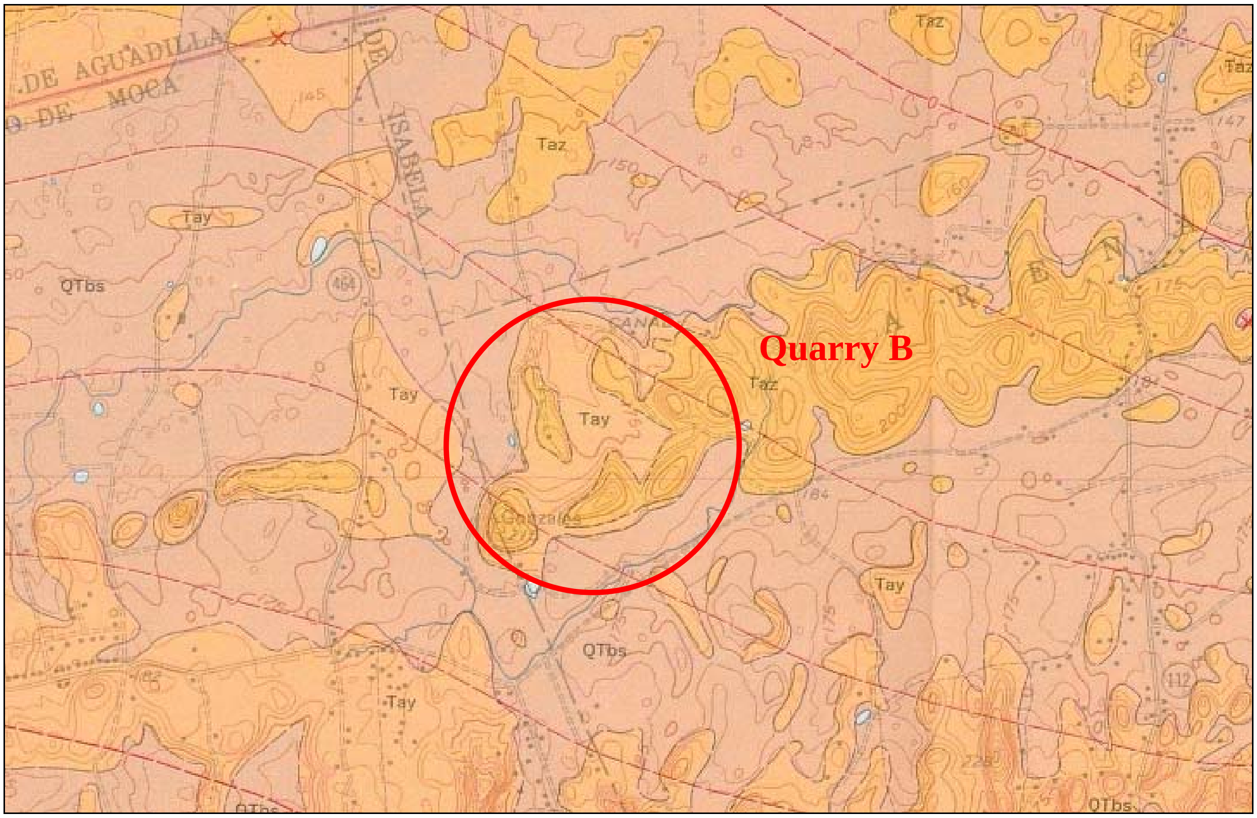

Figure 4.7. Geologic map of the Isabela area near Quarry B. (adapted from Monroe, 1969)

4.4.3. Description of the baseline properties of the parent limestone rock

A summary of the baseline properties of the parent limestone rock for each quarry is shown in Table 4.1. Tests such as maximum and minimum dry density, porosity, water absorption, and specific gravity were carried out on the crushed limestone aggregate at time zero, as received from the quarries. Point load tests were carried out in the limestone rock itself, at time zero days as received from the quarries. The compressive strength is an estimated parameter from an empirical correlation explained in detail in Chapter 3.

Table 4.1. Summary of the baseline properties of the parent limestone rock.

		CLA QUARRY		
Property	**Units**	**A**	**B**	**Comments**
γ_{dmax}	lb/ft^3	124	91.03	From CLA characterization
γ_{dmin}	lb/ft^3	120	89.13	From CLA characterization
Porosity	%	1.95	7.93	From CLA characterization
Water Absorption	%	1.29	3.88	From CLA characterization
Gs	-	2.74	2.74	From CLA characterization
Point Load Index $I_{s(50)}$	ksi	0.45	0.46	t=0 days as received samples
Compressive Strength (q_u)	ksi	10.72	11.12	t=0 days as received samples
Formation	-	Aymamon	Cuevas Limestone	

Figure 4.8 shows an irregular rock specimen from Quarry A and Quarry B as received from the quarries. It can be observed from the figure that the specimen E from Quarry A has a smoother surface than specimen A from Quarry B, whose surface is more porous. The diameter of the limestone rock were 47.20 and 46.8 for specimen E and A, respectively.

Figure 4.8. Photos of a typical limestone rock as received from the Quarry (a) specimen from Quarry A and (b) specimen from Quarry B.

Chapter 5. Moisture Effects on Short-Term Durability and Mechanical Properties of Two Puerto Rico Crushed Limestone Aggregates

5.1. Introduction

A series of tests such as slake durability tests, Los Angeles abrasion tests, and point load tests were performed after being submerged on the selected aggregates to determine their durability when exposed to moisture changes. Also a series of triaxial compression tests were performed on the two selected crushed limestone aggregates under two different moisture conditions: fresh and salt water at 90 and 150 days of submergence to determine its geotechnical properties. The procedure used for these tests is described in Chapter 4. This chapter presents and discusses the results obtained from each one of the tests.

5.2. Description of Crushed Limestone Aggregate (CLA)

The main focus of this investigation was to study the short and long term mechanical and durability properties of two high calcium carbonate crushed limestone of Puerto Rico under different moisture conditions. The experimental program includes a comparison between the soils tested at time zero (as received from the quarry) and the soils submerged in fresh and salt water at 90 and 150 days. The soil samples from both quarries were retrieved from the surface using a shovel. Figure 5.1 shows the soils collected from Quarry A and Quarry B.


Figure 5.1. 3/8" soil specimen from Quarry B (left) and 5/16" soil specimen from Quarry A (right)

Information for both test crushed limestone soils regarding soil description and classification, mineralogy and shear strength are discussed in the following subsections.

5.2.1. General description of the tested crushes limestone soils

As previously mentioned, two different crushed limestone aggregates were used in this investigation:

1- Quarry A – South Karst Formation (Cuevas Limestone): 5/16" to 3" crushed limestone soils with angular grains gray to white in color.

2- Quarry B – North Karst Formation (Aymamon Limestone): 3/8" to 3" crushed limestone soils with subrounded to subangular grains yellow to pink in color.

As mentioned in Chapter 4 seven different tests were conducted to both of the selected crushed limestone soils for characterization. Natural water content was recorded before each test in order to control moisture changes, if any, but every test was performed at dry conditions with w≈0%. Crushed limestone soils were washed and dried after testing to minimize the fine content. Table 5.1 presents a summary of the tests and results for the soil characterization. We can observe from this table that both of the selected crushed limestone soils are classified as GP-*Poorly Graded Gravel* according to the Unified Soil Classification System (USCS).

Table 5.1. Index properties of the two selected CLA materials.

Parameter	CLA Quarry A	CLA Quarry B	Standard
D_{10} (mm)	3.4	3	ASTM D422-63 (2002)
D_{30} (mm)	5	4.5	
D_{50} (mm)	5.9	5	
D_{60} (mm)	6	5.5	
C_u	1.76	1.83	
C_c	1.23	1.23	
G_s	2.74	2.74	ASTM D 854
e_{max}	0.878	0.918	ASTM D4254-00
γ_{dmin} (lb/ft^3)	91.03	89.13	
e_{min}	0.378	0.423	ASTM D 1557
γ_{dmax} (lb/ft^3)	124	120	
U.S.C.S.	GP	GP	ASTM D 2488-00
Porosity (%)	1.95	7.93	ALTERNATIVE METHOD[1]
Absorption	1.29	3.88	ASTM C 97

Note: [1] Description explained in Appendix A

Figure 5.2 shows the grain size distribution for the 5/16" CLA material from Quarry A and the 3/8" CLA material from Quarry B. The gradation curves presented in Figure 5.2 shows that both crushed limestone soil samples exhibits a fairly uniform gradation with grain sizes ranging from 2 mm to 9 mm and no fines. According to the Unified Soil Classification System (ASTM D 2488-00) both soils are classified as poorly graded gravels (GP).

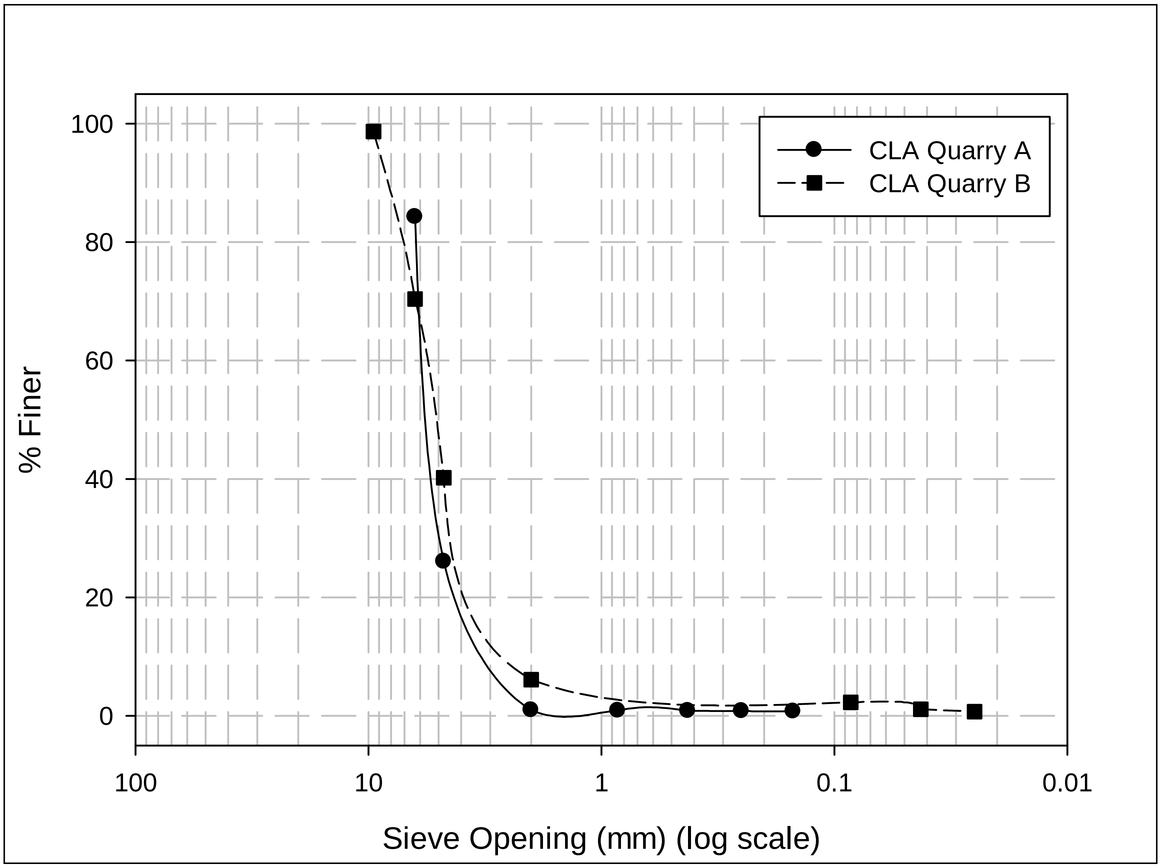

Figure 5.2. Grain size distribution for the 5/16" crushed limestone soil sample from Quarry A and for the 3/8" crushed limestone soil sample from Quarry B.

5.3. Mineralogy of CLA materials

5.3.1. X-ray diffraction

Quarry A and B crushed limestone soil samples were subjected to X-Ray Diffraction analysis to determine qualitatively their mineral content. Tests were performed at the UPR-NSF Earth X-ray Analysis Center (EXACt) using an x-ray diffractometer model SIEMENS D5000. The X-Ray diffractogram for Quarry A and Quarry B are shown in the Figures 5.3 to 5.5, respectively. As expected, both of the diffractograms reveals a predominance of carbonate materials such as calcite and magnesium calcite at 2θ = 29 to 30°.

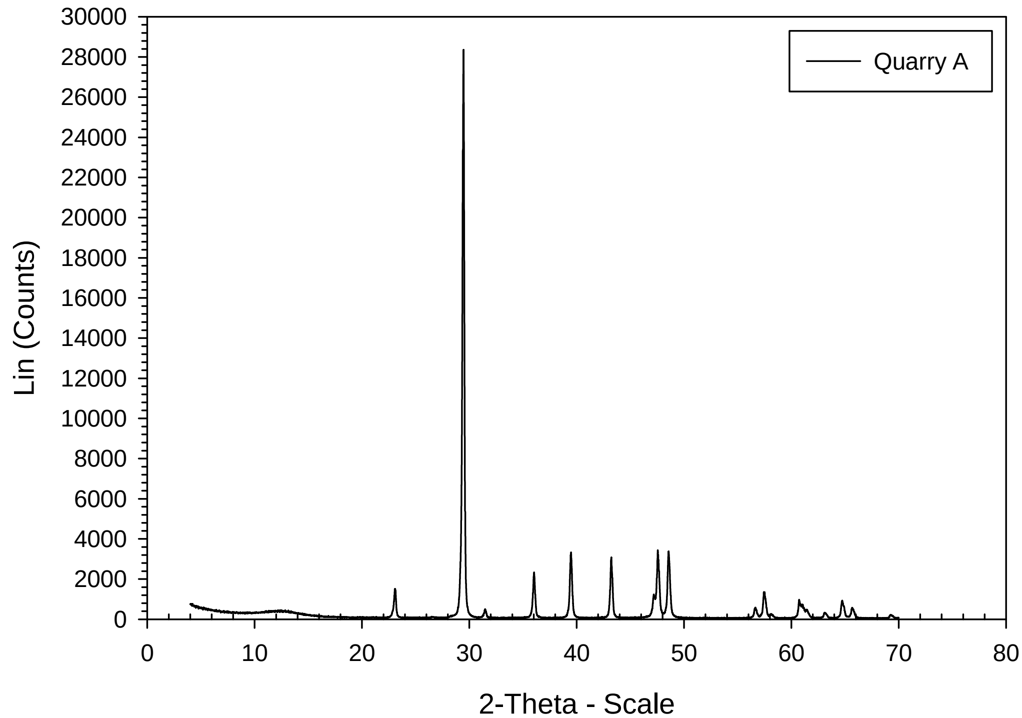

Figure 5.3. X-ray diffraction for Quarry A.

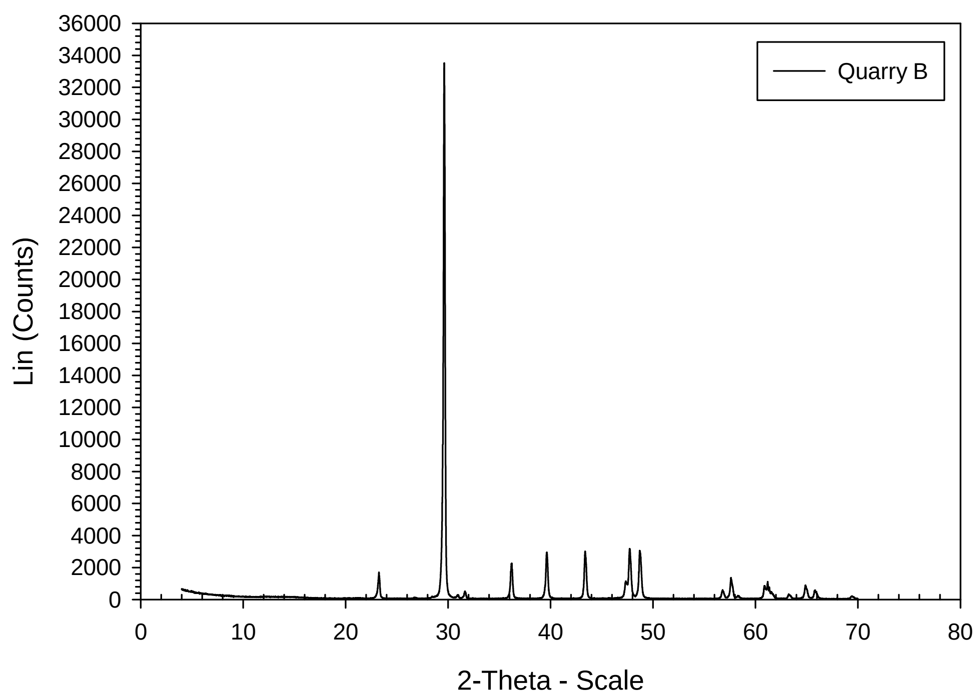

Figure 5.4. X-ray diffraction for Quarry B.

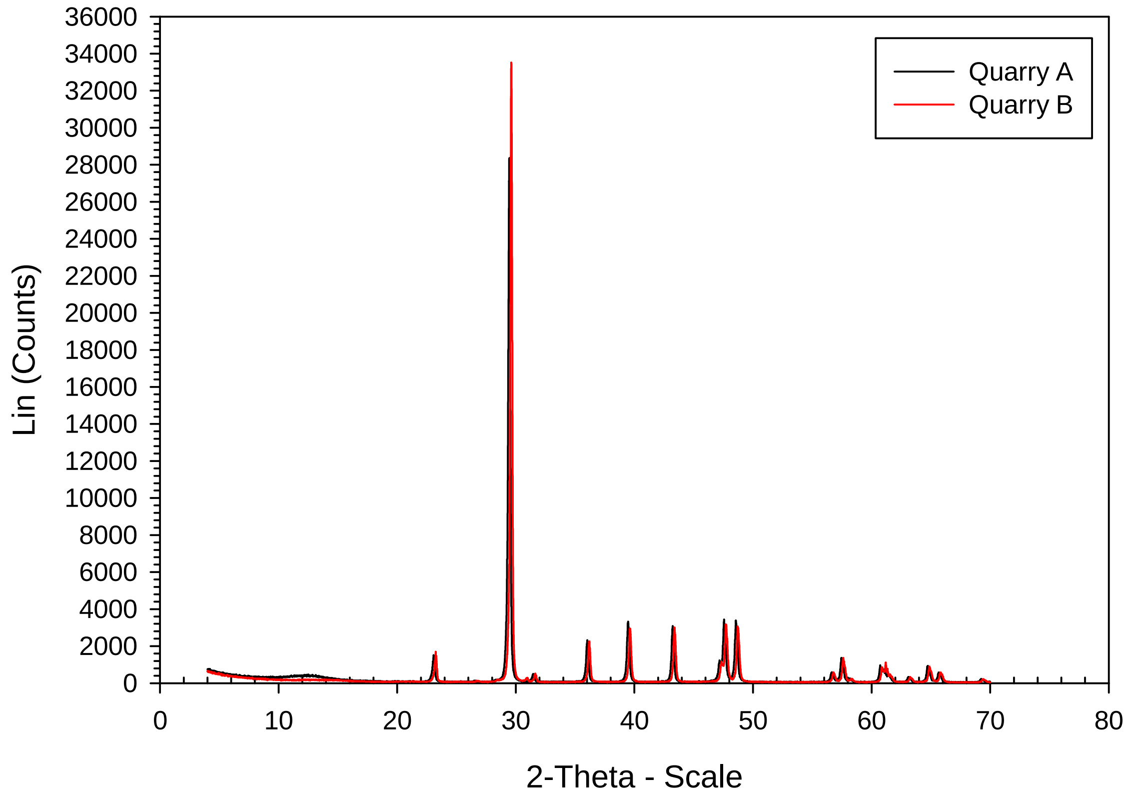

Figure 5.5. X-ray difrraction for Quarry A and B.

5.3.2. Thermo-gravimetric analysis

Quarry A and B soil samples were subjected to thermo-gravimetric analysis to quantitatively determine the amount of calcium carbonate content ($CaCO_3$). A summary of the results is presented in Table 5.2. Thermo-gravimetric analysis confirms the predominance of carbonate materials in both soil samples. Quarry A exhibited a more calcium carbonate content equal to 97.44% of the total mass.

Table 5.2. Summary of Thermo-gravimetric analysis results.

Crushed Limestone	Initial Mass (mg)	Mass Loss (mg)	$CaCO_3$ Content (%)
Quarry A	36.76	15.75	97.44
Quarry B	35.277	14.5541	93.8

Figures 5.6 and 5.7 shows the results for the TGA carried out in the selected crushed limestone aggregates. As shown from the figures, it can be observed that the mass loss of CO_2 starts at around 675°C and finishes around 950°C, as discussed in section 3.3.3.

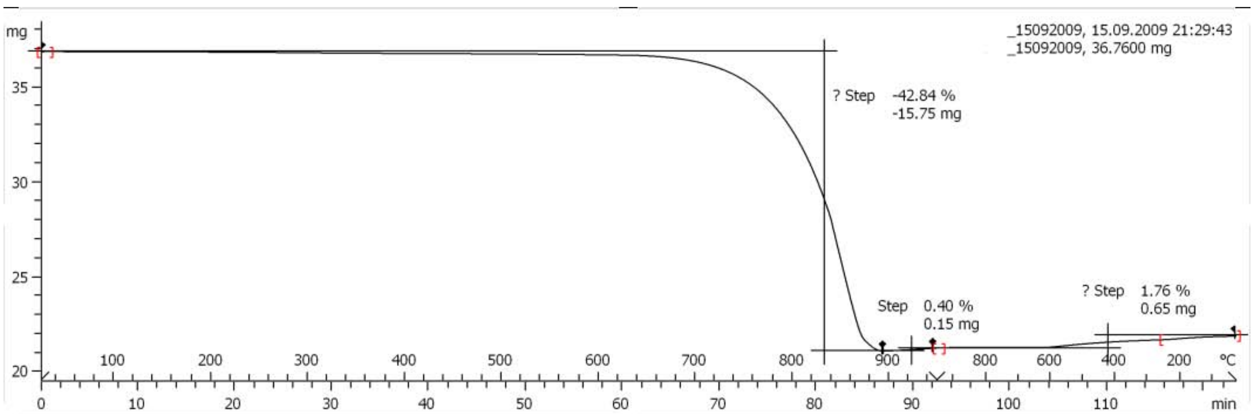

Figure 5.6. TGA results for the CLA from Quarry A.

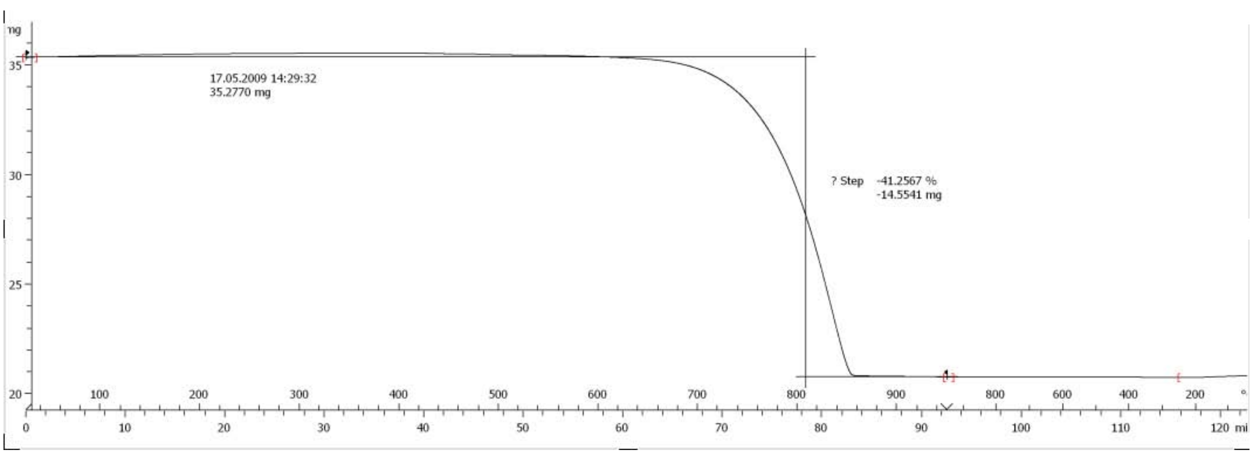

Figure 5.7. TGA results for CLA from Quarry B.

5.4. Moisture effects on slake durability tests on aged CLA materials

Durability characteristics of the two selected crushed limestone aggregates materials was evaluated by means of the slake durability test. This test can be used to compute the slake durability index that is based on the material loss after subjecting the sample to various cycles of wetting and drying by means of a rotating drum that is partially submerged in fresh water. For each slake durability test approximately 450 grams of CLA material was used. Prior to each slake test, the CLA material selected were carefully cleaned with a brush to remove all dust or fines on the particles. The slake durability test procedure was described in Chapter 4. One slake was carried out per aging condition (water type and date). The slake test results (particularly the slake durability index) were reached as a function of submergence time. Table 5.3 describes the durability classification based on the slake durability index and Table 5.4 shows a classification based on a verbal description for the slake durability test.

Table 5.3. Durability classification based on the slake durability index (adapted from Goodman, 1989)

Durability	Slake Durability Index I_d %
Very High	> 98 %
High	95 – 98 %
Medium-High	85 – 95 %
Medium	60 – 85 %
Low	30 – 60 %
Very Low	< 30 %

Table 5.4. Standard verbal description for slake durability test (adapted from ASTM D 4644-87).

Standard Verbal Description for Slake Durability Test	
Type I	Retained pieces remain virtually unchanged
Type II	Retained materials consist of large and small pieces
Type III	Retained material is exclusively small fragments

A summary of the slake durability test results for both CLA material types and different aging conditions are presented in Table 5.5.

Table 5.5. Summary of slake durability test results of CLA materials.

Quarry	Time (days)	Water Condition	Slake Durability Index (I_d) %	ASTM Type
A	0	As received	99.5	I
A	90	Fresh	99.7	I
A	90	Salt Water	99.5	I
A	150	Fresh	99.7	I
A	150	Salt Water	99.5	I
B	0	As received	98.6	I
B	90	Fresh	99.2	I
B	90	Salt Water	98.7	I
B	150	Fresh	98.9	I
B	150	Salt Water	98.9	I

As shown in Table 5.4, all slake durability index values fall into the ASTM-Type I category which correspond to slake durability tests where the retained pieces in the drum remained virtually unchanged. The slake durability test results for both CLA materials and both water submergence conditions, indicate in all cases slake durability index values above 98%. After 150 days of exposure no measurable degradation was observed in terms of reduction of I_d values. Statistically values of I_d measured at time zero days are equivalent to the values measured at the maximum level of exposure of 5 months. It can be concluded that at least in terms of the slake durability tests no short term degradation of the CLA was observed after submergence in fresh or salt water for 150 days. More detailed results from the slake durability tests are presented in Appendix B.

5.5. Moisture effects on point load tests on aged parent limestone rock samples.

The compressive strength of the parent limestone rock for both of the quarries was evaluated by means of the Point Load Test. This test was described in Chapter 4. A summary of the point load test results obtained from unaged and aged samples of the parent limestone rock of both quarries is presented in Table 5.6. This table includes information for each of the set of tests corresponding to a particular aged condition. Information presented includes: number of test per set, average moisture content, and average and standard deviation of the point load measurements. This table also presents the average point load index ($I_{s(50)}$) for each set of tests and the estimated average unconfined compressive strength (q_u) that was evaluated using the empirical correlation established in the ASTM D 5731-95. Additional information is included in Appendix C.

Table 5.6. Summary of results from the Point load test.

Quarry	Time of exposure(days)	Water Condition	Number of Tests	Average Water Content (%)	Average Peak Load (kip)	Standard Deviation of Peak Load (kips)	Average $I_{s(50)}$	Estimated Average q_u (ksi)
A	0	N/A	17	0.06	2.24	2.24	0.45	10.72
A	90	Fresh	14	0.05	2.14	2.1	0.39	10.31
A	90	Salt	14	0.08	2.70	1.06	0.44	10.86
A	150	Fresh	17	0.2	1.98	2.19	0.41	9.98
A	150	Salt	16	0.3	1.86	1.88	0.43	10.18
B	0	N/A	10	0.16	2.33	1.54	0.46	11.12
B	90	Fresh	10	0.04	2.59	1.17	0.50	12.19
B	90	Salt	11	0.06	1.76	2.66	0.43	10.51
B	150	Fresh	11	0.4	2.22	1.22	0.52	12.23
B	150	Salt	12	1.27	2.39	3.02	0.50	12.06

Note: (*) Estimated q_u using empirical correlation (equation 3.8)

For the limestone rock samples after submergence in fresh and salt water for 90 and 150 days water content was calculated after a minimum of two days of air drying. In general, both limestone rock types absorbed very little moisture. For the maximum submergence time of 150 days the moisture content (by weight) values for the limestone from Quarry A were 0.2% and 0.3% for fresh water and salt water, respectively. For this same submergence time the moisture content values for the limestone from Quarry B were 0.4% and 1.27% for fresh and salt water conditions, respectively. From these results it appears that the limestone from Quarry B is more porous, but the moisture content values recorded at 150 days of submergence are still quite low.

From Table 5.6 it can be observed that after 150 days of submergence there was a slight decrease in average peak load recorded for the limestone from Quarry A. The average reduction levels were 11.6% and 17% for submergence in fresh and salt water, respectively. For the limestone of Quarry B almost no reduction of average peak load values after 150 days and for both types of water. In fact, the average peak load values for this limestone showed a great variability and a clear tendency or trend was not possible to infer.

A similar behavior to the one observed between the peak load and time of submergence was recorded. This is as expected since this index is directly proportional to the values for the peak load. The point load index values for the limestone from Quarry A showed a consistent decreased with increasing time of submergence. As shown in Table 5.6, the point load index values decreased from 8.89% and 4.44% after 150 days of submergence in fresh and sea water, respectively. In contrast, point load index values for the limestone from Quarry B did not show a decreased with submergence in time. The test results for this limestone did not follow the expected trend and in fact showed even an increase with time.

5.6. Moisture effects on Los Angeles abrasion test results on aged CLA materials

The Los Angeles test procedure was described in Chapter 3. As described in the methodology chapter, Los Angeles abrasion test were carried out after different times of submergence in fresh and salt water. For both CLA materials, the maximum time of submergence was 150 days. A summary of the Los Angeles abrasion test results is presented in Table 5.7.

Table 5.7. Summary of results from Los Angeles abrasion test on aged and unaged CLA.

CLA from Quarry	Time of exposure (days)	Water Condition	Soil Initial Mass (grams)	Soil Final Mass (grams)	% Mass Loss
A	0	As received	2055.98	1356.24	34.03
A	90	Fresh	-	-	-
A	90	Salt Water	-	-	-
A	150	Fresh	2055.49	1288.34	37.32
A	150	Salt Water	2055.14	1328.23	35.37
B	0	As received	1939.55	1233.02	36.43
B	90	Fresh	1921.42	1213.38	36.85
B	90	Salt Water	1906.53	1143	40.05
B	150	Fresh	1920.3	1188.16	38.13
B	150	Salt Water	1920.18	1140.82	40.59

Note: No tests were done at 90 days for CLA from Quarry A.

As shown in Table 5.7, both CLA materials showed a decrease in resistance to abrasion, impact, and grinding after 150 days of submergence in both fresh and salt water. The Los Angeles test results for the CLA from Quarry A after 150 days of submergence yielded differences in percentages of mass loss 9.66% and 3.93% higher than the values obtained from unaged CLA samples. A similar trend was observed for the aged CLA materials from Quarry B which yielded differences in mass loss percentages that were 4.67% and 11.42% higher than those recorded from unaged samples. From the Los Angeles abrasion test results in Table 5.7 we can see a slight to moderate degradation in abrasion resistance in both CLA materials after a maximum submergence period of 150 days in both fresh and salt water at room temperature.

5.7. Moisture effects on 1-D Compression test results on aged CLA materials.

This section presents the experimental results of 1-D Compression tests carried out on aged and unaged samples of both CLA material types. The test procedure of the 1-D Compression test was presented in Chapter 3. The stress-strain curves obtained for both unaged CLA materials are shown in Figure 5.8. It can be seen that both CLA materials have a very similar response.

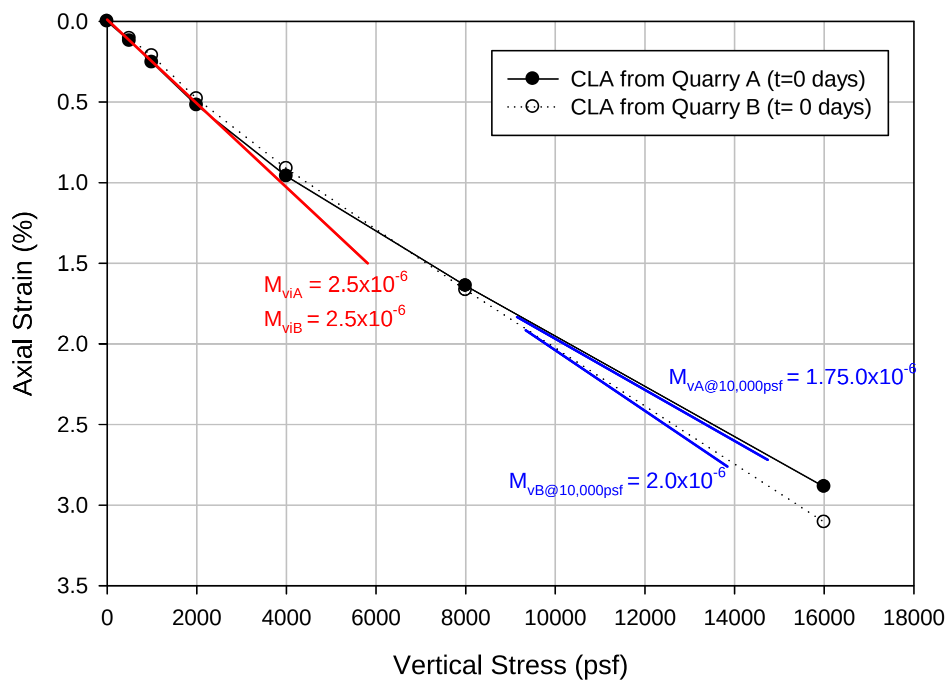

Figure 5.8. Comparisson of 1-D Compression results for unaged CLA materials.

From Figure 5.8 it can be observed that the coefficient of volume compressibility (M_v) of both CLA materials was 2.5x10^{-6} ft^2/lb. The values of m_v for a stress level of 10,000 psf were 2x10^{-6} and 1.8x10^{-6} ft^2/lb for the unaged CLA materials from Quarry A and B, respectively. The stress-strain curves obtained from the 1-D Compression tests on CLA samples submerged 150 days in both fresh and salt water are shown in Figures 5.9 and 5.10 for the CLA materials from quarries A and B, respectively. It can be observed from Figure 5.9 and 5.10 that the CLA from Quarry A submerged in salt water after 150 days experienced higher deformations while the CLA from Quarry B submerged in fresh water after 150 days experienced higher deformations.

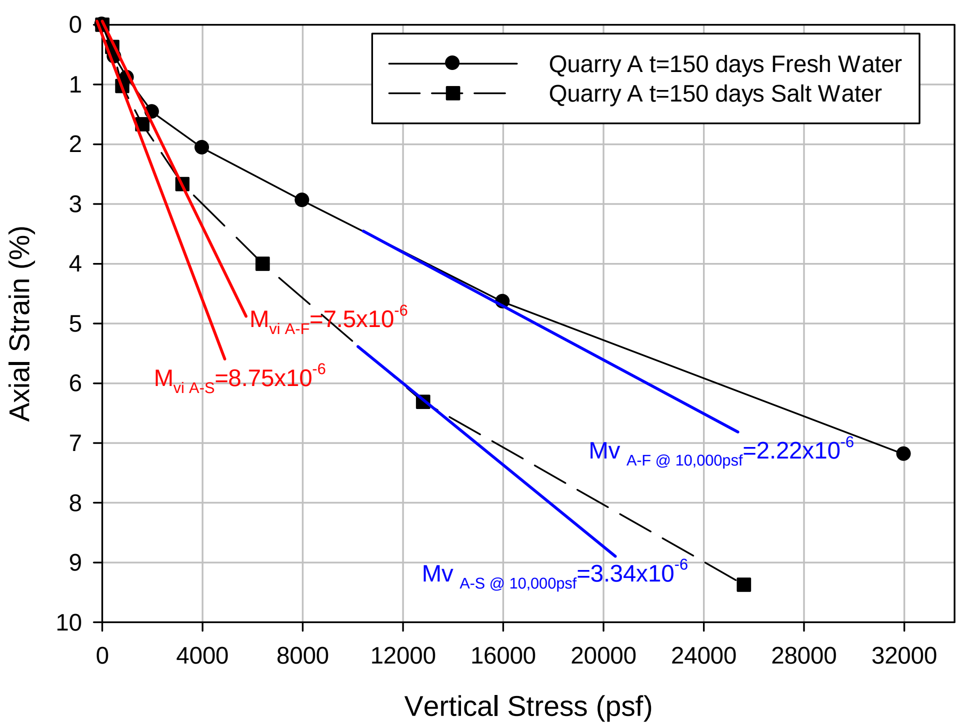

Figure 5.9. Comparisson of 1-D Compression results for CLA of Quarry A aged 150 days.

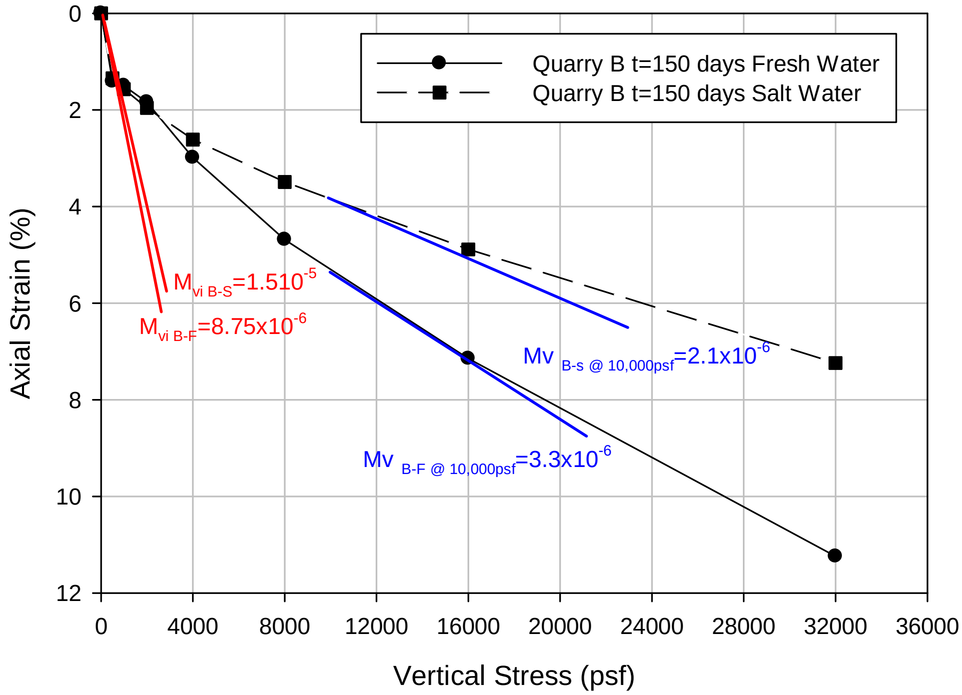

Figure 5.10. Comparisson of 1-D Compression results for CLA of Quarry B aged 150 days.

A summary of the 1-D Compression tests for both CLA materials is shown in Table 5.8. It can be seen from this table that samples were prepared at loose initial states (using procedure describes in Chapter 3). The results indicate that moisture effects, after 150 days of submergence, were considerably in terms of increased compressibility. This can be seen graphically in Figures 5.15 and 5.16 which shows the effects of 150 days of submergence (in both fresh and salt water) on the CLA materials from quarries A and B, respectively. From these figures we can see that both CLA materials have increased 1-D compressibility after 150 days of submergence. However, it is important to point out that unfortunately the initial relative densities of all tests were not uniform. Nevertheless increased compressibility was observed for the tests on aged CLA materials submerged in fresh water for 150 days. These two tests, for both quarries, had higher initial relative densities than the corresponding tests for unaged conditions.

Table 5.8. Summary of results from 1-D Compression Test

CLA from Quarry	Time of exposure(days)	Water Condition	H_f (inches)	e_0	e_f	m_{vi} (in^2/lb) $x10^{-6}$	$m_{v1000psf}$ (in^2/lb) $x10^{-6}$
A	0	As received	0.702	0.960	0.834	2.5	1.75
A	150	Fresh	0.602	0.854	0.488	7.5	2.2
A	150	Salt	0.559	0.958	0.474	8.75	3.4
B	0	As received	0.664	0.955	0.731	2.5	2.0
B	150	Fresh	0.519	0.946	0.346	8.75	3.3
B	150	Salt	0.577	0.981	0.523	0.26	2.1

Note: Initial height of all specimens was 0.75 inches.

CLA material from Quarry B submerged in fresh water for 150 days presented the highest deformation with a change in void ratio of 0.5994 and a change in height of 0.2311. CLA material from Quarry A at zero days exhibited the lowest deformation with a change in void ratio of 0.1251 and a change in height of 0.0479 inches. Figures 5.11 and 5.12 show a comparison for the stress-strain curves from Quarry A and B at time zero and 150 days, respectively. In general, CLA from Quarry B submerged in fresh water after 150 days experience the greatest deformation.

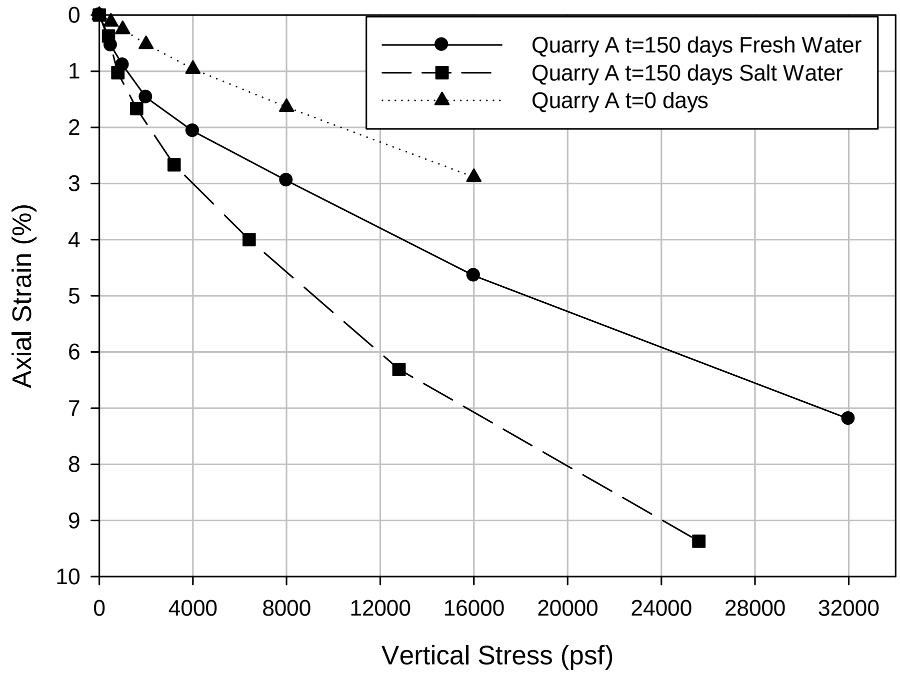

Figure 5.11. Comparisson of 1-D Compression results for CLA of Quarry A as received and after 150 days of submergence in fresh and salt water.

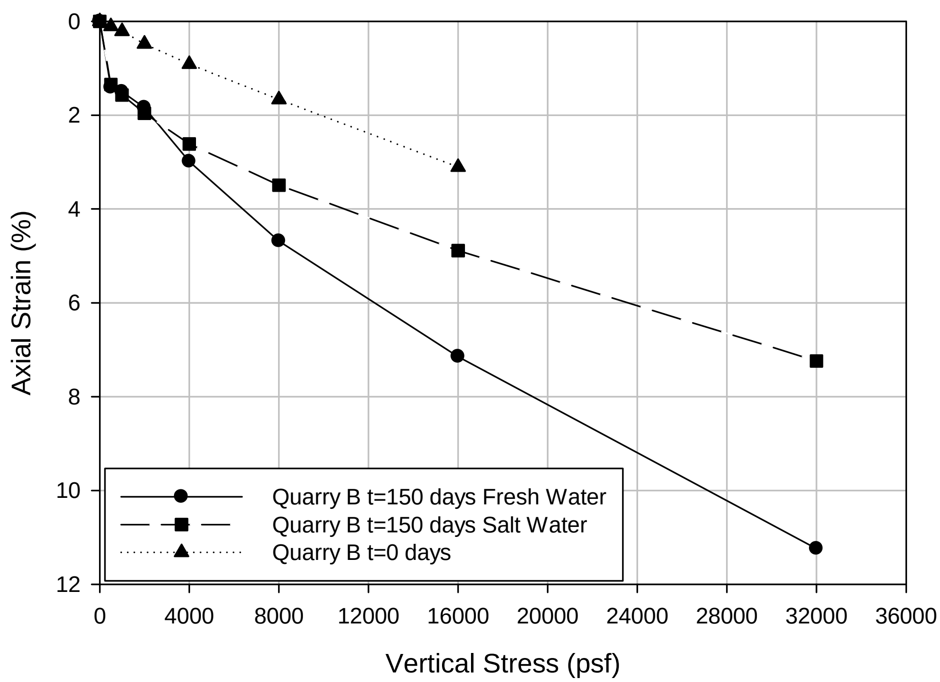

Figure 5.12. Comparisson of 1-D Compression results for CLA of Quarry B as received and after 150 days of submergence in fresh and salt water.

In summary, the moisture effects on the coefficient of volume compressibility obtained from 1-D Compression tests was considerably for both CLA materials after submergence periods of 150 days in both fresh and salt water. The initial coefficient of volume compressibility (M_{vi}) values for the CLA from Quarry A increased 200% and 250% after 150 days of submergence in fresh and salt water, respectively. Similarly, the coefficient of volume compressibility (M_{vi}) values for the CLA from Quarry B increased 250% and 500% after 150 days of submergence in fresh and salt water, respectively. These levels of compressibility increase are not negligible and are considered moderate to high.

5.8. Variation of mechanical properties from triaxial compression tests

For each CLA material type two moisture environments were used to submerge the samples (fresh water and salt water). CLA materials exposed to both moisture environments were tested under triaxial compression conditions after 90 and 150 days of submergence time. The test results are presented in the following subsections and are compared to the results obtained on unaged CLA samples. The procedure of the triaxial compression tests was described in Chapter 3. As indicated in this chapter, the samples were prepared in a dry state, thus no internal pore pressures were developed during application of cell pressure or deviatoric stresses. Therefore the stress-strain curves presented in this section (Figures 5.13 though 5.22) correspond to curves of effective stresses as a function of axial strain for both CLA materials and different aging conditions.

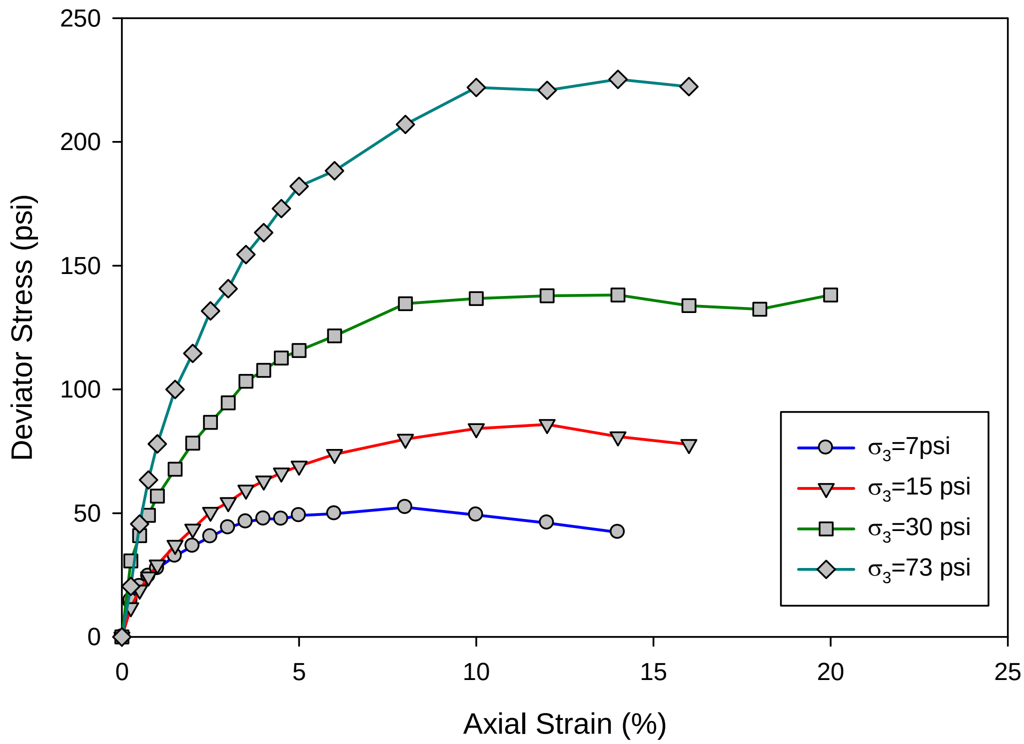

Figure 5.13. Deviator stress versus axial strain for CLA fom Quarry A at zero days.

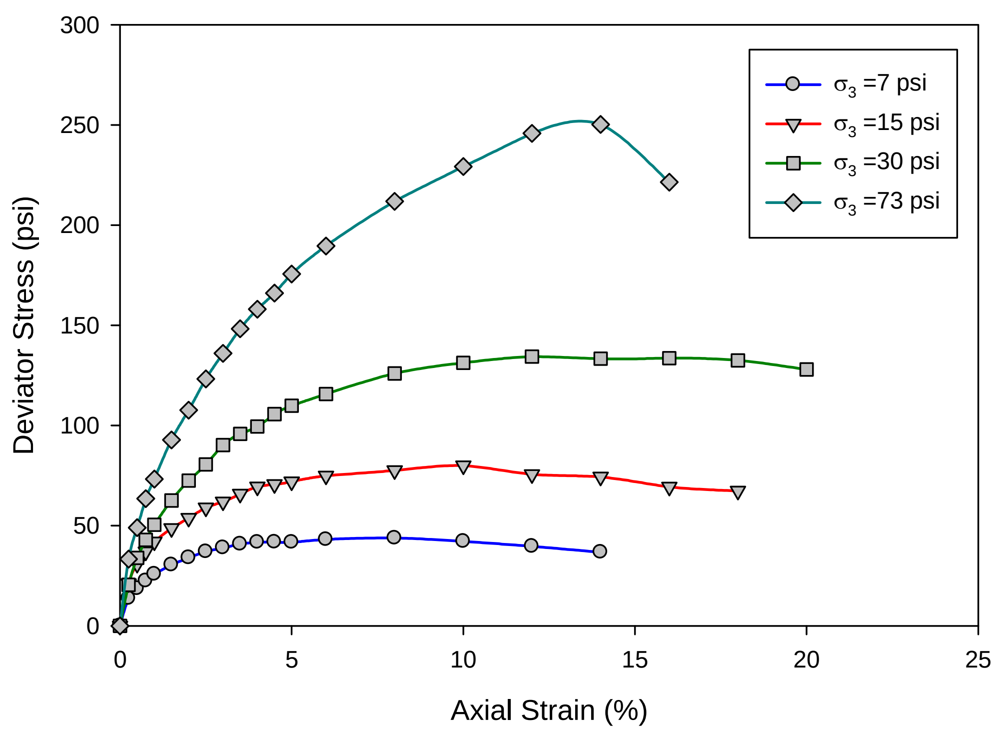

Figure 5.14. Deviator stress versus axial strain for CLA fom Quarry B at zero days.

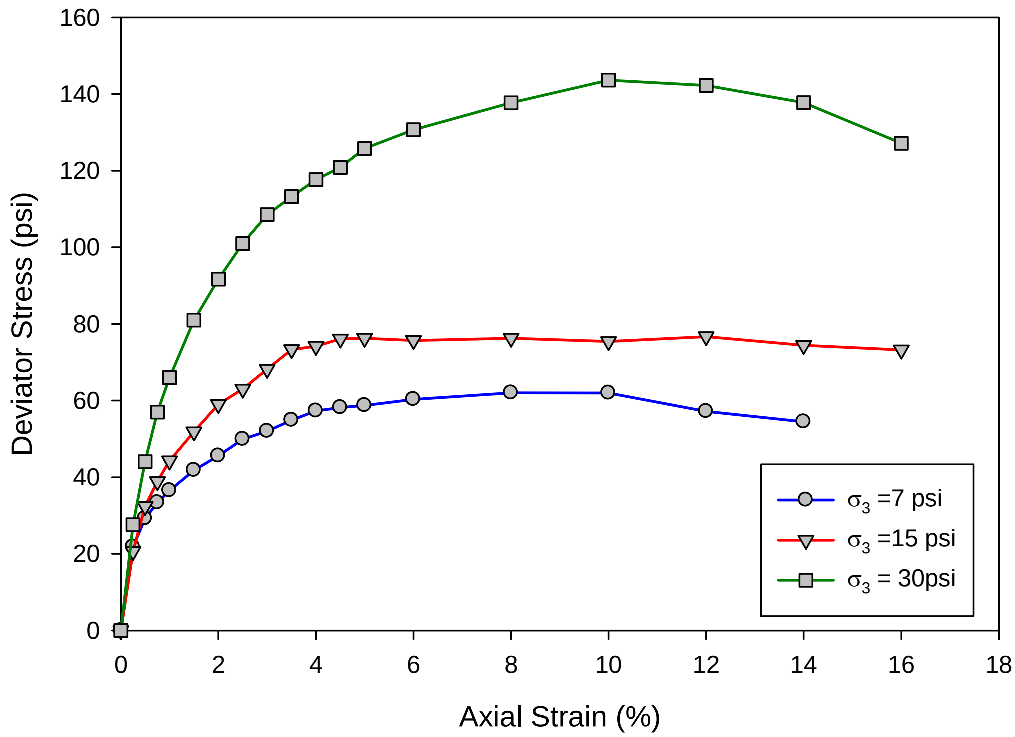

Figure 5.15. Stress versus axial strain for CLA from Quarry A after 90 days submerged in fresh water.

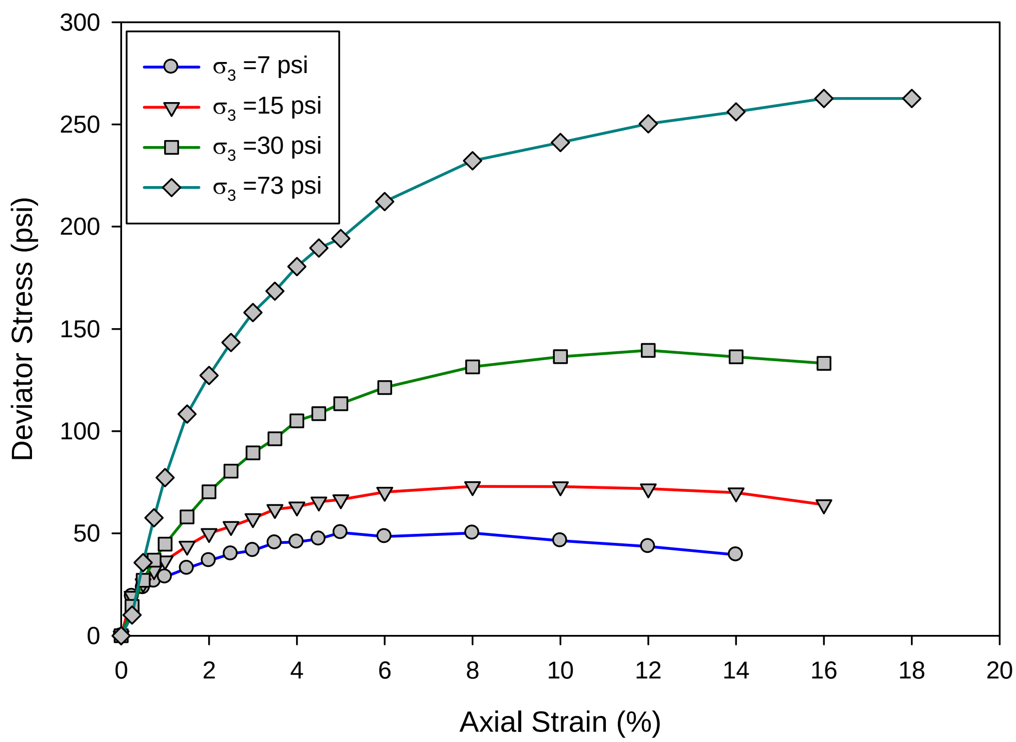

Figure 5.16. Stress versus axial strain for CLA from Quarry A after 90 days submerged in salt water.

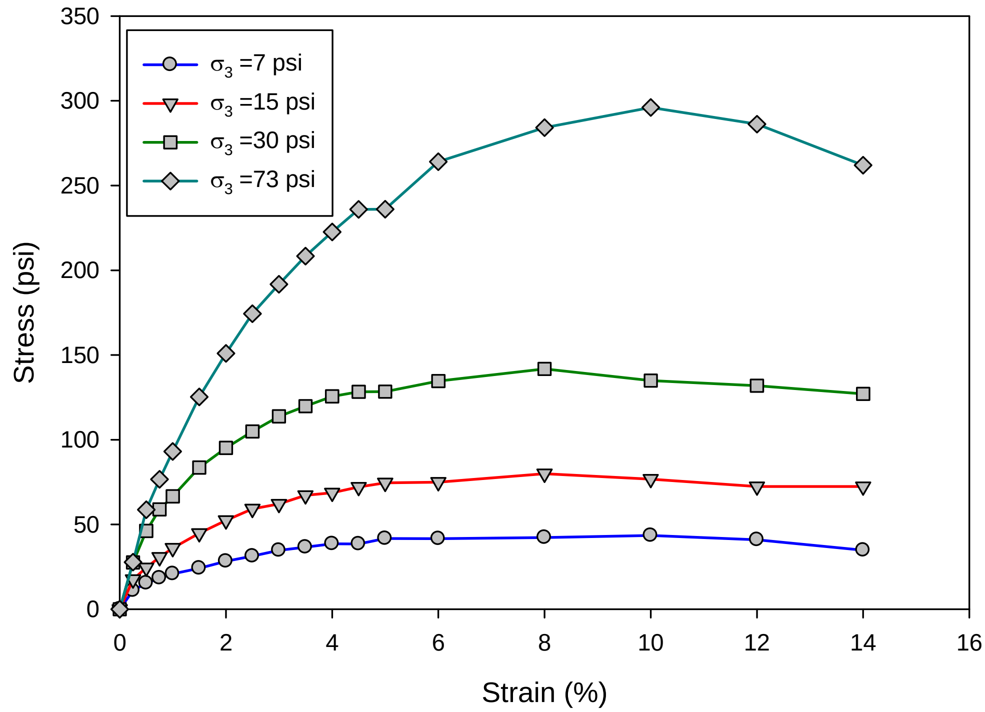

Figure 5.17. Stress versus axial strain for CLA from Quarry B after 90 days submerged in fresh water.

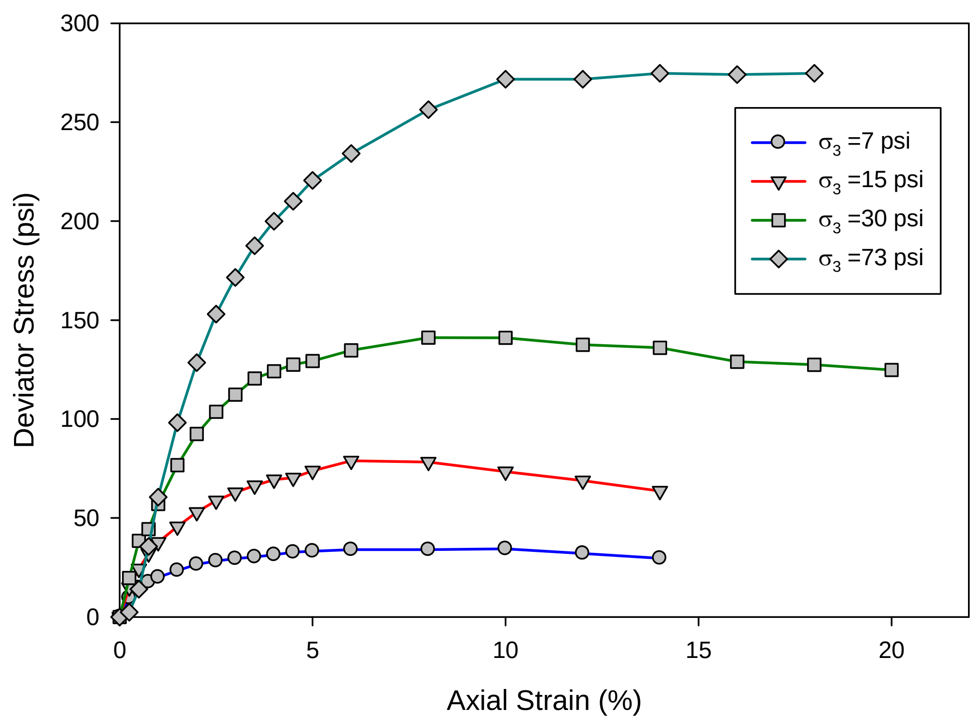

Figure 5.18. Stress versus axial strain for CLA from Quarry B after 90 days submerged in salt water.

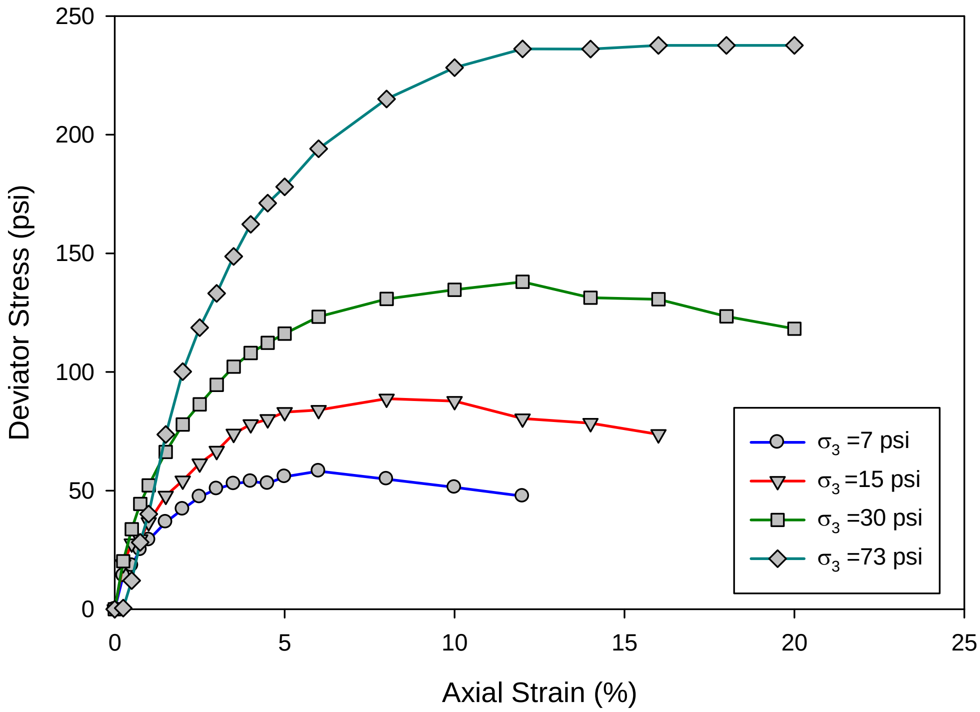

Figure 5.19. Stress versus axial strain for CLA from Quarry A after 150 days submerged in fresh water.

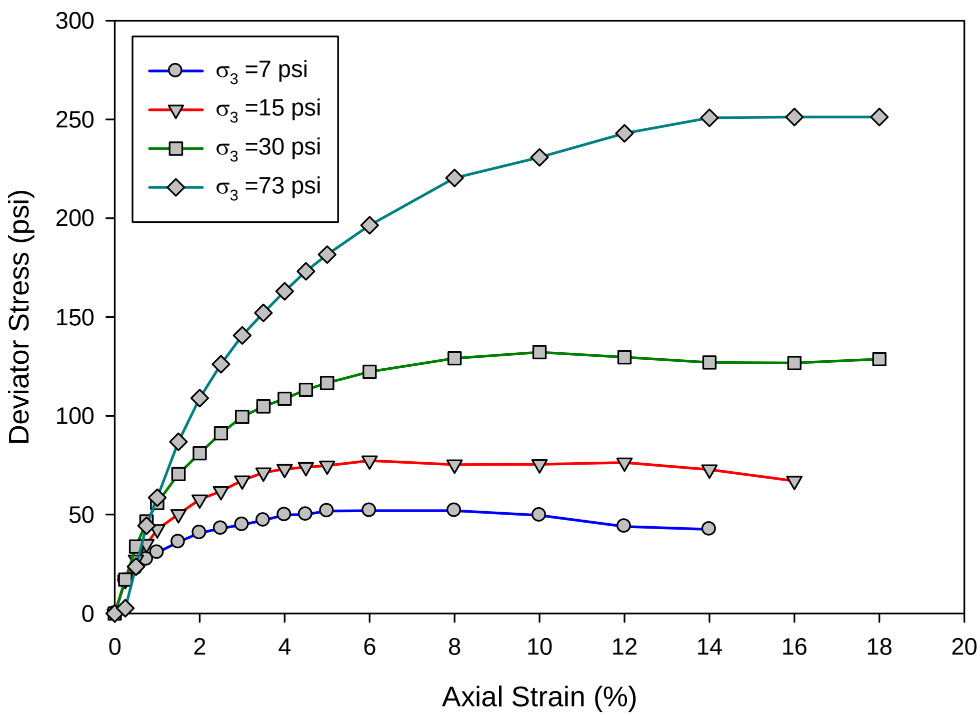

Figure 5.20. Stress versus axial strain for CLA from Quarry A after 150 days submerged in salt water.

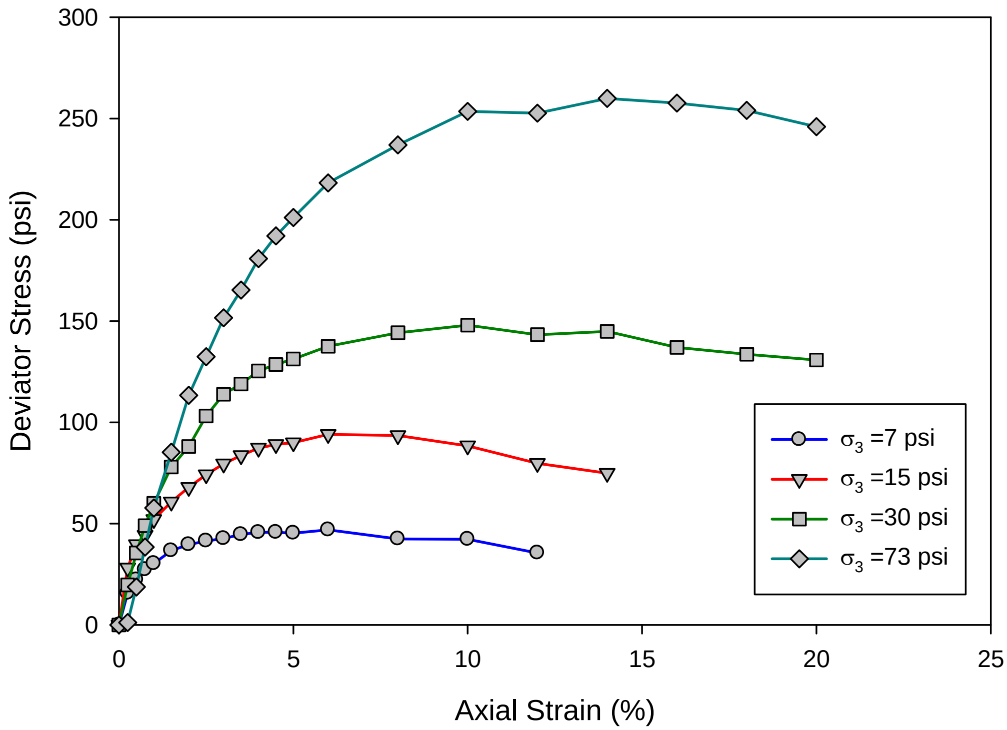

Figure 5.21. Stress versus axial strain for CLA from Quarry B after 150 days submerged in fresh water.

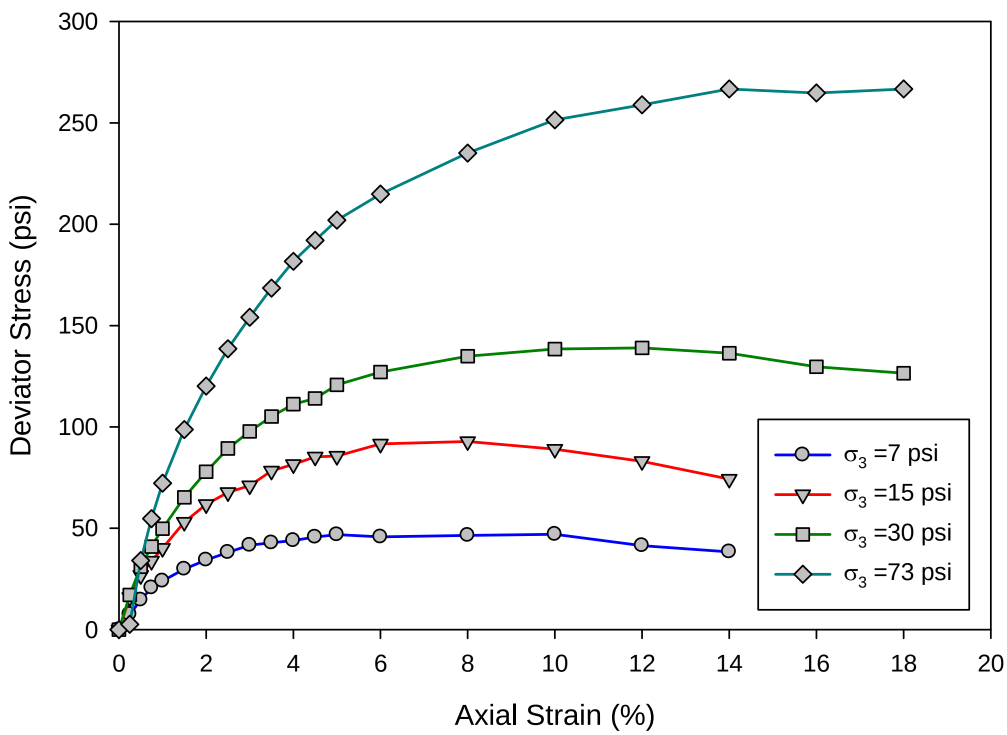

Figure 5.22. Stress versus axial strain for CLA from Quarry B after 150 days submerged in salt water.

The preceding figures showed the stress-strain curves for the two CLA materials after different periods of submergence in both fresh and salt water. The assessment of degradation of mechanical properties was made in terms of shear strength parameters and corresponding envelopes (curved and straight) for peak and 10% axial strain.

Tables 5.9 through 5.12 show a summary of the results of the mechanical properties for both the CLA materials from Quarry A and B. Results correspond to two types of failure criteria: maximum peak shear strength and 10% of the axial strain. As show in these tables, given the size and angularity of the crushed limestone aggregate particles it is not easy to obtain perfectly uniform or constant dry densities.

Table 5.9. Summary of triaxial compression results for CLA from Quarry A using peak strength as failure criterion.

Quarry	Time of exposure (days)	Water Condition	σ_c (psi)	γ_{dry} lb/ft^3	Initial Void Ratio	ε_{axial} @ peak (%)	Φ_{sec} (°)	Φ'_0 (°)	$\Delta\Phi$(°)	Dr (%)
A	0	-	7	97.7	0.75	8	51.53	47.90	14.00	25.6
			15	101	0.69	12	48.37			37.6
			30	98	0.75	20	44.77			25.6
			73	98.6	0.73	14	37.47			29.6
A	90	Fresh	7	96	0.78	8	54.15	48.61	13.88	19.6
			15	96.9	0.764	20	46.52			22.8
			30	96.5	0.77	10	45.43			21.6
			73	-	-	-	-			-
A	90	Salt	7	100.6	0.7	5	50.97	47.14	10.11	35.6
			15	97.6	0.75	8	45.7			25.6
			30	95.2	0.79	12	44.93			17.6
			73	96.9	0.76	16	40.11			23.6
A	150	Fresh	7	98	0.75	6	53.19	48.79	14.74	25.6
			15	94.1	0.82	8	48.9			11.6
			30	95.7	0.79	12	44.75			17.6
			73	93	0.839	18	38.39			7.8
A	150	Salt	7	94.1	0.817	6	51.44	47.36	11.76	12.2
			15	95.2	0.8	6	46.67			15.6
			30	94.8	0.8	10	44.04			15.6
			73	93.8	0.82	20	39.35			11.6

Table 5.10. Summary of triaxial compression results for CLA from Quarry B using peak strength as failure criterion.

Quarry	Time of exposure (days)	Water Condition	σ_c (psi)	γ_{dry} lb/ft^3	Initial Void Ratio	ε_{axial} @ peak (%)	Φ_{sec} (°)	Φ'_0 (°)	$\Delta\Phi$(°)	Dr (%)
B	0	-	7	96.3	0.78	8	48.7	46.48	9.55	27.9
			15	98.9	0.73	10	47.2			38.0
			30	98.3	0.74	12	44.3			36.0
			73	97.9	0.75	14	39.28			33.9
B	90	Fresh	7	91.7	0.86	10	48.58	46.89	6.49	11.7
			15	93.8	0.82	8	47.21			19.8
			30	94.1	0.82	8	45.21			19.8
			73	93.3	0.83	10	42.16			17.8
B	90	Salt	7	95.3	0.79	10	44.71	45.15	4.3	25.9
			15	95.6	0.79	6	46.99			25.9
			30	92.3	0.85	8	45.13			13.7
			73	92.3	0.853	18	40.88			13.1
B	150	Fresh	7	95.1	0.8	6	49.82	48.13	10.37	23.8
			15	94.2	0.81	6	49.85			21.8
			30	95.1	0.8	10	45.92			23.8
			73	94.3	0.81	14	39.93			21.8
B	150	Salt	7	95.7	0.79	10	49.84	47.89	10.13	25.9
			15	96.5	0.77	8	49.62			29.9
			30	96.4	0.78	12	44.87			27.9
			73	95.4	0.79	18	40.38			25.9

Table 5.11. Summary of triaxial compression results for CLA from Quarry A for ε_{axial}=10%.

Quarry	Time of exposure (days)	Water Condition	σ_c (psi)	γ_{dry} (lb/ft^3)	Initial Void Ratio	Φ_{sec} (°)	Φ'_0 (°)	$\Delta\Phi$(°)	Dr (%)
A	0	-	7	97.7	0.75	50.58	47.37	13.37	25.6
			15	101	0.69	48.05			37.6
			30	98	0.75	44.59			25.6
			73	98.6	0.73	37.22			29.6
A	90	Fresh	7	96	0.78	54.13	48.51	14.46	19.6
			15	92	0.85	46.24			5.6
			30	96.5	0.77	45.43			21.6
			73	-	-	-			
A	90	Sea	7	103.4	0.65	49.62	46.39	10.41	45.6
			15	97.6	0.75	45.68			25.6
			30	95.2	0.79	44.57			17.6
			73	96.9	0.76	38.65			23.6
A	150	Fresh	7	98	0.75	51.24	47.82	13.75	25.6
			15	94.1	0.82	48.72			11.6
			30	95.7	0.79	44.34			17.6
			73	93	0.84	37.7			7.6
A	150	Sea	7	92.7	0.85	50.72	46.82	12.40	5.6
			15	95.2	0.8	46.25			15.6
			30	94.8	0.8	44.04			15.6
			73	93.8	0.82	37.89			11.6

Table 5.12. Summary of triaxial compression results for CLA from Quarry B for ε_{axial}=10%.

Quarry	Time of exposure (days)	Water Condition	σ_c (psi)	γ_{dry} (lb/ft^3)	Initial Void Ratio	Φ_{sec} (°)	Φ'_0 (°)	$\Delta\Phi$(°)	Dr (%)
B	0	-	7	96.3	0.78	48.07	46.02	10.54	27.88
			15	98.9	0.73	47.2			37.98
			30	98.3	0.74	43.91			35.96
			73	97.9	0.75	37.77			33.94
B	90	Fresh	7	91.7	0.86	48.58	46.5	6.47	11.72
			15	93.8	0.82	46.54			19.80
			30	94.1	0.82	44.36			19.80
			73	93.3	0.83	42.16			17.78
B	90	Sea	7	95.3	0.79	50.58	47.68	10.04	25.86
			15	95.6	0.79	48.05			25.86
			30	92.3	0.85	44.59			13.74
			73	91.3	0.87	40.69			9.70
B	150	Fresh	7	95.1	0.8	48.13	47.13	9.02	23.84
			15	94.2	0.81	48.86			21.82
			30	95.1	0.8	45.92			23.84
			73	94.3	0.81	39.5			21.82
B	150	Sea	7	95.7	0.79	49.84	47.58	10.91	25.86
			15	96.5	0.77	48.96			29.90
			30	96.4	0.78	44.8			27.88
			73	95.4	0.79	39.36			25.86

5.8.1. *Moisture effects on shear strength, circles at failure, K_f lines, and failure envelopes for CLA from Quarry A*

The CLA material showed a non-linear shear strength failure envelope. Therefore the secant friction angle approach, as described by Duncan and Wright (2005), was used as follows:

$$\phi_{sec} = \phi_0 - (\Delta\phi * Log(\sigma_3 / P_a)) \quad \ldots\ldots\ldots\ldots\ldots\ldots\ldots\ldots\ldots\ldots\ldots\ldots\ldots\ldots\ldots\ [5.3]$$

Where: σ_3 = confining pressure,
Pa = atmospheric pressure,
Φ_o = the value of Φ' for σ_3'=1atm, and
ΔΦ=the reduction in Φ' for a 10-fold increase in confining pressure.

The curved shear strength envelopes for the CLA from Quarry A submerged in fresh water 0, 90, and 150 days are shown in Figures 5.23 through 5.27, respectively. The corresponding values of Φ_o and ΔΦ computed for each case are shown in the different figures. These graphs correspond to the peak shear strength failure criterion.

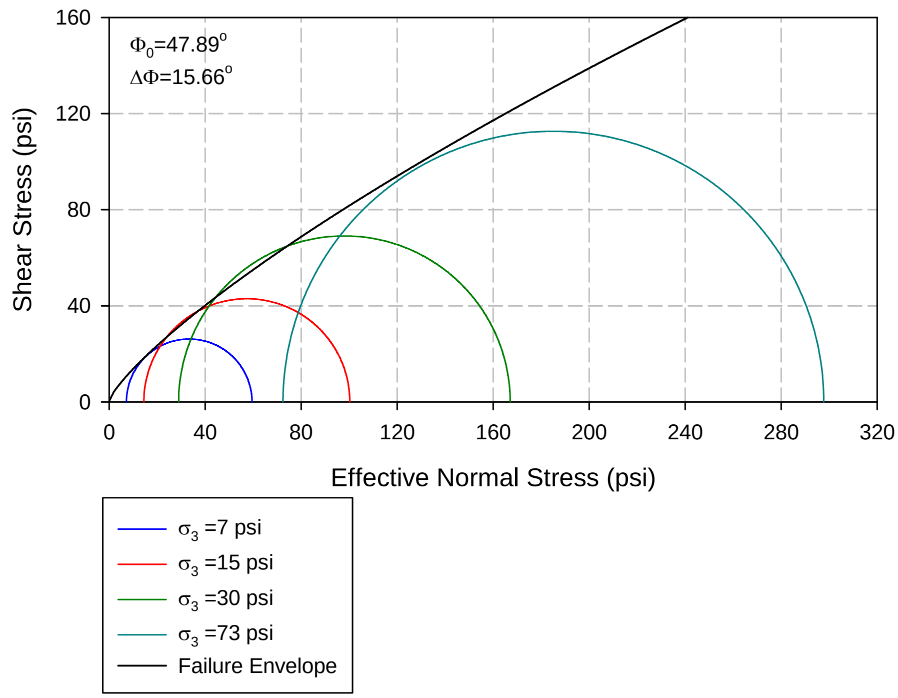

Figure 5.23. Mohr circles at peak and corresponding failure envelope for CLA from Quarry A at zero days.

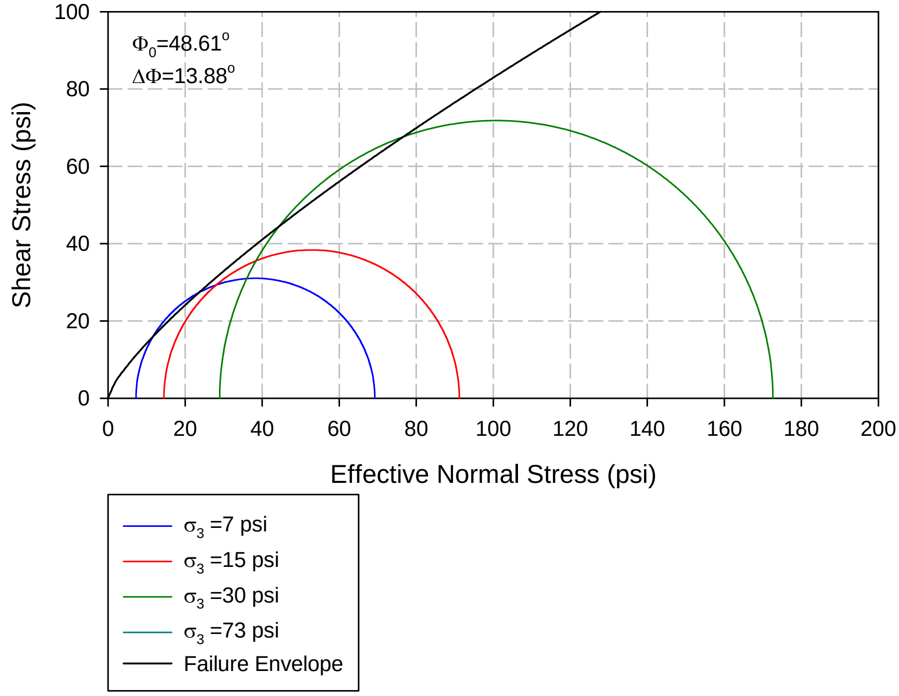

Figure 5.24. Mohr circles at peak and corresponding failure envelope for CLA from Quarry A after 90 days of submergence in fresh water.

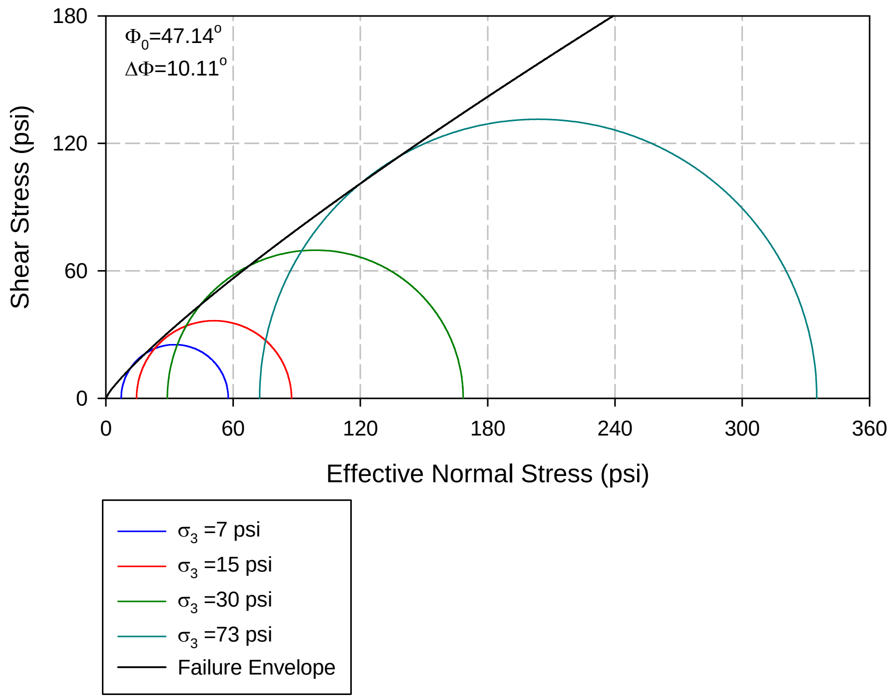

Figure 5.25. Mohr circles at peak and corresponding failure envelope for CLA from Quarry A after 90 days of submergence in salt water.

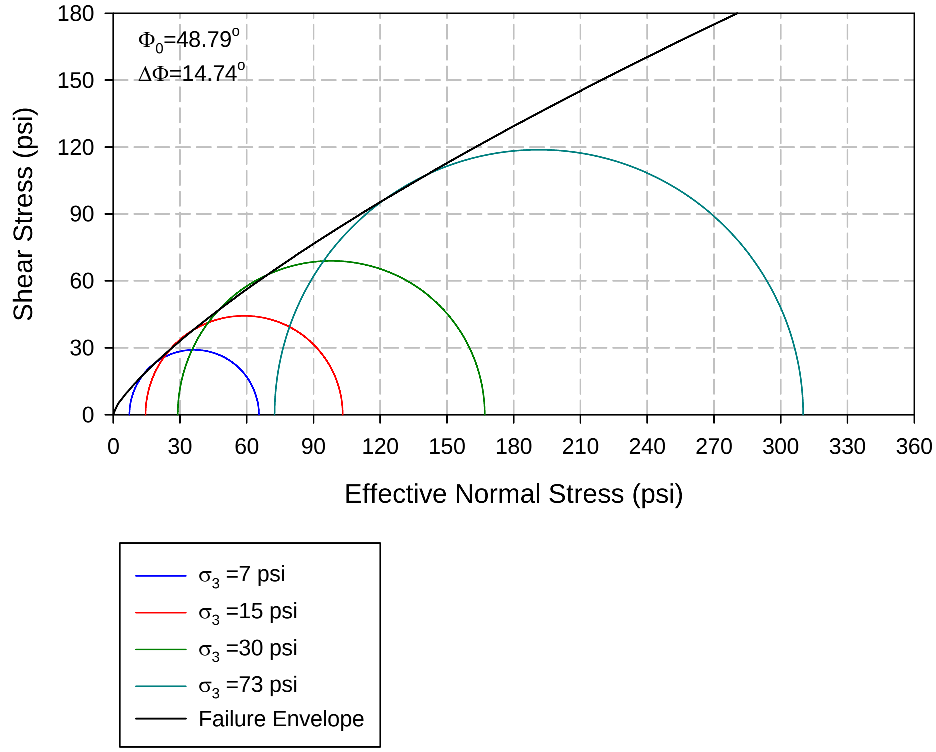

Figure 5.26. Mohr circles at peak and corresponding failure envelope for CLA from Quarry A after 150 days of submergence in fresh water.

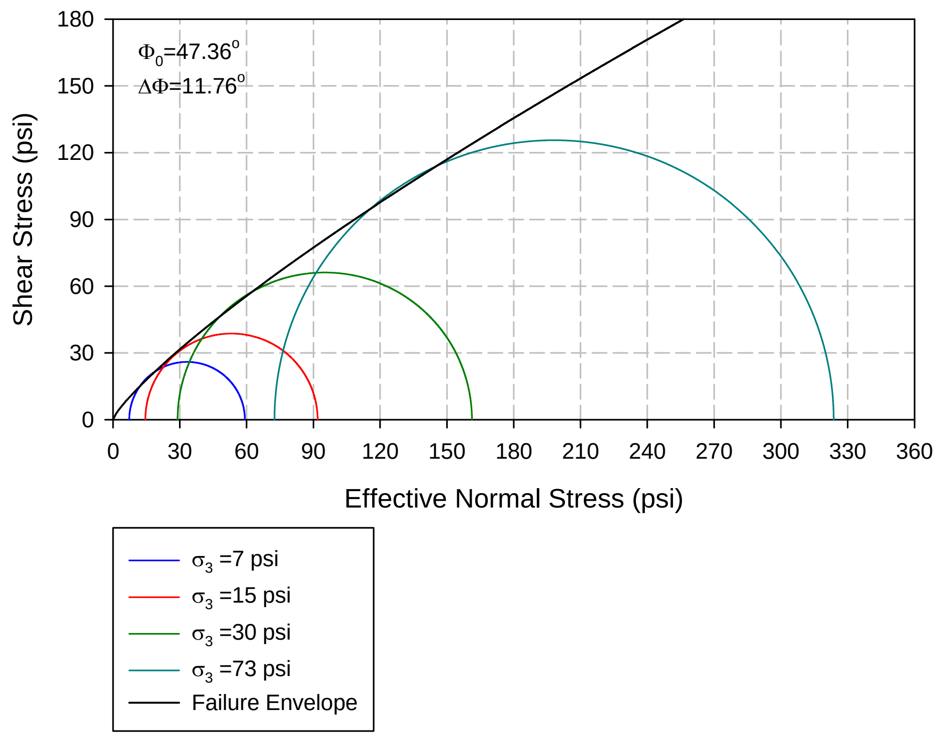

Figure 5.27. Mohr circles at peak and corresponding failure envelope for CLA from Quarry A after 150 days of submergence in salt water.

The curved shear strength envelopes for the CLA from Quarry A submerged in fresh water 0, 90, and 150 days are shown in Figures 5.28 through 5.32, respectively. The corresponding values of Φ_o and $\Delta\Phi$ computed for each case are shown in the different figures. These graphs correspond to the 10% axial strain failure criterion.

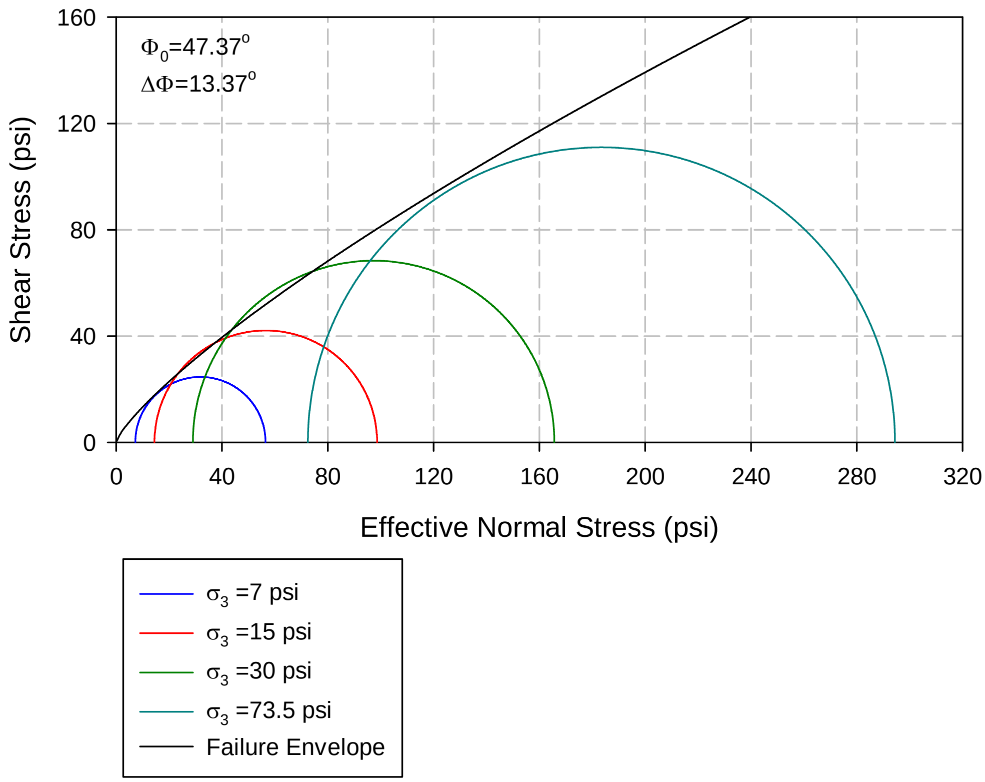

Figure 5.28. Mohr circles at ε_{axial}=10% and corresponding failure envelope for CLA from Quarry A at zero days.

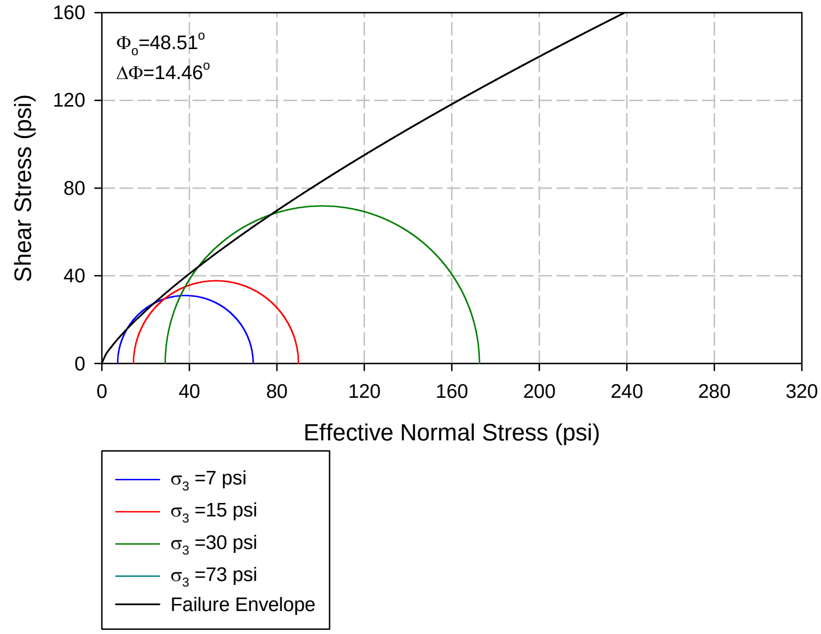

Figure 5.29. Mohr circles at ε_{axial}=10% and corresponding failure envelope for CLA from Quarry A after 90 days of submergence in fresh water.

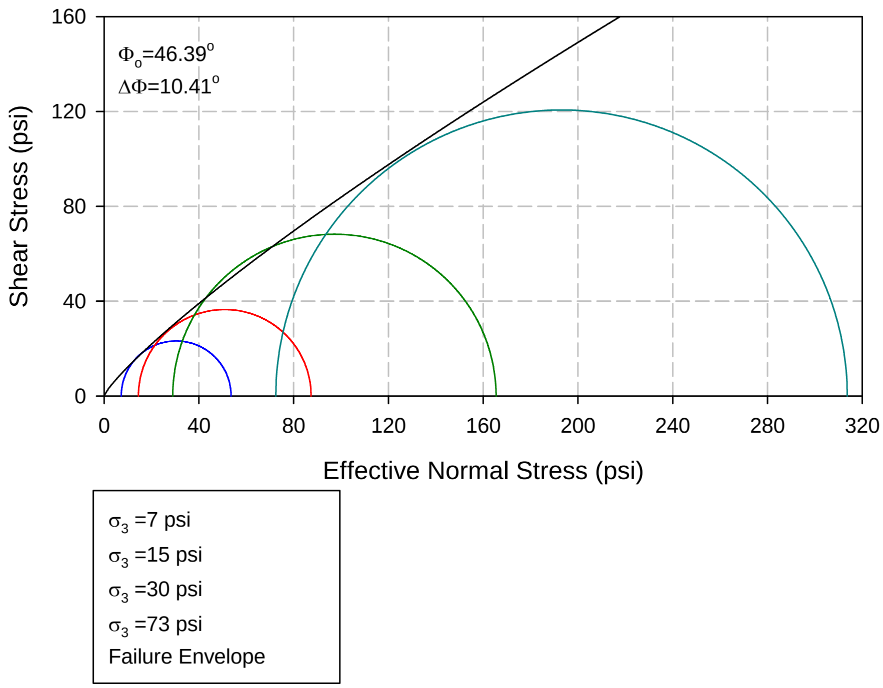

Figure 5.30. Mohr circles at ε_{axial}=10% and corresponding failure envelope for CLA from Quarry A after 90 days of submergence in salt water.

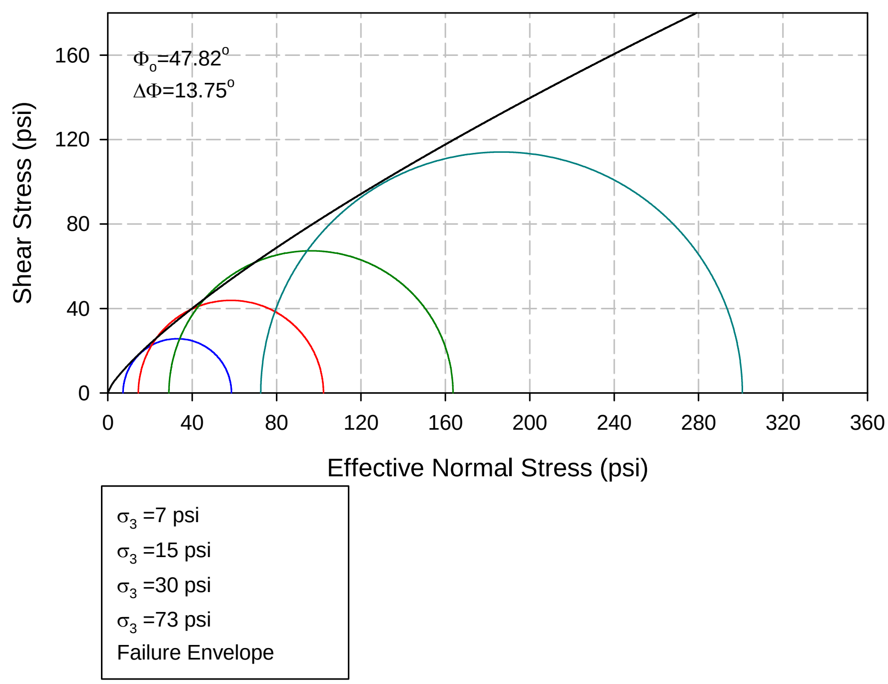

Figure 5.31. Mohr circles at ε_{axial}=10% and corresponding failure envelope for CLA from Quarry A after 150 days of submergence in fresh water.

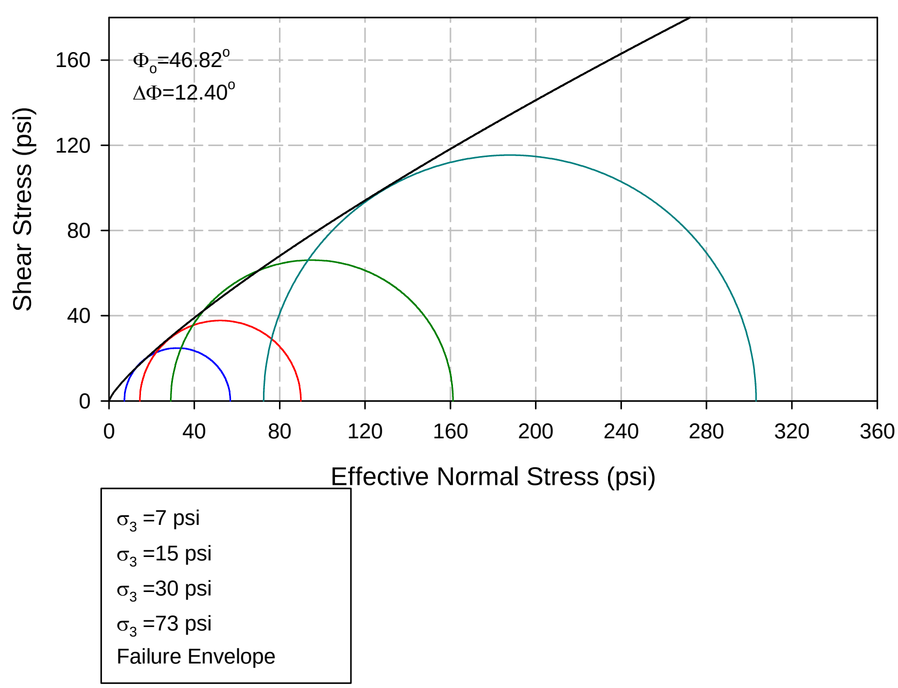

Figure 5.32. Mohr circles at ε_{axial}=10% and corresponding failure envelope for CLA from Quarry A after 150 days of submergence in salt water.

The variation of secant friction angle as a function of the confining pressure level used in the triaxial compression tests are shown in Figures 5.33 and 5.34 for fresh and salt water respectively. These figures correspond to peak shear strength failure.

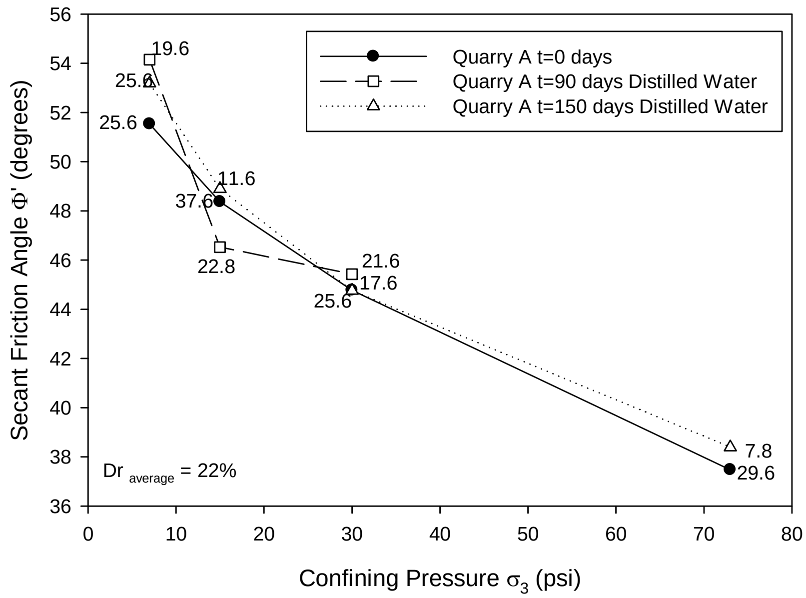

Figure 5.33. Variation of the secant friction angles as a function of the confining pressure for CLA from Quarry A submerged in fresh water at zero, 90, and 150 days (peak strength criterion).

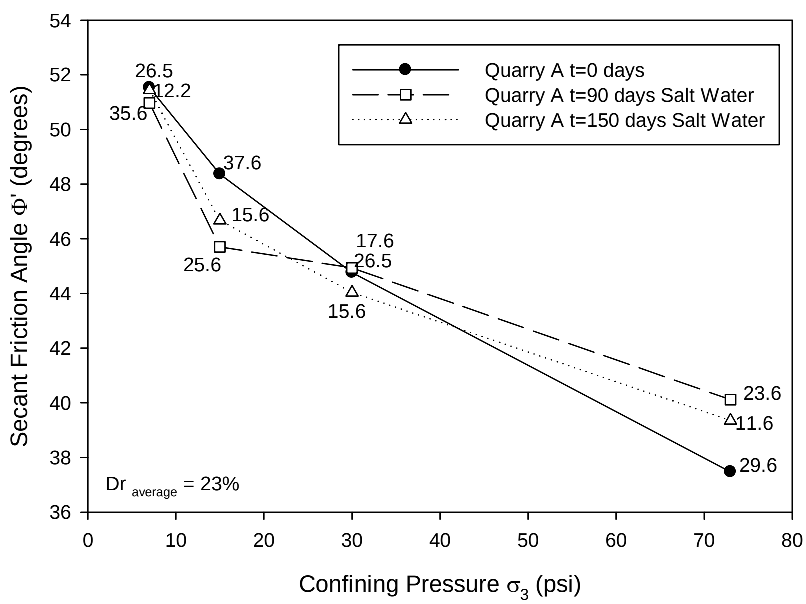

Figure 5.34. Variation of the secant friction angles as a function of the confining pressure for CLA from Quarry A submerged in salt water at zero, 90, and 150 days (peak strength values).

The CLA materials submerged in fresh water exhibited the expected behavior, in terms of decreasing secant friction angles as the confining pressure increased. However, no noticeable degradation of secant friction angles was observed. Figure 5.34 shows very similar secant friction angles curves for zero and 150 days. It should be pointed out that at confining pressure values of 73 the membrane always broke around 12% of the axial strain. For 90 days submergence in fresh water this test could not be completed.

Figures 5.35 and 5.36 show the variation of secant friction angle for fresh and salt water respectively, corresponding to the 10% of axial strain failure criterion. It can be observed from Figure 5.35 that secant friction angles at time zero and 150 days are very similar. The curves show some differences in the secant friction angles as a function of submergence time at low confining pressure levels. However, there was no consistent trend observed. The difference of secant friction angle values can be explained from differences in the initial relative density of the different tests.

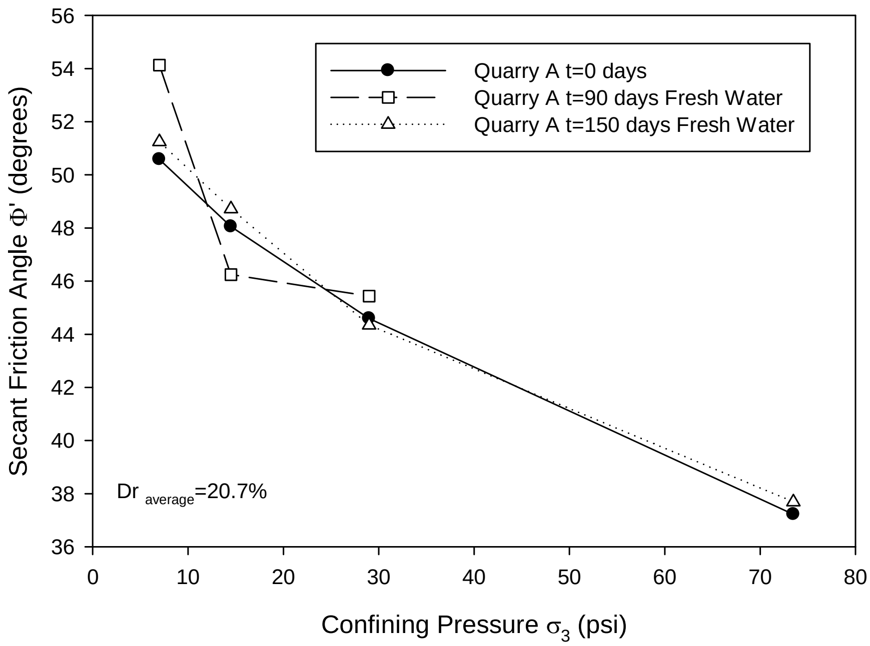

Figure 5.35. Variation of the secant friction angles as a function of the confining pressure for CLA from Quarry A submerged in fresh water at zero, 90, and 150 days (ε_{axial}=10%).

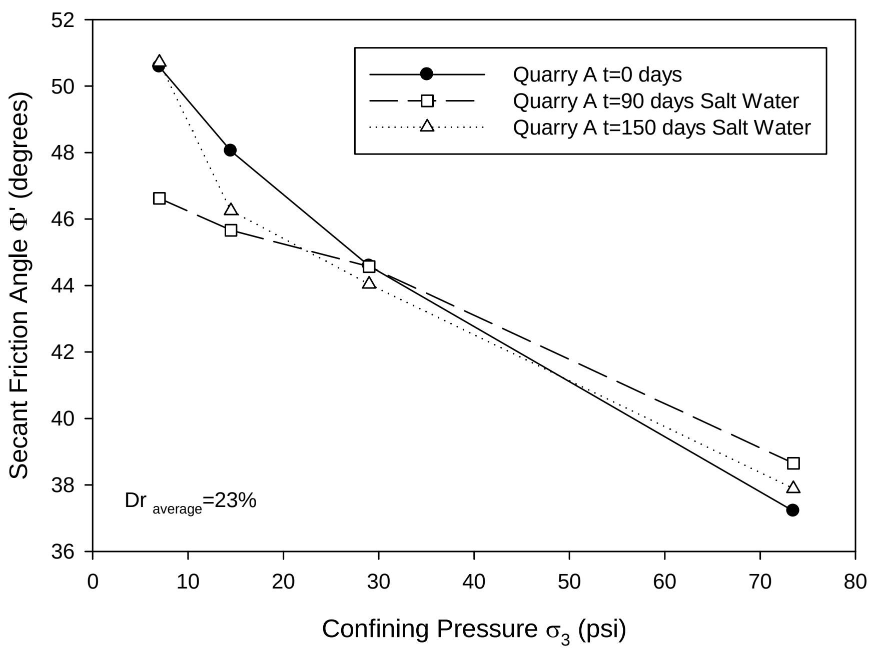

Figure 5.36. Variation of the secant friction angles as a function of the confining pressure for CLA from Quarry A submerged in salt water at zero, 90, and 150 days (ε_{axial}=10%).

Figure 5.37 and 5.38 shows the curved shear strength envelopes for CLA materials from Quarry A submerged in fresh and salt water, respectively. The envelopes for the CLA materials from Quarry A submerged in fresh water were very similar, hence no variation in the shear strength envelope was observed. The envelopes for CLA materials from Quarry A submerged in salt water showed some differences, particularly for normal stresses above 100 psi. However, the variation observed did not follow the expected degradation trend. These two figures show failure envelopes corresponding to peak shear strength.

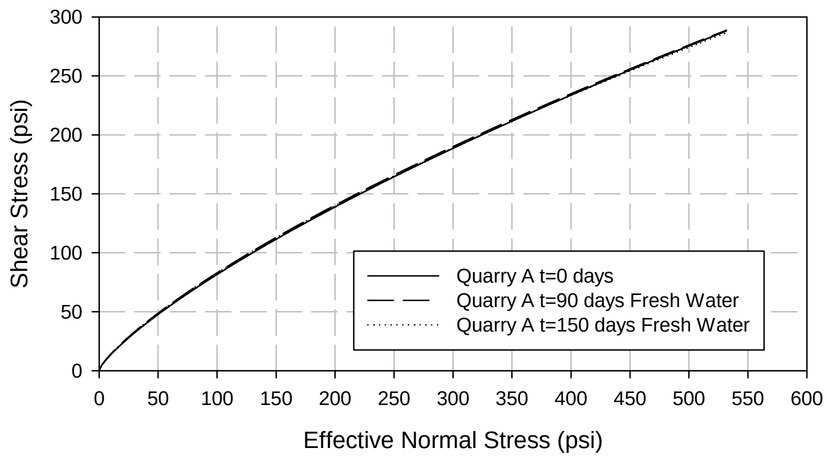

Figure 5.37. Comparisson of curved failure envelopes for CLA material from Quarry A submerged in fresh water (peak shear criterion).

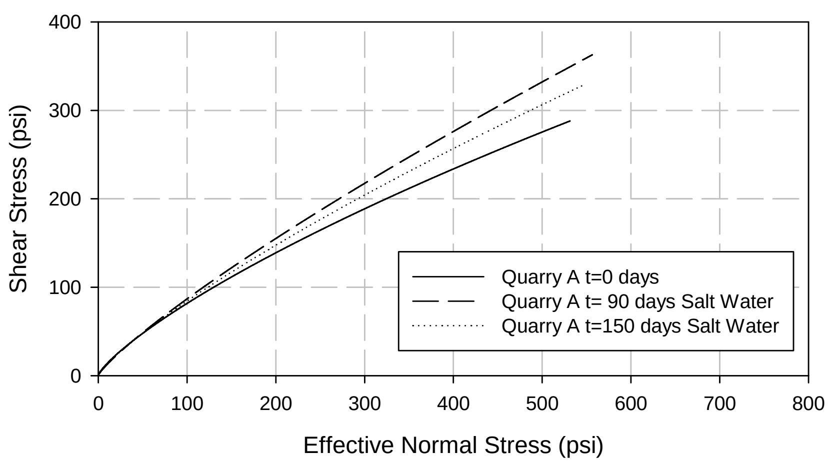

Figure 5.38. Comparisson of curved failure envelopes for CLA material from Quarry A submerged in salt water (peak shear criterion).

The K_f line is an equivalent line to the curved shear strength failure envelopes presented previously. However these K_f lines are linear and they are obtained from the stress path curves that have coordinates *p'* and *q*, defined as follow:

p'=center coordinates of the shear strength circle = $(\sigma'_{1f} + \sigma'_{3f})/2$

q=ratio coordinates of the shear strength circle == $(\sigma'_{1f} - \sigma'_{3f})/2$

Figures 5.39 and 5.40 present the ratio coordinates as a function of the center coordinates of the shear strength circle for the CLA materials from Quarry A after 0, 90, and 150 days of submergence in fresh and salt water, respectively.

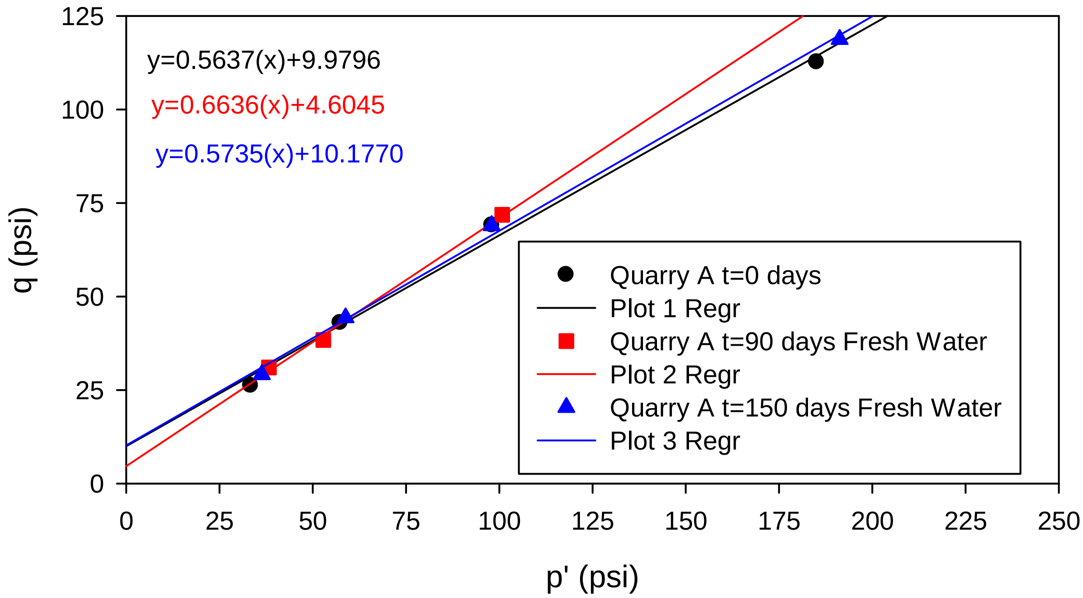

Figure 5.39. Ratio coordinates (q) versus center coordinates (p') comparison for CLA from Quarry A submerged in fresh water after 0,90, and 150 days.

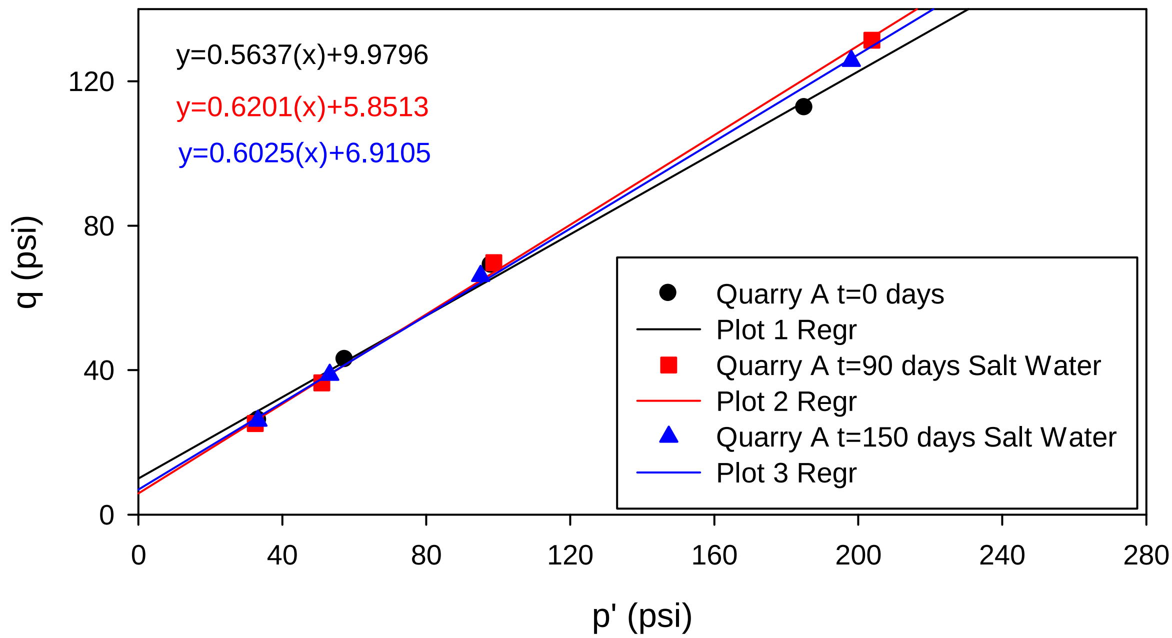

Figure 5.40. Ratio coordinates (q) versus center coordinates (p') comparison for CLA from Quarry A submerged in salt water after 0,90, and 150 days.

As shown in Figure 5.40, CLA materials at time zero and after 150 days of submergence in salt water exhibited very similar values, hence no variation in the shear strength was observed. The K_f lines for CLA materials from Quarry A submerged in fresh water showed some differences, particularly for normal stresses above 100 psi. However, the variation observed did not follow the expected degradation trend. These two figures show failure envelopes corresponding to peak shear strength.

5.8.2. Moisture effects on shear strength, circles at failure, K_f lines, and failure envelopes for CLA from Quarry B

The triaxial tests results for the CLA material from Quarry B was summarized in Tables 5.10 and 5.12, for failure criteria corresponding to peak strength and ε_{axial}=10%, respectively. The curved shear strength envelopes (for peak strength) for the CLA from Quarry B submerged in fresh water 0, 90, and 150 days are shown in Figures 5.41 through 5.45, respectively. The corresponding values of Φ_o and $\Delta\Phi$ computed for each case are shown in the different figures.

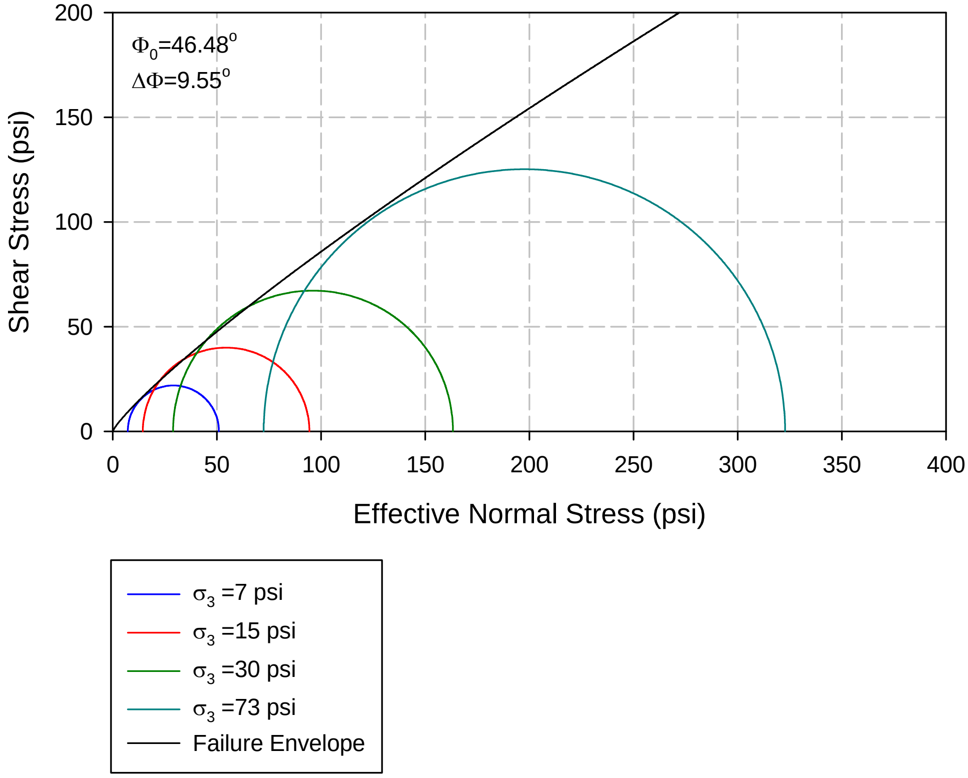

Figure 5.41 Mohr circles at ε_{axial}=10% and corresponding failure envelope for CLA from Quarry B at zero days.

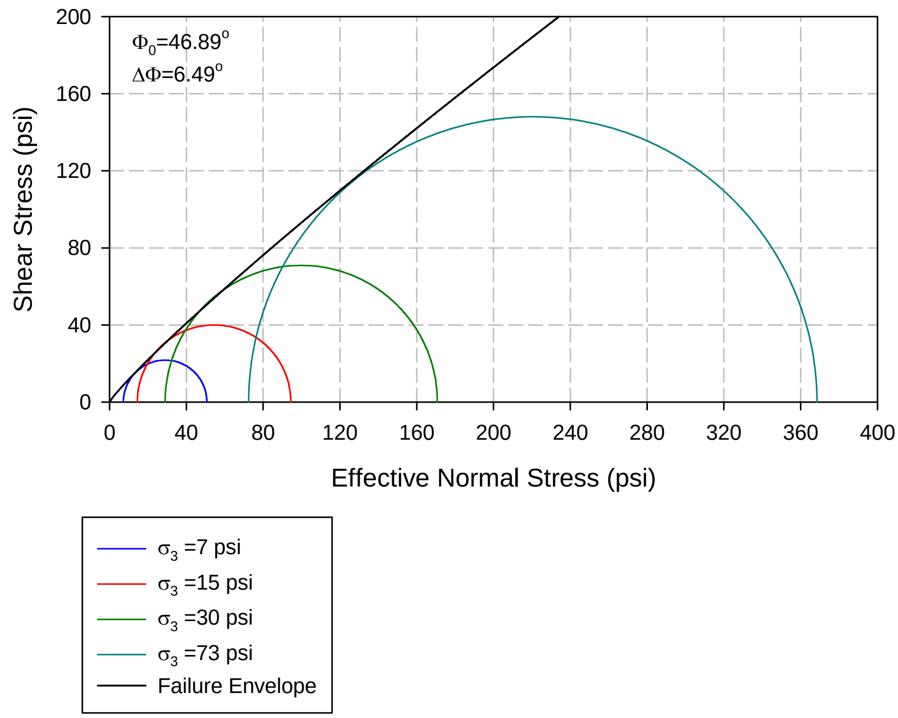

Figure 5.42. Mohr circles at peak and corresponding and failure envelope for CLA from Quarry B after 90 days submerged in fresh water (peak strength criterion).

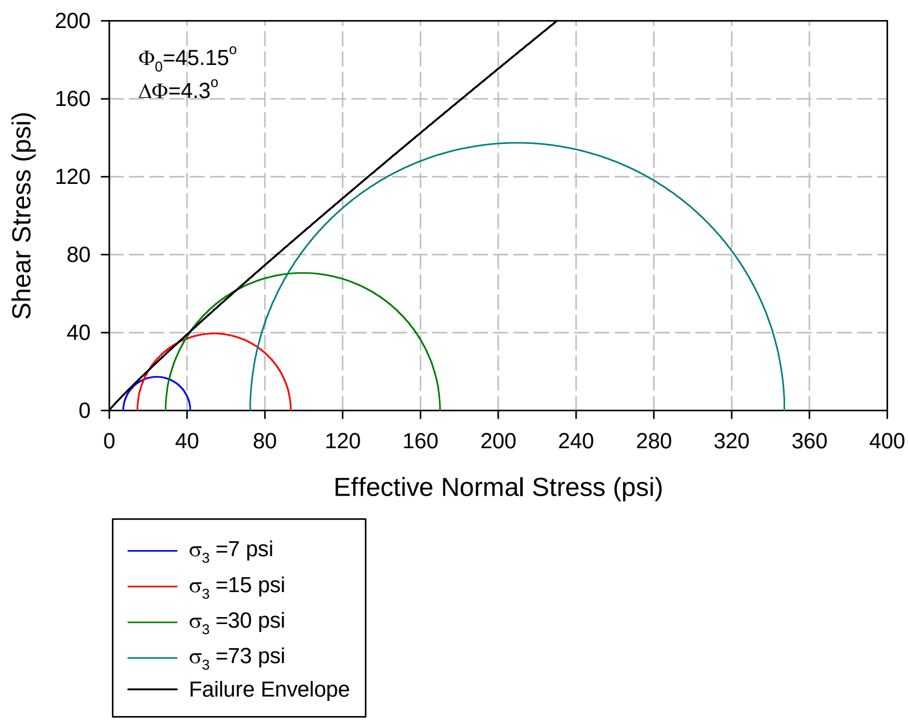

Figure 5.43. Mohr circles at peak and corresponding and failure envelope for CLA from Quarry B after 90 days submerged in salt water (peak strength criterion).

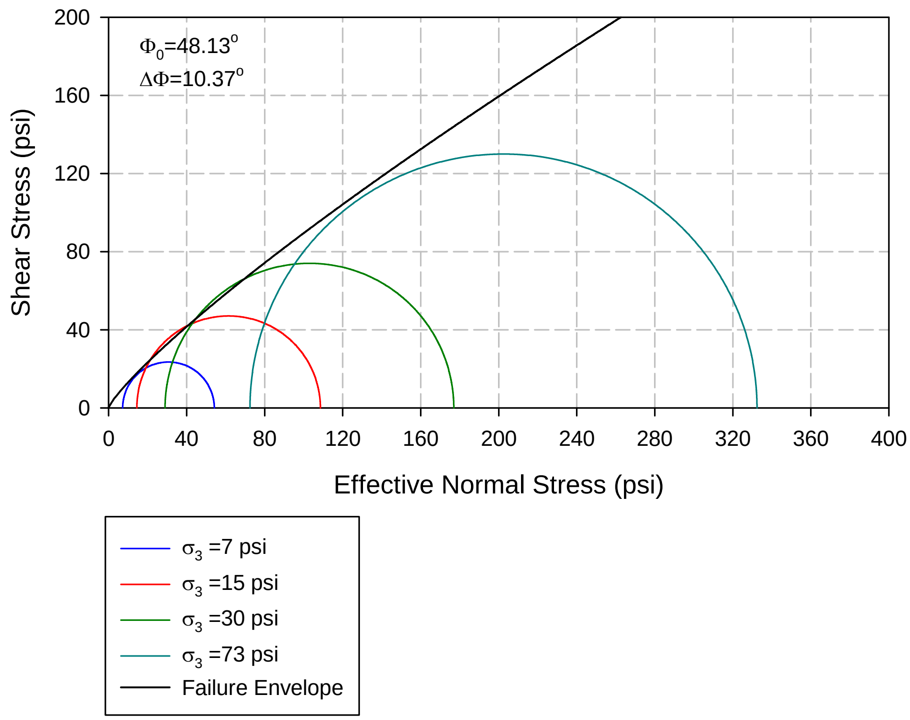

Figure 5.44. Mohr circles at peak and corresponding and failure envelope for CLA from Quarry B after 150 days submerged in fresh water (peak strength criterion).

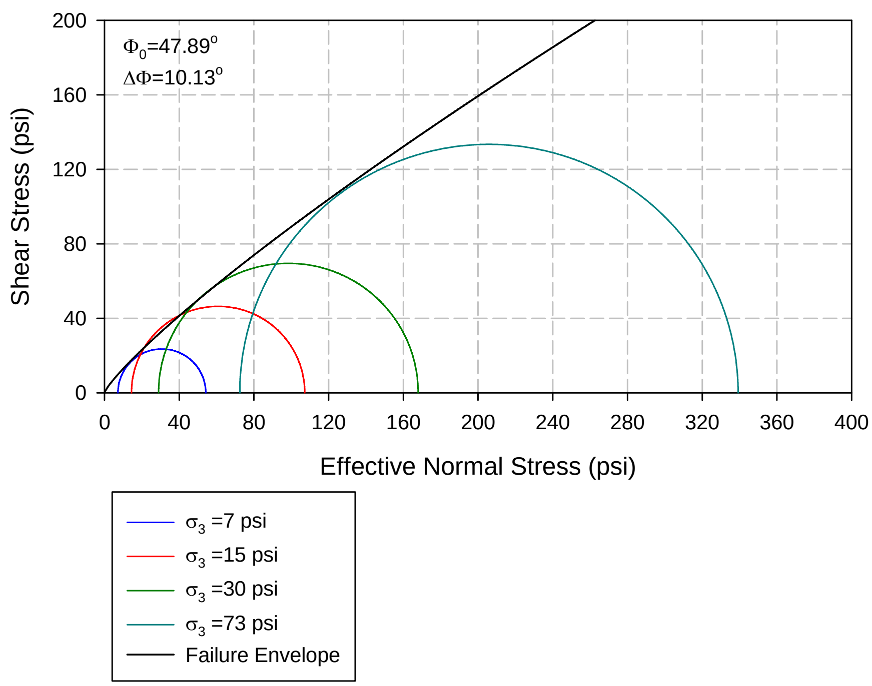

Figure 5.45. Mohr circles at peak and corresponding and failure envelope for CLA from Quarry B after 150 days submerged in salt water (peak strength criterion).

The following figures (5.46 through 5.50) correspond to the shear strength circles and failure envelopes for the 10% of the axial strain failure criterion.

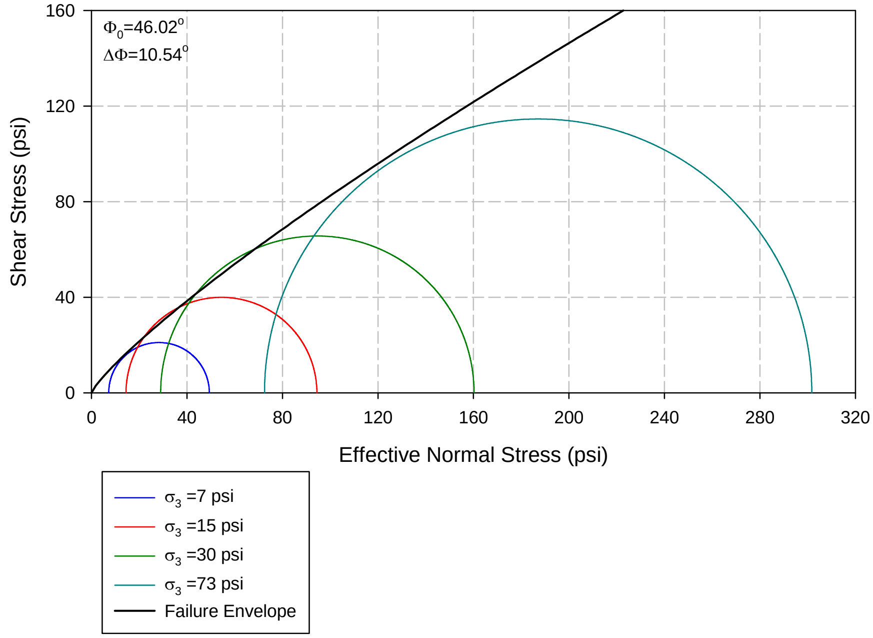

Figure 5.46. Mohr circles and failure envelope for CLA from Quarry B at zero days (ε_{axial}=10%).

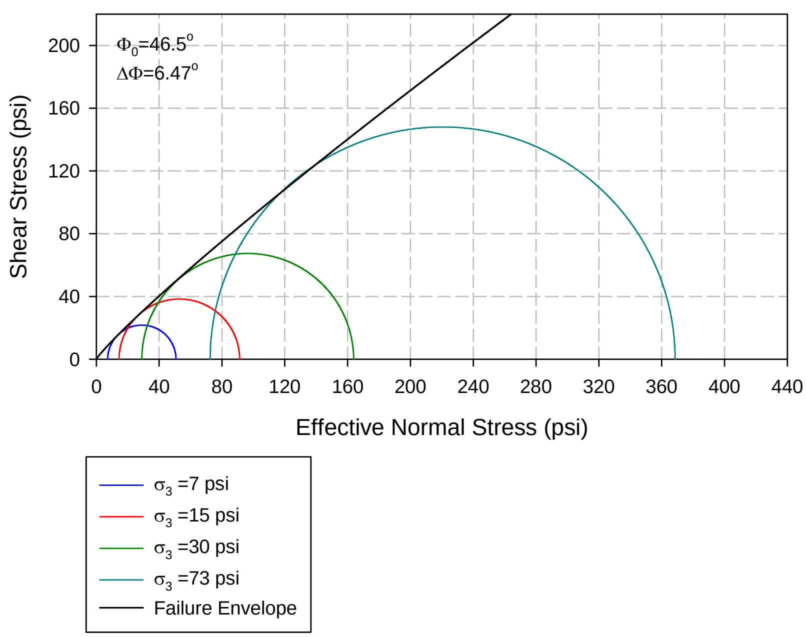

Figure 5.47. Mohr circles and failure envelope for CLA Quarry B after 90 days submerged in fresh water (ε_{axial}=10%).

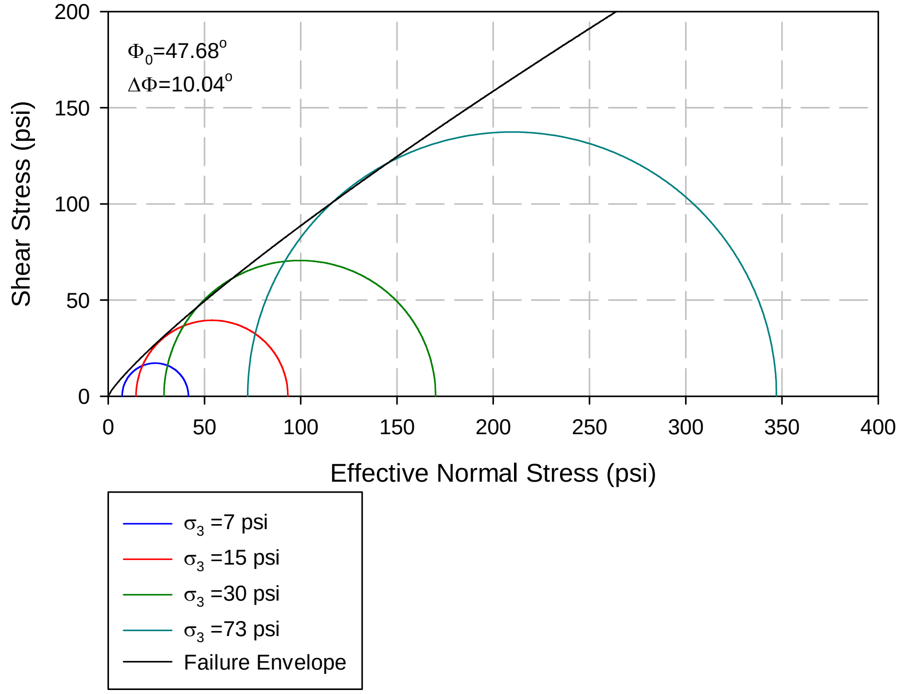

Figure 5.48. Mohr circles and failure envelope for CLA Quarry B after 90 days submerged in salt water (ε_{axial}=10%).

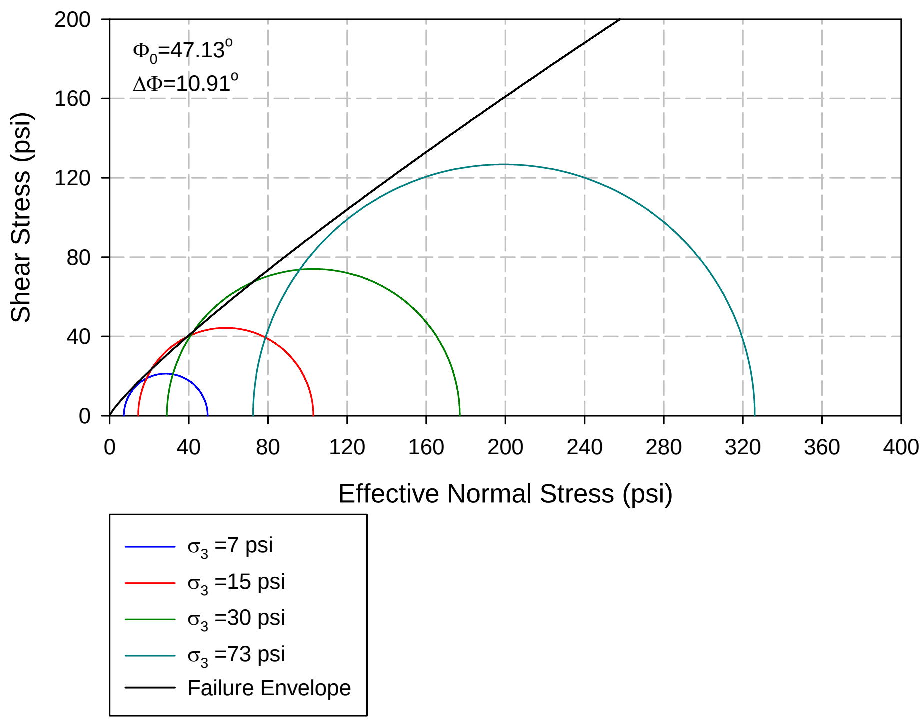

Figure 5.49. Mohr circles and failure envelope for CLA Quarry B after 150 days submerged in fresh water (ε_{axial}=10%).

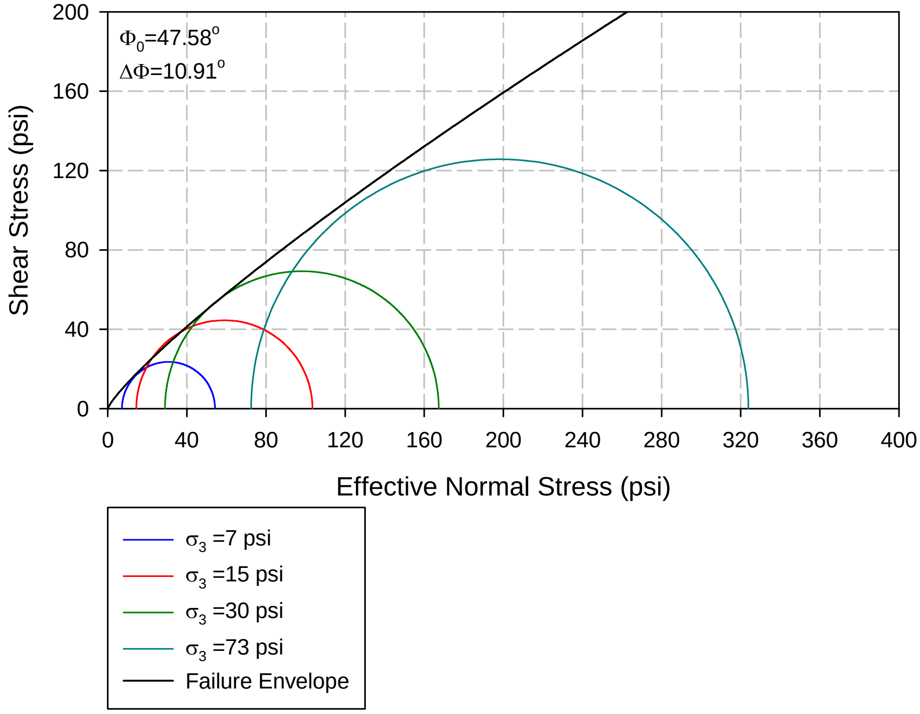

Figure 5.50. Mohr circles and failure envelope for CLA Quarry B after 150 days submerged in salt water (ε_{axial}=10%).

The variation of secant friction angle as a function of the confining pressure level used in the triaxial compression tests are shown in Figures 5.51 and 5.52 for fresh and salt water respectively. These figures correspond to peak shear strength failure.

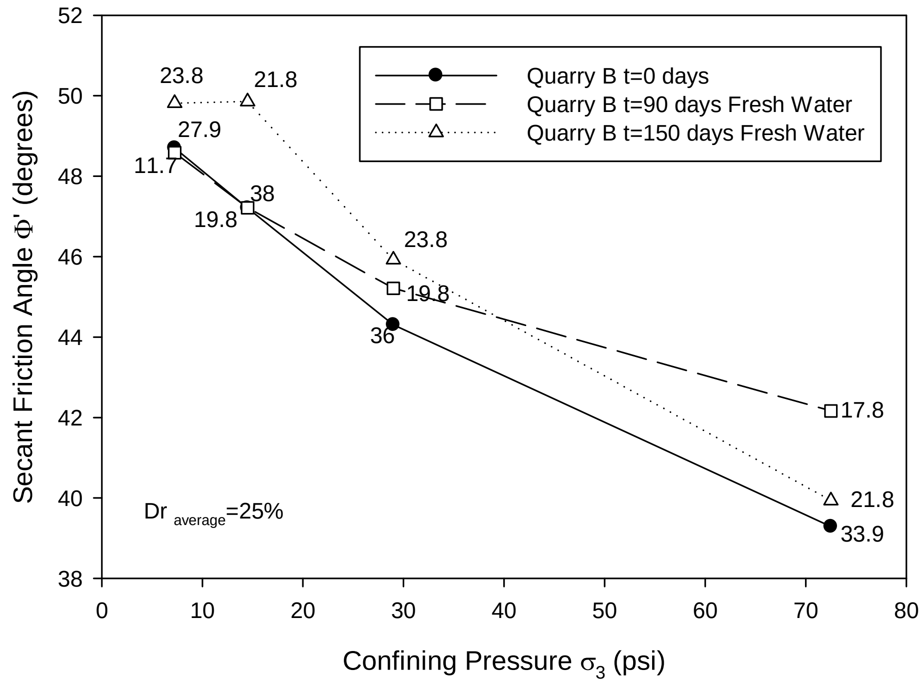

Figure 5.51. Variation of the secant friction angles as a function of the confining pressure for CLA from Quarry B submerged in fresh water at zero, 90, and 150 days (peak strength criterion).

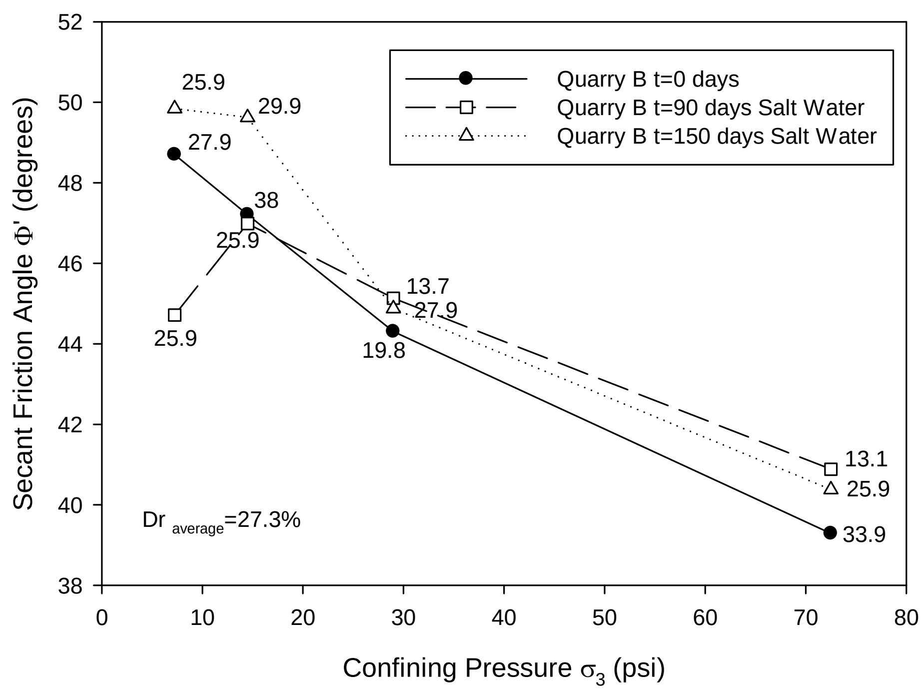

Figure 5.52. Variation of the secant friction angles as a function of the confining pressure for CLA from Quarry B submerged in salt water at zero, 90, and 150 days (peak strength criterion).

The CLA materials submerged in fresh water exhibited the expected behavior, in terms of decreasing secant friction angles as the confining pressure increased. However, no noticeable degradation of secant friction angles was observed. Figure 5.51 shows very similar secant friction angles curves for zero and 150 days.

Figures 5.53 and 5.54 show the variation of secant friction angle for fresh and salt water respectively, corresponding to the 10% of axial strain failure criterion. It can be observed from Figure 5.53 that secant friction angles at time zero and 150 days are very similar. The curves show some differences in the secant friction angles as a function of submergence time at low confining pressure levels. However, there was no consistent trend observed. The difference of secant friction angle values can be explained from differences in the initial relative density of the different tests.

Marsal et al. (1980) studied the geotechnical behavior of coarse grained materials with triaxial testing under different and high confining pressures. He stated that as the confining pressure increased the value for the angle of internal friction decreased due to the crushing of the particles and to the fact that high levels of tension are required when dealing with this type of materials. This type of behavior is also presented in our crushed limestone aggregates as shown in previous figures.

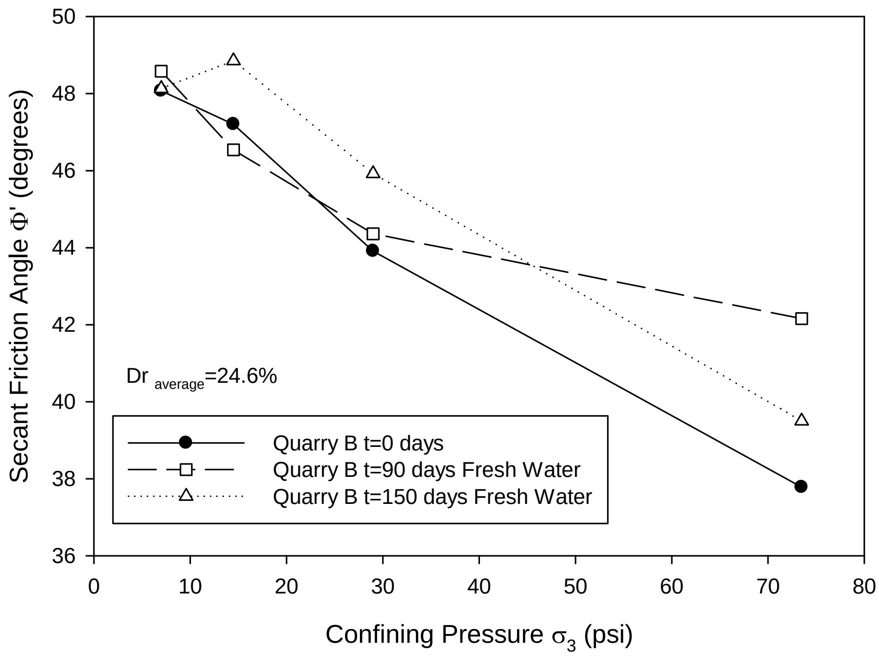

Figure 5.53. Variation of the secant friction angles as a function of the confining pressure for CLA from Quarry B submerged in fresh water at zero, 90, and 150 days (ε_{axial}=10%).

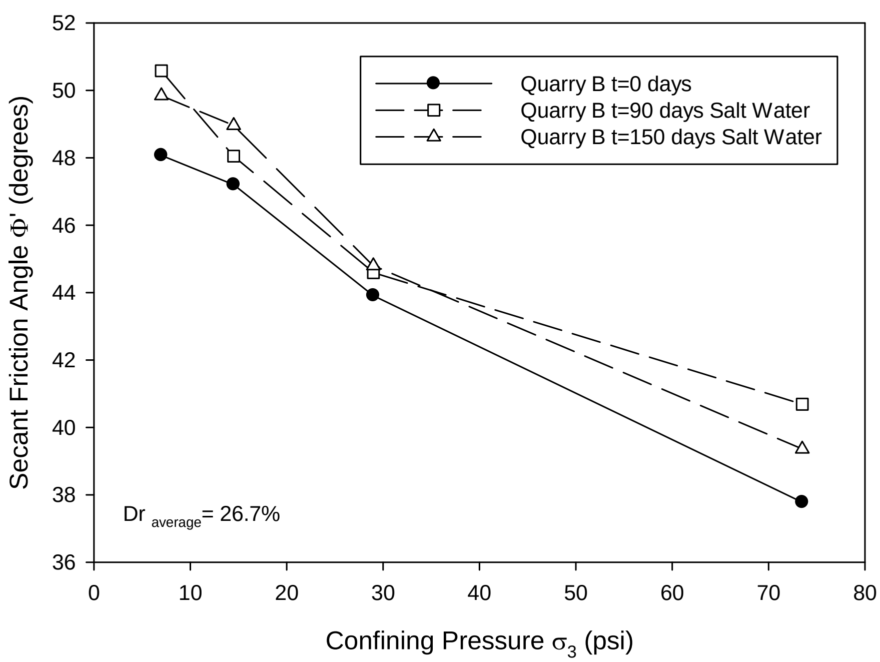

Figure 5.54. Variation of the secant friction angles as a function of the confining pressure for CLA from Quarry B submerged in salt water at zero, 90, and 150 days (ε_{axial}=10%).

Figure 5.55 and 5.56 show the curved shear strength envelopes for CLA materials from Quarry B submerged in fresh and salt water respectively. The CLA materials submerged in fresh water and salt water showed a similar behavior in terms of their curved shear strength envelope. The envelopes for CLA materials from Quarry B submerged in both fresh and salt water showed some differences, particularly for normal stresses above 100 psi. However, the variation observed did not follow the expected degradation trend. These two figures show failure envelopes corresponding to peak shear strength.

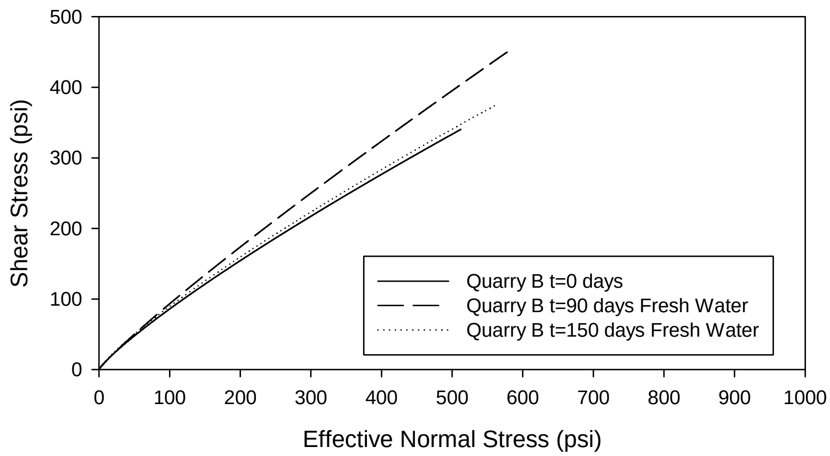

Figure 5.55. Comparisson of curved failure envelopes for CLA material from Quarry B submerged in fresh water (peak shear criterion).

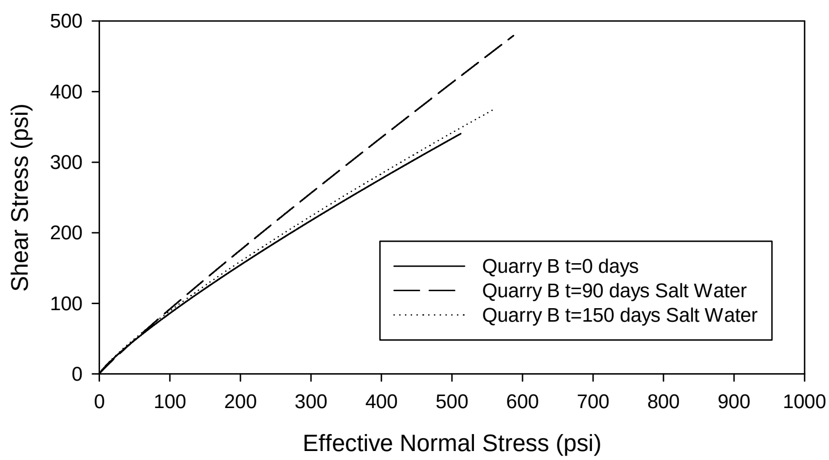

Figure 5.56. Comparisson of curved failure envelopes for CLA material from Quarry B submerged in salt water (peak shear criterion).

Figure 5.57 shows a comparison of all the curved shear strength envelopes for both of the quarries at all the moisture environments and time conditions. As shown in the figure, at all times and under all the moisture environments Quarry B exhibited higher failure envelopes which indicates that the crushed limestone from quarry B have more resistance and needed higher stresses to experience failure. Specimens from Quarry B cured 90 days in salt water present the greatest curved shear strength failure envelope.

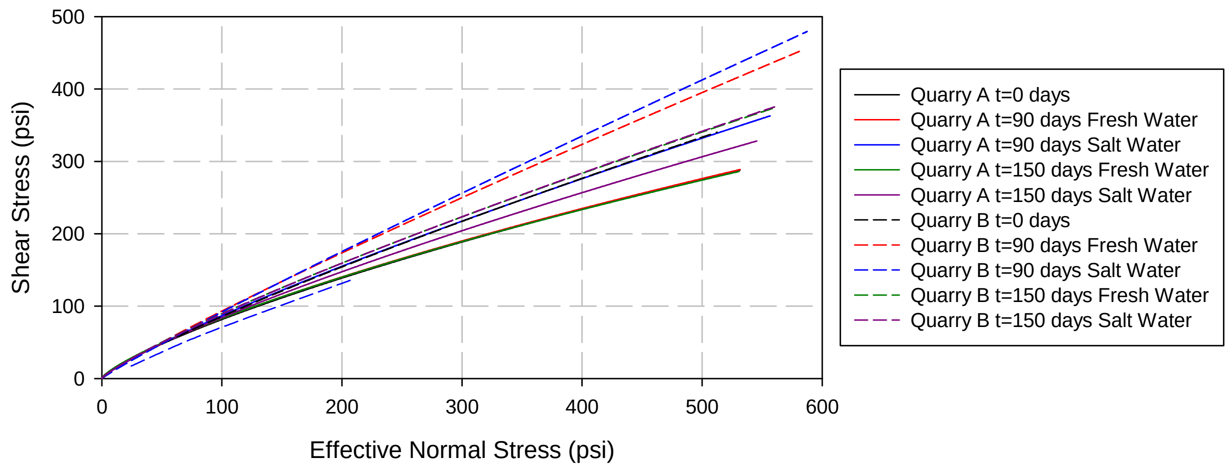

Figure 5.57. Comparison of the failure envelope for Quarry A and B at zero, 90, and 150 days submerged in fresh and salt water.

Figures 5.58 and 5.59 present the ratio coordinates as a function of the center coordinates of the shear strength circle for the CLA materials from Quarry B after 0,90, and 150 days of submergence in fresh and salt water, respectively. CLA materials submerged in fresh and salt water showed very similar behaviors. The values of the K_f lines slopes vary from 0.6 to 0.64.

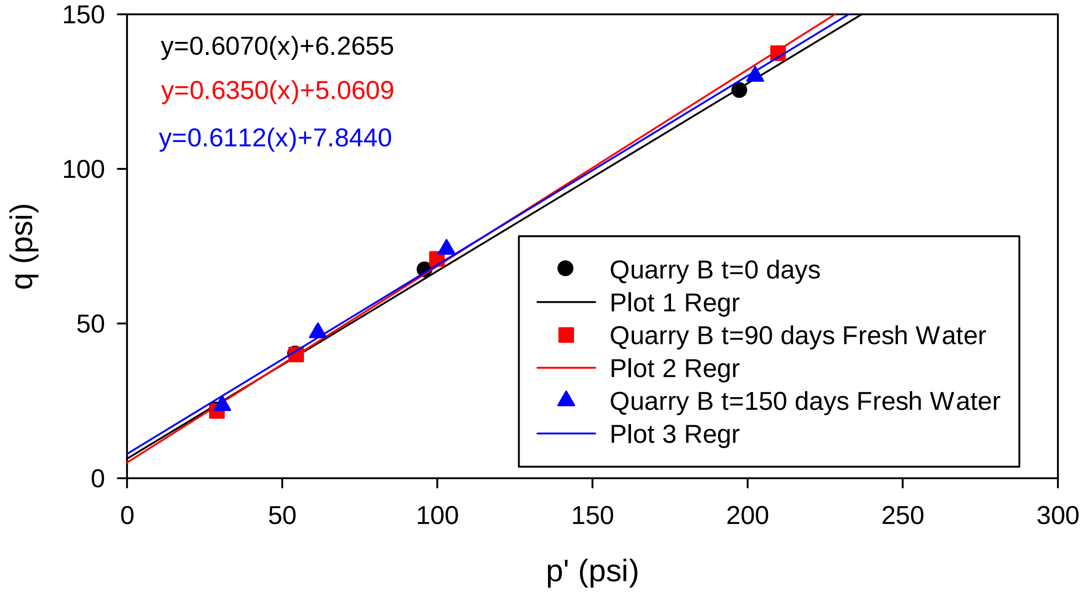

Figure 5.58.Ratio coordinates (q) versus center coordinates (p') comparison for CLA from Quarry B submerged in fresh water after 0, 90, and 150 days.

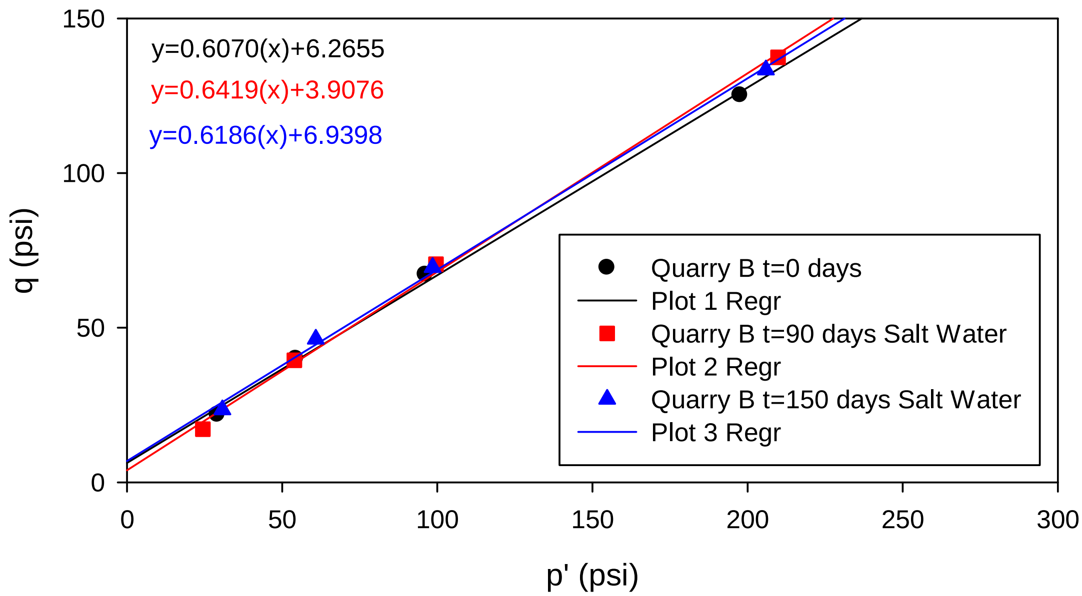

Figure 5.59.Ratio coordinates (q) versus center coordinates (p') comparison for CLA from Quarry B submerged in salt water after 0, 90, and 150 days.

The CLA materials submerged in fresh water and salt water showed a similar behavior in terms of their K_f lines. The K_f lines for CLA materials from Quarry B submerged in both fresh and salt water showed rather small differences. This can be checked with the linear regression equations. However, the variation observed did not follow the expected degradation trend. These two figures show failure envelopes corresponding to peak shear strength.

Figures 5.60 through 5.62 show a comparison of the K_f lines from Quarry A and Quarry B at time zero and after 90 and 150 days of submergence in fresh and salt water.

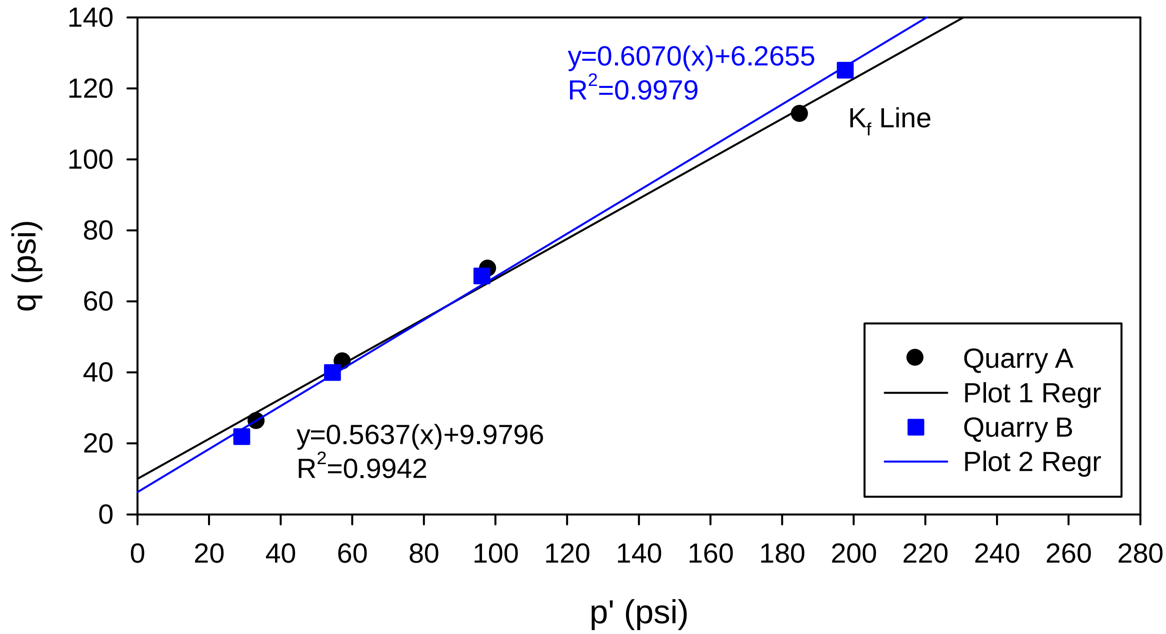

Figure 5.60. Ratio coordinates (q) versus center coordinates (p') comparison for Quarry A and B specimens at zero days.

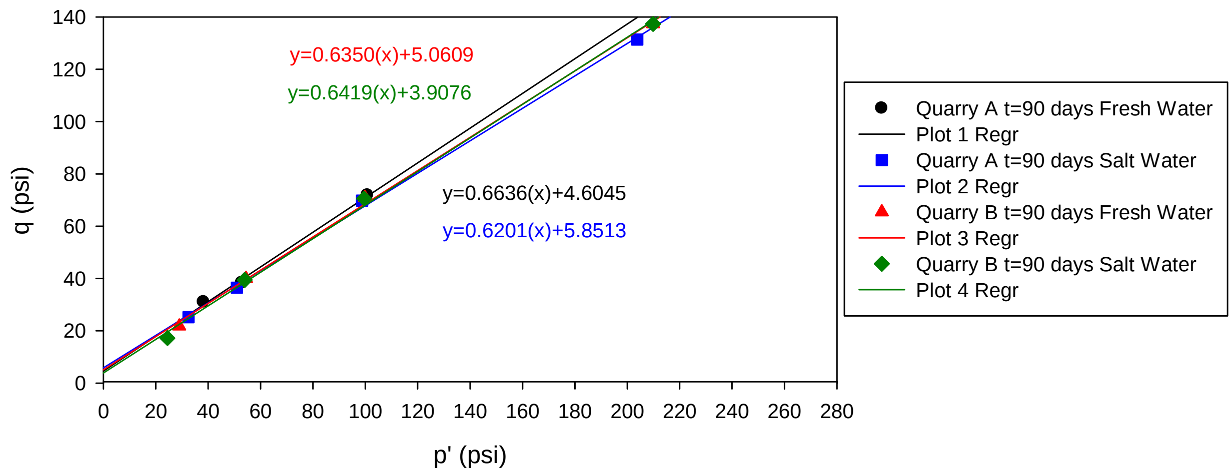

Figure 5.61. Ratio coordinates versus (q) versus center coordinates (p') comparison for Quarry A and B specimens after 90 days of submergence in fresh and salt water.

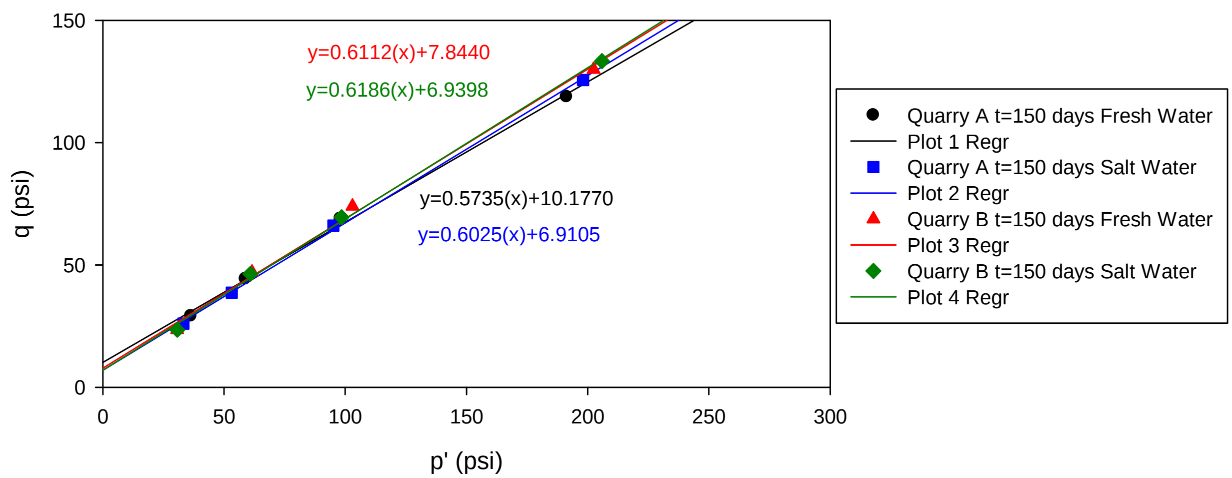

Figure 5.62. Ratio coordinates (q) versus center coordinates (p') comparison for Quarry A and B specimens after 150 days of submergence in fresh and salt water.

CLA from Quarry A and B at zero days showed a similar behavior in terms of the K_f lines. This similar behavior was also experienced in the CLA from Quarry A and B after a submergence of 90 and 150 days in fresh and salt water. After a normal stress of 100 psi these CLA showed some differences. However, the variation observed did not follow the expected degradation trend.

5.8.3. *Comparison of the results for the secant friction angle for CLA materials from both quarries.*

Figures 5.63 through 5.65 show a comparison for the secant friction angles as a function of the confining pressure for the CLA materials for both quarries for submergence times of 0, 90, and 150 days, respectively.

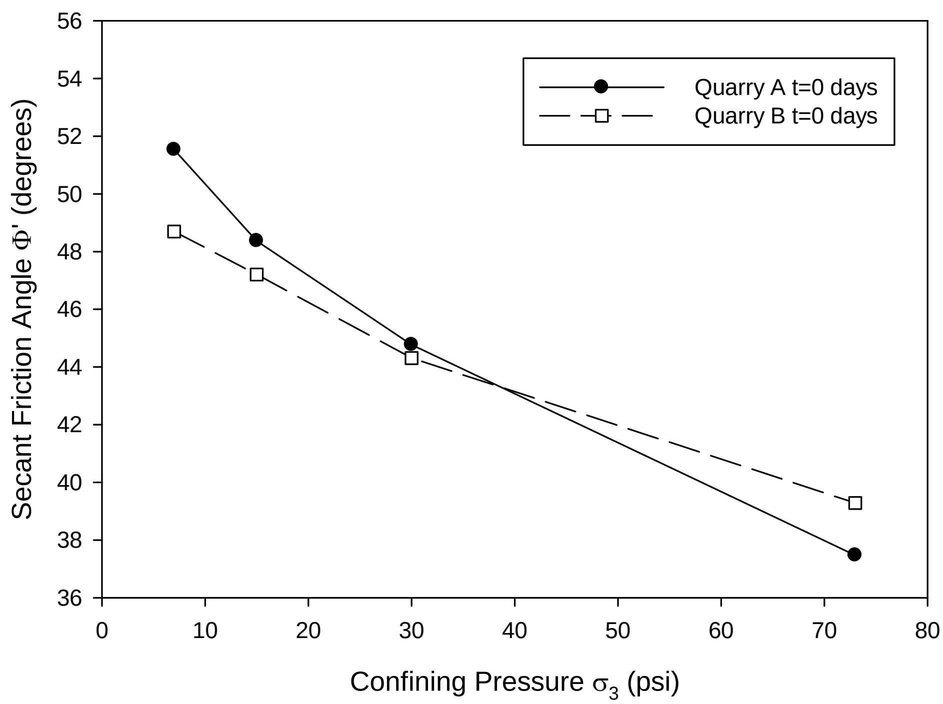

Figure 5.63. Comparisson of secant friction angles as a function of confining pressure for unaged CLA materials for Quarry A and B.

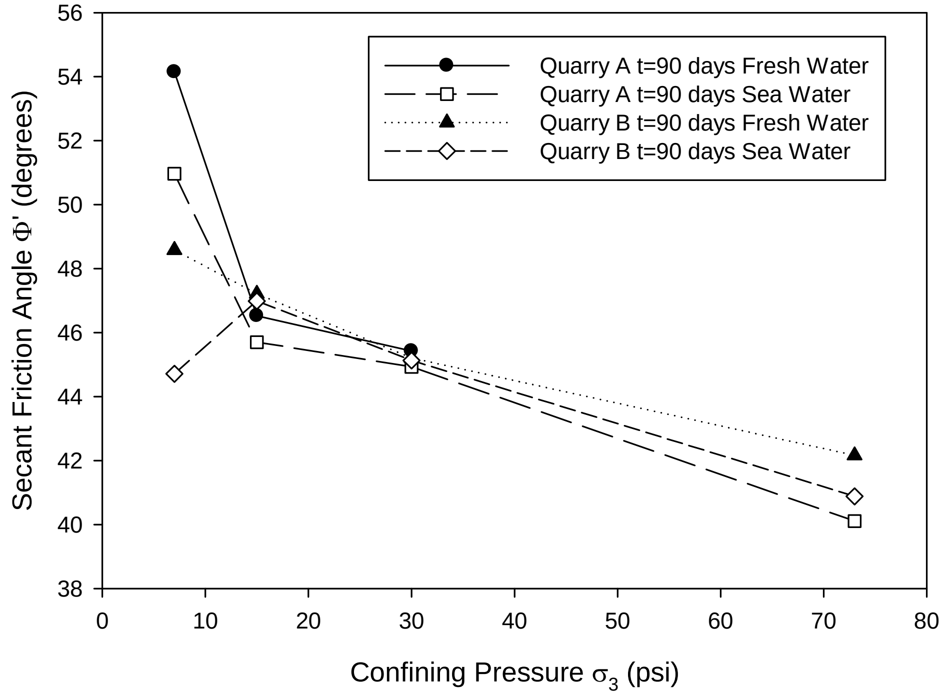

Figure 5.64. Comparisson of secant friction angles as a function of confining pressure and water type for the CLA materials at 90 days of submergence.

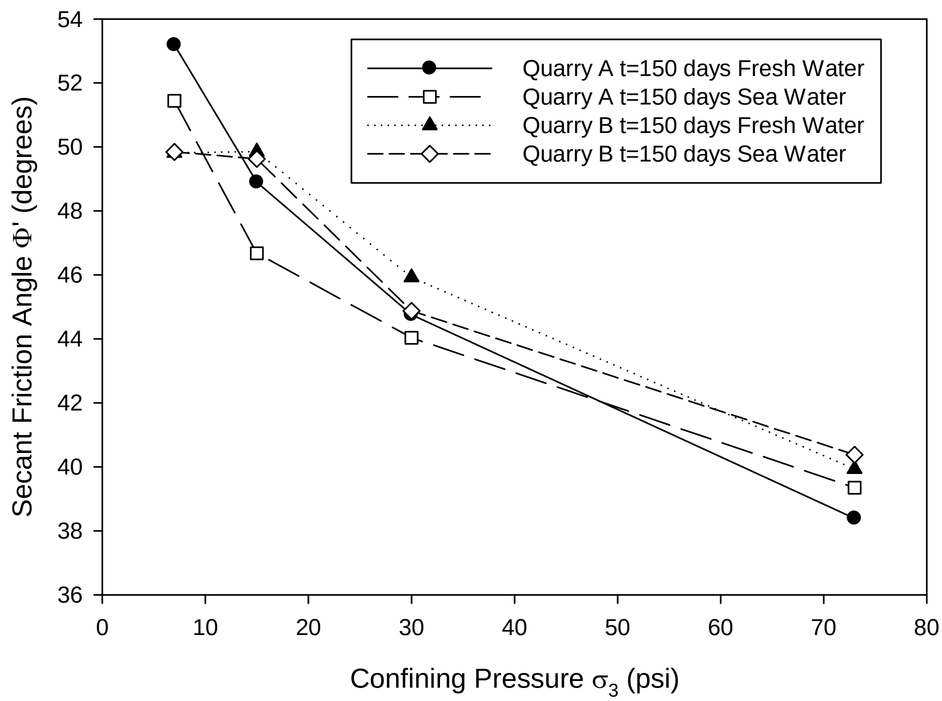

Figure 5.65. Comparisson of secant friction angles as a function of confining pressure and water type for the CLA materials at 150 days of submergence.

The difference between the values of the angles of internal friction for the crushed limestone aggregates from Quarry A and Quarry B is barely noticeable. However, in general higher friction angles were observed for the CLA from Quarry A under similar testing and aging conditions. The differences ranged from 1.8 and 5.2 degrees. This small difference could be attributed to differences in angularity and to a lesser extent on the average site of the aggregate. Mineralogy is not considered a factor as the two CLA materials were found to have a similar mineralogy (see Section 5.3).

5.8.4. Moisture effects on CLA stiffness values measured from triaxial compression tests.

From the stress-strain curves obtained with the different triaxial compression tests one can assess the effects of the moisture environments on the deformation properties of the two CLA materials investigated in this thesis. For this research project two elastic stiffness parameters were assessed from the triaxial compression tests: the initial stiffness (Ei) computed from the initial slope of the stress-strain curve and secant stiffness ($Es_{2\%}$) computed between axial stresses of 0 and 2%. Figure 5.66 shows schematically these two elastic moduli.

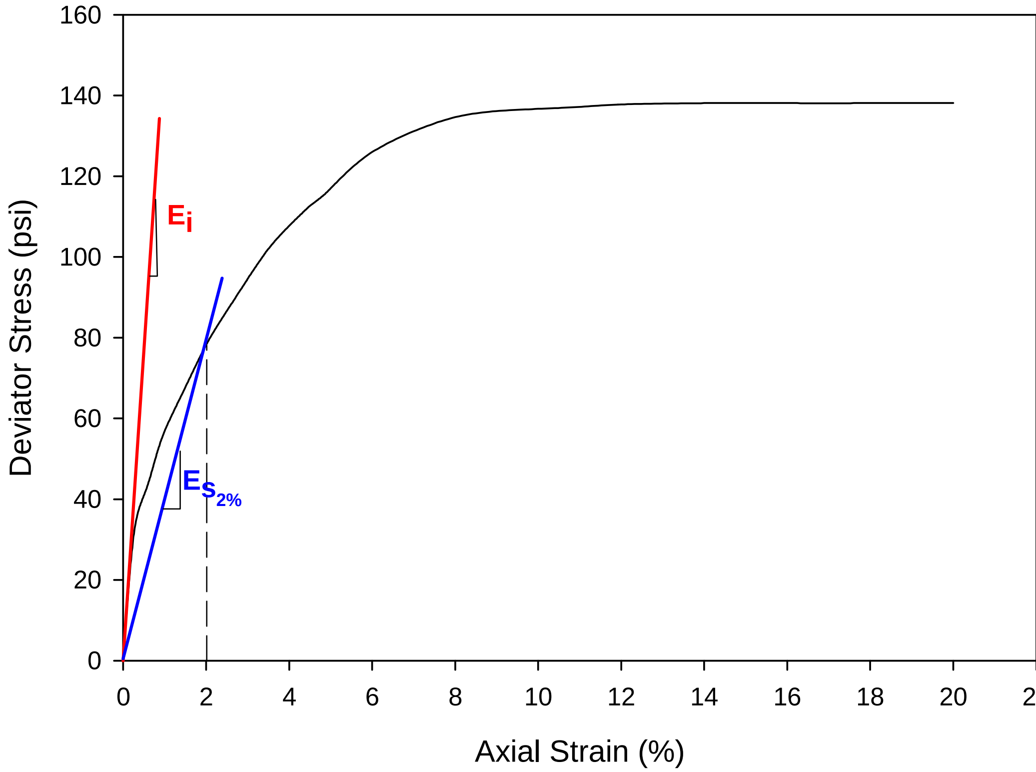

Figure 5.66. Illustration of the initial stiffness moduli and the secant stiffness moduli.

The stress-strain curves for the CLA of Quarry A and B were presented in Figures 5.13 through 5.22. From this curves the values of the initial stiffness (E_i) and secant stiffness ($E_{s2\%}$) moduli were obtained as a function of confining stress (σ_3') and time of submergence.

A summary of the initial stiffness moduli (E_i) and secant stiffness moduli (E_s) is shown in Tables 5.13 and 5.14.

Table 5.13.Summary of the initial stiffness moduli and secant stiffness moduli values for CLA from Quarry A.

Quarry	Time of exposure(days)	Water Condition	σ_c (psi)	γ_{dry} (lb/ft^3)	Initial Void Ratio	ε_{axial} @ peak (%)	Φ_{sec} (°)	E_i (psi)	$E_{s-2\%}$ (psi)	Dr%
A	0	-	7	97.7	0.75	8	51.53	5319.2	1834.4	25.6
			15	101	0.69	12	48.37	6000	2179.8	37.6
			30	98	0.75	20	44.77	14000	3911.4	25.6
			73	98.6	0.73	14	37.47	21276	5728.1	29.6
A	90	Fresh	7	96	0.78	8	54.15	12000	2278.6	19.6
			15	96.9	0.764	20	46.52	16000	2948.6	22.8
			30	96.5	0.77	10	45.43	20000	4583	21.6
			73	-	-	-	-	-	-	-
A	90	Salt	7	100.6	0.7	5	50.97	6666.7	1834.3	35.6
			15	97.6	0.75	8	45.7	8000	2502.3	25.6
			30	95.2	0.79	12	44.93	10000	3514.5	17.6
			73	96.9	0.76	16	40.11	16216	6361.1	23.6
A	150	Fresh	7	98	0.75	6	53.19	4081.6	2105.4	25.6
			15	94.1	0.82	8	48.9	5714.3	2708.5	11.6
			30	95.7	0.79	12	44.75	7142.9	3891.5	17.6
			73	93	0.839	18	38.39	7500	4700	7.8
A	150	Salt	7	94.1	0.817	6	51.44	5000	2036	12.2
			15	95.2	0.8	6	46.67	6000	2882.7	15.6
			30	94.8	0.8	10	44.04	8888.9	4050.1	15.6
			73	93.8	0.82	20	39.35	10000	5150	11.6

Table 5.14. Summary of the initial stiffness moduli and secant stiffness moduli values for CLA from Quarry B.

Quarry	Time of exposure (days)	Water Condition	σ_c (psi)	γ_{dry} (lb/ft^3)	Initial Void Ratio	ε_{axial} @ peak (%)	Φsec (°)	E_i (psi)	$E_{s\text{-}2\%}$ (psi)	Dr%
B	0	-	7	96.3	0.78	8	48.7	4000	1698	27.88
			15	98.9	0.73	10	47.2	6250	2689.6	37.98
			30	98.3	0.74	12	44.3	10000	3622.9	35.96
			73	97.9	0.75	14	39.28	18750	5379.3	33.94
B	90	Fresh	7	91.7	0.86	10	48.58	4000	1413.5	11.72
			15	93.8	0.82	8	47.21	6000	2617.1	19.80
			30	94.1	0.82	8	45.21	13333	4759.5	19.80
			73	93.3	0.83	10	42.16	20000	7546.6	17.78
B	90	Salt	7	95.3	0.79	10	44.71	2857.1	1327.1	25.86
			15	95.6	0.79	6	46.99	5000	2645.1	25.86
			30	92.3	0.85	8	45.13	6666.7	4623.5	13.74
			73	92.3	0.853	18	40.88	8000	5950	13.13
B	150	Fresh	7	95.1	0.8	6	49.82	4000	1981.8	23.84
			15	94.2	0.81	6	49.85	5000	3396.9	21.82
			30	95.1	0.8	10	45.92	7272.7	4401.9	23.84
			73	94.3	0.81	14	39.93	7500	5669.1	21.82
B	150	Salt	7	95.7	0.79	10	49.84	2666.7	5500	25.86
			15	96.5	0.77	8	49.62	4285.7	3086.6	29.90
			30	96.4	0.78	12	44.87	5000	3891.7	27.88
			73	95.4	0.79	18	40.38	10000	6000	25.86

The variation of the initial stiffness (E_i) as a function of confining stress (σ_3') and submergence time for fresh and salt water for CLA materials from Quarry A are shown in Figures 5.67 and 5.68, respectively. Similarly, the variation of the secant stiffness (E_s) for fresh and salt water is shown in Figures 5.69 and 5.70, respectively. Results for CLA materials from Quarry B are shown in Figures 5.71 through 5.72.

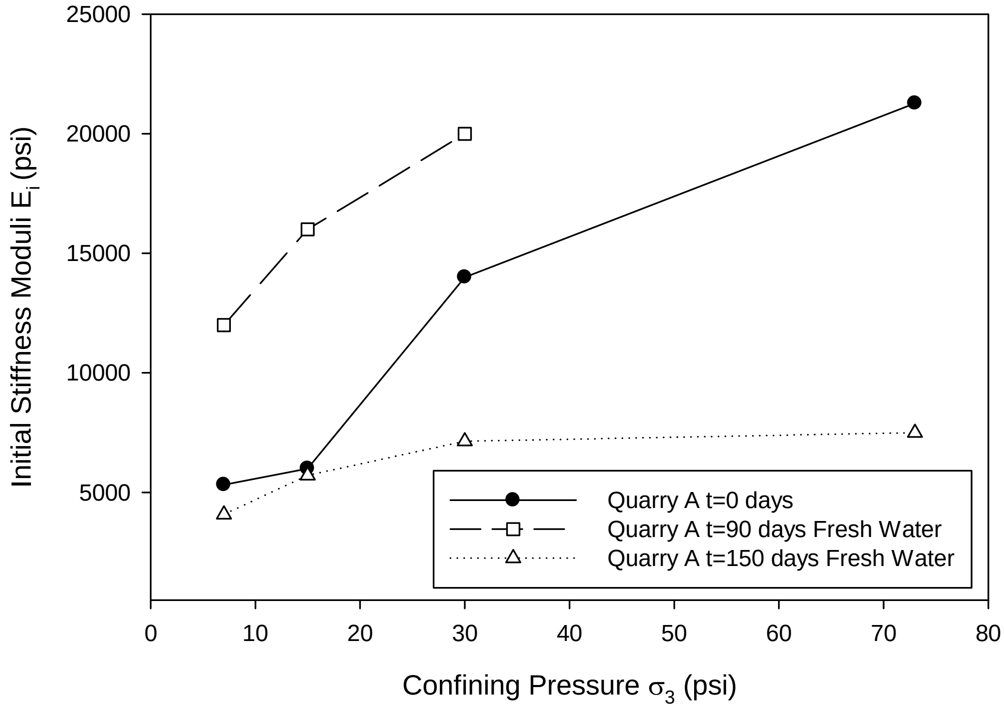

Figure 5.67. Moisture effects in the initial stiffness obtained from triaxial compression tests of CLA from Quarry A when submerged in fresh water.

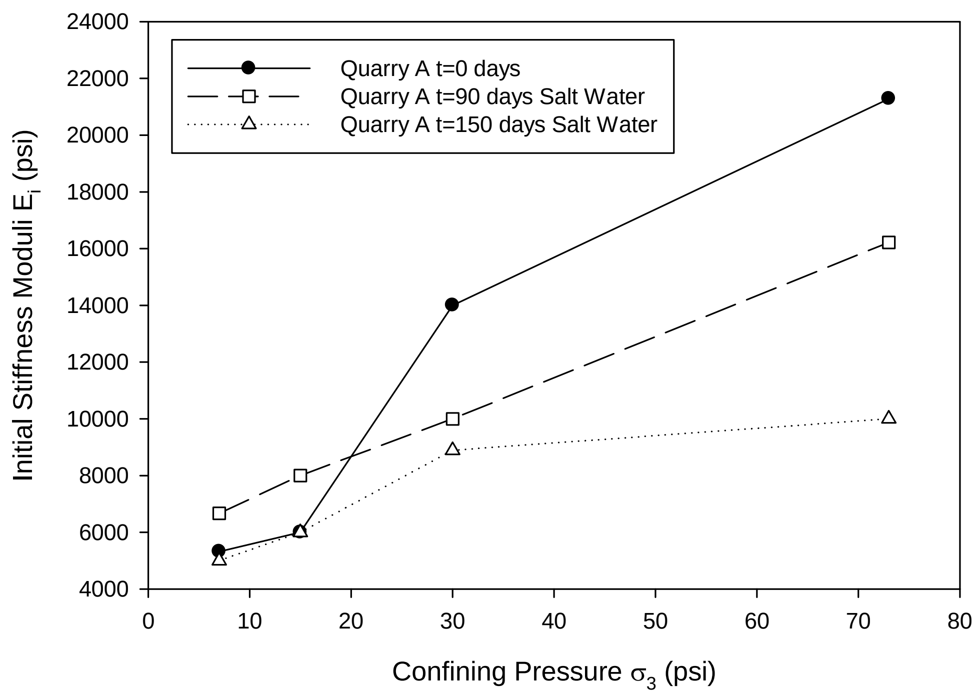

Figure 5.68. Moisture effects in the initial stiffness obtained from triaxial compression tests of CLA from Quarry A when submerged in salt water.

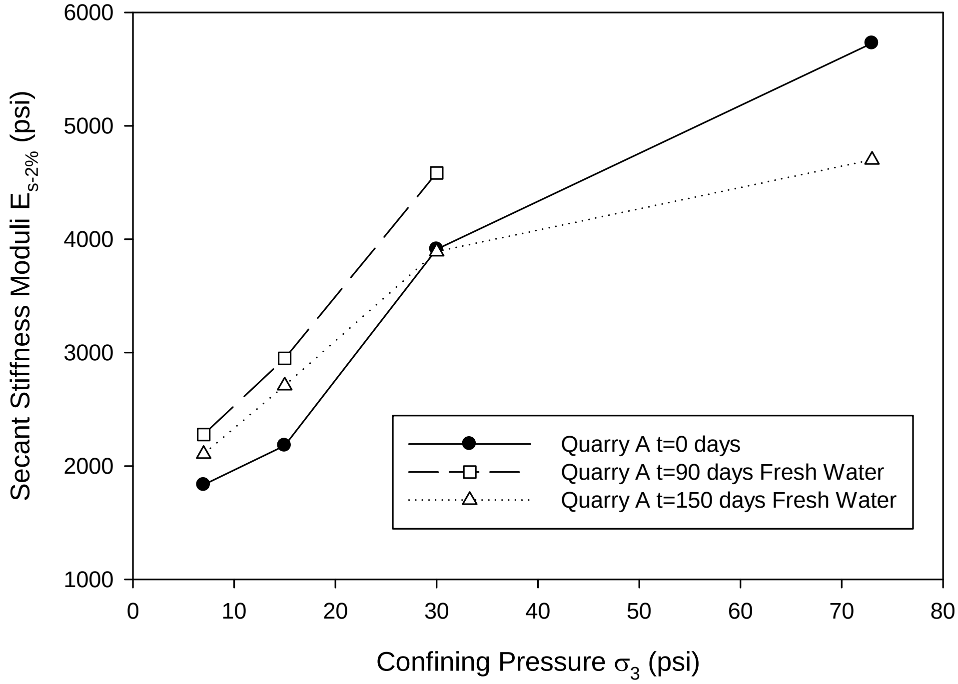

Figure 5.69. Moisture effects in the secant stiffness obtained from triaxial compression tests of CLA from Quarry A when submerged in fresh water.

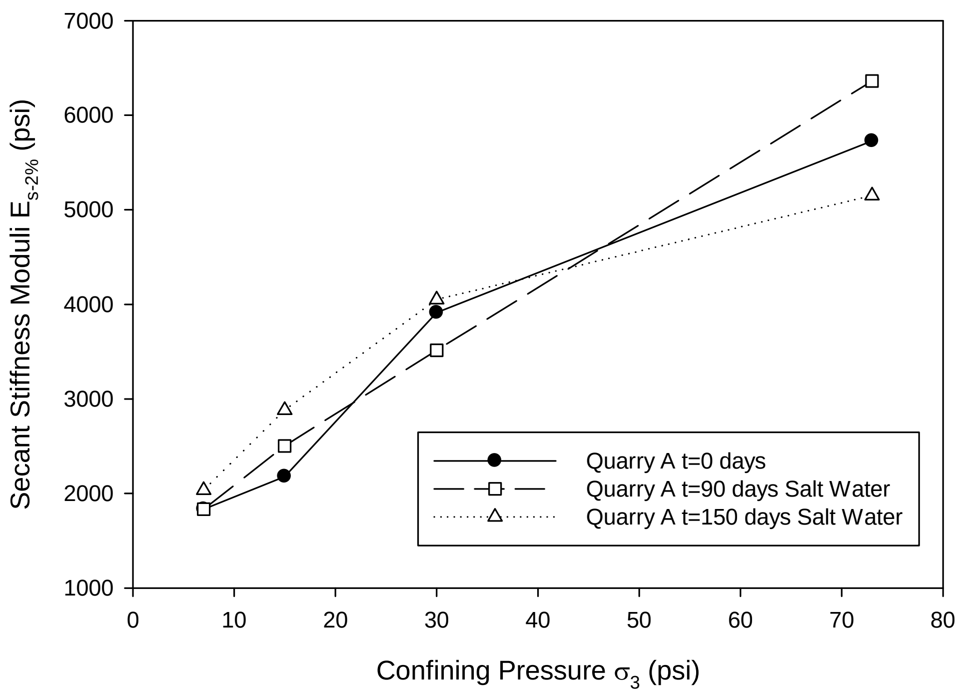

Figure 5.70. Moisture effects in the secant stiffness obtained from triaxial compression tests of CLA from Quarry A when submerged in salt water.

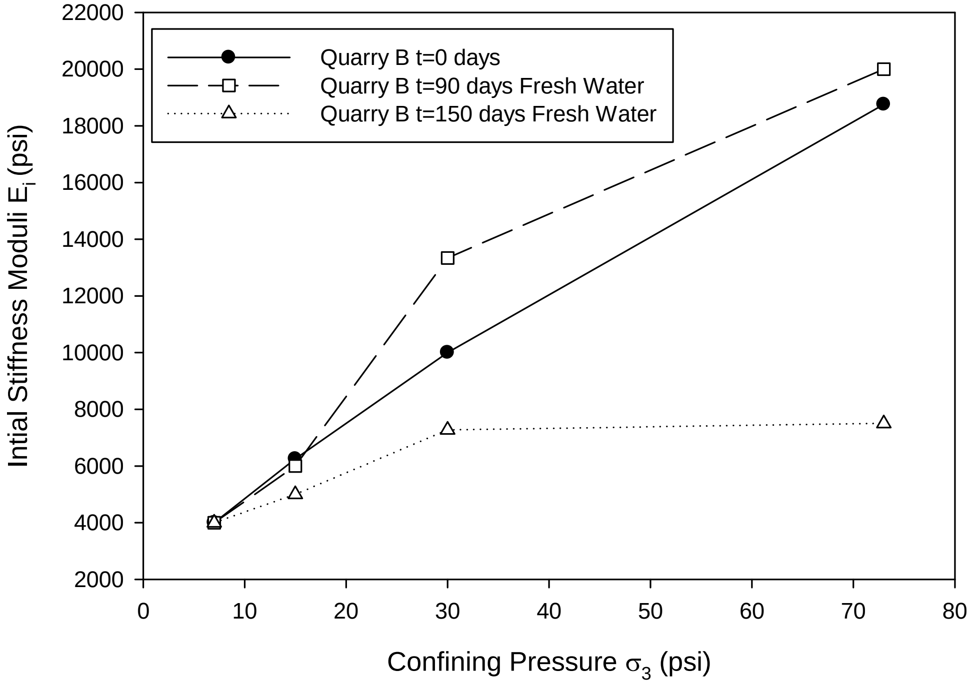

Figure 5.71. Moisture effects in the initial stiffness obtained from triaxial compression tests of CLA from Quarry B when submerged in fresh water.

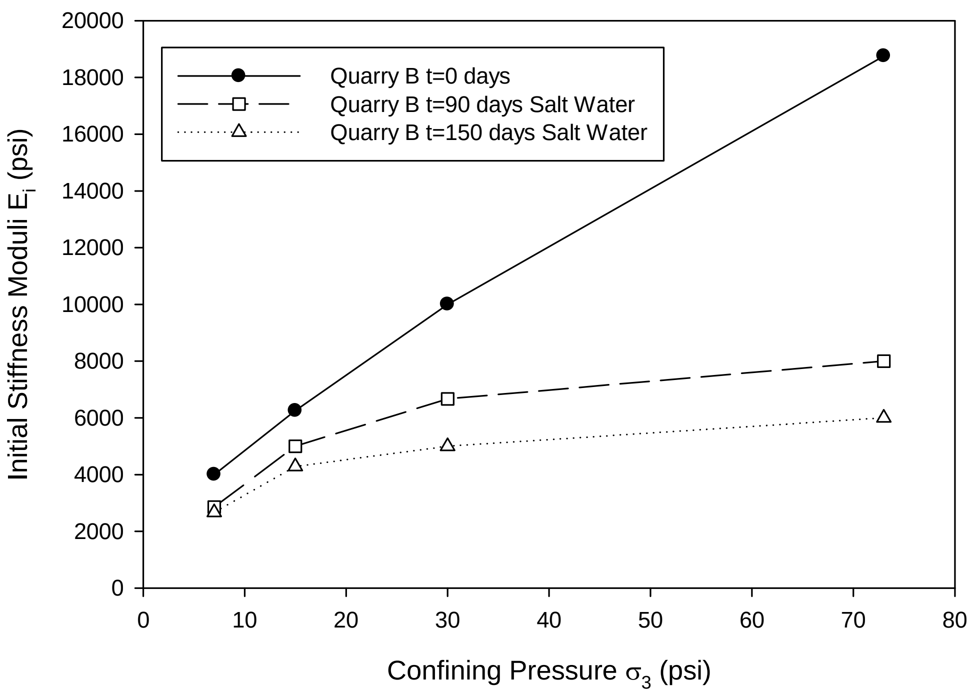

Figure 5.72. Moisture effects in the initial stiffness obtained from triaxial compression tests of CLA from Quarry B when submerged in salt water.

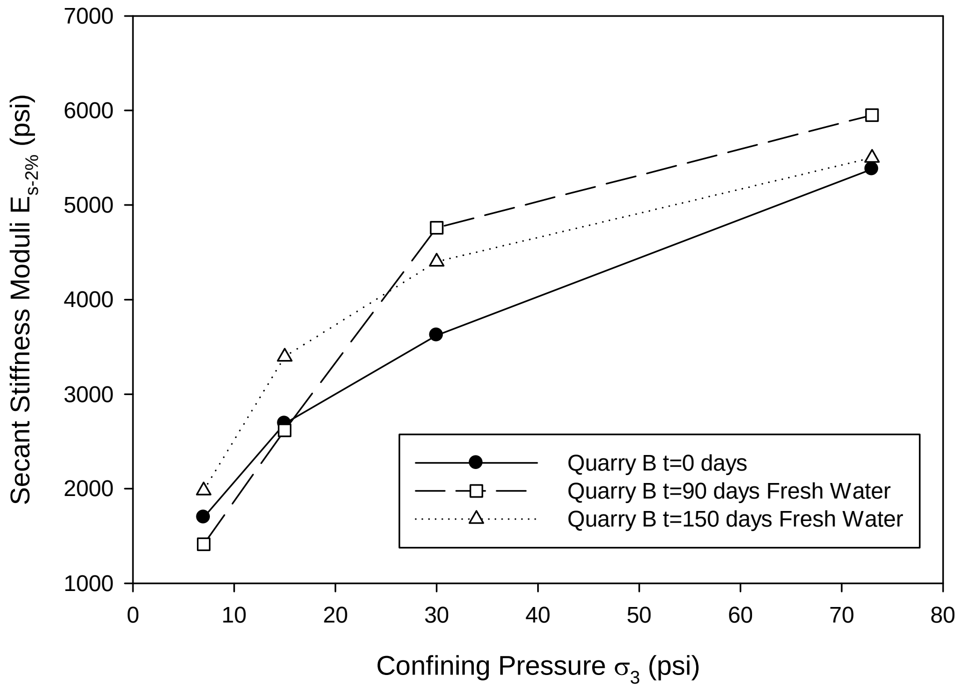

Figure 5.73. Moisture effects in the secant stiffness obtained from triaxial compression tests of CLA from Quarry B when submerged in fresh water.

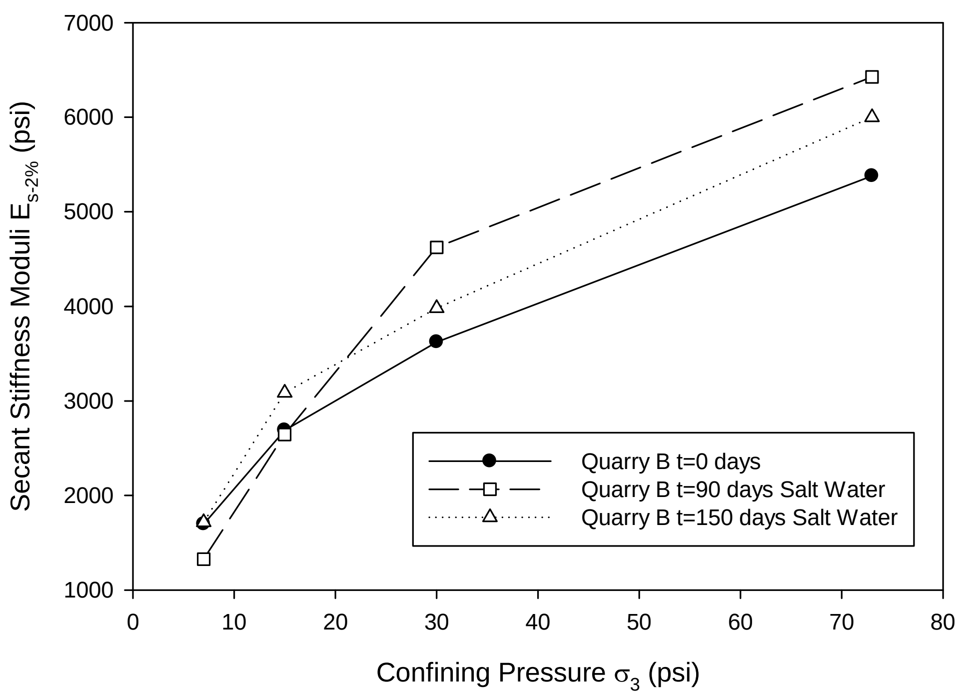

Figure 5.74. Moisture effects in the secant stiffness obtained from triaxial compression tests of CLA from Quarry B when submerged in salt water.

Results from the moisture effects in the initial stiffness moduli and secant stiffness moduli do not address a specific behavior or similar pattern of results. For example: for the CLA materials from Quarry A submerged in fresh water the initial stiffness moduli and secant moduli reaches its higher value when tested at time zero but for the CLA materials from Quarry B the pattern is different. The initial stiffness moduli reach its maximum value after a submergence of 150 days and its minimum value after when tested after zero days. For the CLA materials from Quarry A and B submerged in salt water results are similar. The initial stiffness moduli and the secant stiffness moduli reaches its maximum value after a submergence of 150 and 90 days, respectively and its lowest initial stiffness moduli at zero days . The greatest the initial stiffness moduli the lower the deformation the CLA materials is going to experiment.

5.8.5. Crushing Potential Analyses

A) Crushing in the Modified Proctor Test:

Table 5.15 shows the result of the crushing potential for the CLA from Quarry A and B. These results range from 0.73 to 0.95 which indicates a particle breakage factor very high. Results showed the expected behavior given that these aggregates were subjected to a compaction effort of 56,000 lb-ft/ft^3.

Table 5.15. Particle Breakage Factor for the Modified Proctor Test.

Modified Proctor Test					
Quarry	Time of exposure (days)	Water Condition	D_{10i} (mm)	D_{10f} (mm)	Particle Breakage Factor (B_{10})
A	0	As received	3	0.15	0.95
B	0	As received	3.7	1	0.73

B) 1-D Compression Test:

Results of the particle breakage factor are shown in Table 5.16. It can be observed that B_{10} ranged from 0 to 0.12 which indicates that these CLA barely crushed during the 1-D Compression Test. It was observed at the end of the test that the particles remained virtually unchanged.

Table 5.16. Particle Breakage Factor for the 1-D Compression Test.

1-D Compression Test					
Quarry	Time of exposure (days)	Water Condition	D_{10i} (mm)	D_{10f} (mm)	Particle Breakage Factor (B_{10})
A	0	As received	3.2	3.2	0
A	150	Fresh	3.4	3	0.12
A	150	Salt	3.4	3.4	0
B	0	As received	3.5	3.5	0
B	150	Fresh	4.9	4.4	0.1
B	150	Salt	3.3	3.3	0

C) Triaxial Compression Test:

Table 5.17 and 5.18 shows the particle breakage factor for the triaxial compression tests from Quarry A and B. As seen from these tables the particles breakage factor ranges from 0 to 0.37 and 0 to 0.41 for Quarry A and B, respectively. As the confining pressure increases the particle breakage factor also increases. In general, Quarry B showed higher B_{10} and it can be attributed to its higher porosity value, even tough results were very similar.

Table 5.17. Particle Breakage Factor for the Triaxial Compression Test for Quarry A.

Triaxial Compression Test						
Quarry	Water Condition	Time	Pressure (psi)	D_{10i} (mm)	D_{10f} (mm)	B_{10}
A	N/A	0 days	7	3.45	3.1	0.10
			15	3.1	2.8	0.10
			30	3.1	2.5	0.19
			73	3.3	2.2	0.33
A	Fresh	90 days	7	3.3	2.7	0.18
			15	3.3	2.9	0.12
			30	3.4	2.7	0.21
			73	-	-	-
A	Salt	90 days	7	-	-	-
			15	3.3	2.99	0.09
			30	3.1	2.7	0.13
			73	3.2	2.3	0.28
A	Fresh	150 days	7	3.4	3	0.12
			15	-	-	-
			30	3.4	2.8	0.18
			73	3.2	2.2	0.31
A	Salt	150 days	7	-	-	-
			15	3.4	3.2	0.06
			30	3.5	2.8	0.20
			73	3.5	2.2	***0.37***

Table 5.18. Particle Breakage Factor for the Triaxial Compression Test for Quarry B.

Triaxial Compression Test						
Quarry	Water Condition	Time	Pressure (psi)	D_{10i} (mm)	D_{10f} (mm)	B_{10}
B	N/A	0 days	7	3.5	3	0.14
			15	3.6	3.4	0.06
			30	3.5	2.9	0.17
			73	2.7	2	0.26
B	Fresh	90 days	7	4.5	4.02	0.11
			15	4.99	4.4	0.12
			30	5	4	0.20
			73	5.1	4.2	0.18
B	Salt	90 days	7	3.3	3	0.09
			15	3	2.9	0.03
			30	3.1	2.6	0.16
			73	3.2	2.3	0.28
B	Fresh	150 days	7	-	-	-
			15	4.5	4	0.11
			30	3.45	2.9	0.16
			73	4.6	2.7	***0.41***
B	Salt	150 days	7	3.2	3.1	0.03
			15	-	-	-
			30	3.1	2.8	0.10
			73	3.5	2.4	0.31

5.9. Summary and Conclusions

This chapter provided the results for the moisture effects on the short term mechanical properties of the selected crushed limestone soils from Quarry A and Quarry B. A series of slake durability tests, Los Angeles abrasion test, and point load tests were performed to determine the durability properties of the crushed limestone aggregates. 1-D Compression tests and triaxial compression tests were performed to determine the geotechnical properties of the materials. Results, for both the durability and geotechnical properties, were used for comparison purposes.

The ***slake durability test*** results for both CLA materials and both water submergence conditions, indicated in all cases slake durability index values above 98%. After 150 days of exposure no measurable degradation was observed in terms of reduction of I_d values. It can be concluded that at least in terms of the slake durability tests no short term degradation of the CLA was observed after submergence in fresh or salt water for 150 days.

For the ***Point Load Test*** it can be said that in general the selected parent limestone rocks absorbed very little moisture. It was observed that after 150 days of submergence there was a slight decrease in average peak load recorded for the limestone from Quarry A. The average reduction levels were 11.6% and 17% for submergence in fresh and salt water, respectively. For the limestone of Quarry B almost no reduction of average peak load values after 150 days and for both types of water. In fact, the average peak load values for this limestone showed a great variability and a clear tendency or trend was not possible to infer. A similar behavior with the point load index to the one observed between the peak load and time of submergence was recorded. The point load index values for the limestone from Quarry A showed a consistent decreased with increasing time of submergence. In contrast, point load index values for the limestone from Quarry B did not show a decreased with submergence in time. The test results for this limestone did not follow the expected trend and in fact showed even an increase with time.

For the ***Los Angeles Abrasion test***, both CLA materials showed a decrease in resistance to abrasion/attrition/impact/and griding after 150 days of submergence in both fresh and salt water. The Los Angeles test results for the CLA from Quarry A after 150 days of submergence yielded percentages of mass loss 9.66% and 3.93% higher than the values obtained from unaged CLA samples. A similar trend was observed for the aged CLA materials from Quarry B which yielded mass loss percentages that were 4.67% and 11.42% higher than those recorded from unaged samples. It was observed a slight to moderate degradation in abrasion resistance in both CLA materials after a maximum submergence period of 150 days in both fresh and salt water at room temperature.

In summary, the moisture effects on the coefficient of volume compressibility obtained from ***1-D Compression tests*** was considerably for both CLA materials after submergence periods of 150 days in both fresh and salt water. The initial coefficient of volume compressibility (m_{vi}) values for the CLA from Quarry A increased 300% and 350% after 150 days of submergence in fresh and salt water, respectively. Similarly, the coefficient of volume compressibility (m_{vi}) values for the CLA from Quarry B increased 350% and 60% after 150 days of submergence in fresh and salt water, respectively. These levels of compressibility increase are not negligible and are considered moderate to high.

In the stress versus strain graphs we observed that the peak stresses increased as the confining pressure increased. This type of behavior is the one expected and explained in technical literatures. The maximum axial strain permitted for the soils to experience was 20%. Only a couple of specimens reach its peak stress at a 20% of the axial strain. In general, materials experienced failure at approximately 8-16% of the axial strain. Typically the maximum axial strain permitted is around 15% but coarse grained materials required higher stress levels to failure.

The higher curved shear strength envelope that exhibited Quarry B indicates that the crushed limestone soils have more resistance and needed higher stresses to experience failure. This result in lower values for the internal friction angle, even though the difference between the values for this angle for Quarry A and B is barely noticeable. Internal friction angle was evaluated under two different failure criteria: maximum peak strength and at 10% of the axial strain. Results were very similar for both criteria. The values for the internal friction angle were found to decrease as the confining pressure increased. For Quarry A crushed limestone soils value of the internal angle of friction ranges from 54.13° to 37.22°. Values for the internal friction angle for the crushed limestone soils from Quarry B ranged from 50.58° to 37.77°.

Stiffness moduli was experimentally determined from the initial slope of the stress versus strain curve generated after triaxial testing. It was found that this value was stress and strain dependent, which means that it can change as the stress and strain condition changes. Also it was found that as the confining pressure increases the stiffness moduli also increases. Results from the moisture effects in the initial stiffness moduli and secant stiffness moduli do not address a specific behavior or similar pattern of results. For example: for the CLA materials from Quarry A submerged in fresh water the initial stiffness moduli and secant moduli reaches its higher value when tested at time zero but for the CLA materials from Quarry B the pattern is different.

From the crushability analyses it was observed that the CLA subjected to a compaction effort of 56,000 lb-ft/ft^3 in the Modified Proctor experienced the highest particle breakage factor (0.73 to 0.95), as expected. For the CLA materials subjected to 1-D Compression test the particle breakage factor recorded was in the range of 0 to 0.10 and 0 to 0.12 for Quarry A and B, respectively. For the triaxial compression test the particle breakage factor exhibited ranged from 0 to 0.37 and from 0 to 0.41 for the CLA materials from Quarry A and B, respectively.

Chapter 6. Summary, conclusions, and recommendations for future work

6.1. Introduction

This investigation described the mechanical behavior and durability properties of the two selected high-calcium carbonate crushed limestone soils: one from the Puerto Rico North karst landform and the other from the Puerto Rico South karst landform under different moisture conditions. Mechanical behavior was evaluated by means of 1-D Compression test and triaxial compression tests while the durability properties were assessed by means of slake durability tests, Los Angeles abrasion tests, and point load tests. This chapter present a summary of the work realized followed by conclusions and recommendations for future work.

6.2. Summary

The results of this investigation were presented in 6 chapters. Chapter two presents a general definition and description of the term *limestone*. It was explained that the limestone properties vary widely and depends in several factors such as physical and chemical properties. The limestone formations found in Puerto Rico were mentioned and described. Figures illustrating the Puerto Rico karst lanform and the geologic formation of the North coast limestone area were presented. A general description of the mayor limestone formations in the Northern and Southern karst landform was presented in a table. Physical properties of common crushed-stone were shown and the importance of the crushability of soils was explained. A general literature review and previous investigations in Puerto Rico was included.

Chapter three presented a description of the experimental plan followed to achieve the goals of this investigation. A detailed laboratory program was included and all the suggested methods to determine the soil classification, soil mineralogy, soil durability properties, and soil geotechnical properties were described.

Chapter four described the area from which the crushed limestone soils were collected. A general description of the area of study and the corresponding soil taxonomy of the area was mentioned. A general map of the Puerto Rico soils was shown and the selected areas of study were illustrated. A specific geological description for the selected quarries was included with aerial photos and geological and soil taxonomy maps. A description of the selected crushed limestone soils and its baseline properties for this investigation and the details for the water collection for the aging of the samples is also included.

Results of the soil classification, soil mineralogy, soil durability and geotechnical properties under different moisture and water submergence conditions were presented in chapter five. First, soil classification results such as grain size analysis, specific gravity, USCS classification, porosity, absorption, and unit weight were discussed.

Soil mineralogy was evaluated by means of X-ray diffraction and thermo-gravimetric analysis. From the diffractograms of both quarries is clearly stated that the mineral content of the crushed limestone soils is almost identical. The main carbonates found were calcite and magnesium calcite. From the thermo-gravimetric analysis we were able to determine quantitatively the amount of calcium carbonate in the samples. For the crushed limestone soil sample from Quarry A the amount of calcium carbonate found was 97.44% and 93.8% for Quarry B.

Slake durability tests were performed in crushed limestone soil samples as received from the quarries and in CLA materials submerged in fresh and salt water for a period of 90 and 150 days. Results for both CLA materials and both water submergence conditions, indicate in all cases slake durability index values above 98%. Slake durability tests results revealed that both of the materials studied were resistant to wetting and drying cycle and when subjected to the slake durability test the pieces remained virtually unchanged.

Point load test on parent limestone rock samples in general absorbed very little moisture. It was observed that after 150 days of submergence there was a slight decrease in average peak load recorded for the limestone from Quarry A. The average reduction levels were 11.6% and 17% for submergence in fresh and salt water, respectively. For the limestone of Quarry B almost no reduction of average peak load values after 150 days and for both types of water. In fact, the average peak load values for this limestone showed a great variability and a clear tendency or trend was not possible to infer. A similar behavior with the point load index to the one observed between the peak load and time of submergence was recorded. The point load index values for the limestone from Quarry A showed a consistent decreased with increasing time of submergence. In contrast, point load index values for the limestone from Quarry B did not show a decreased with submergence in time. The test results for this limestone did not follow the expected trend and in fact showed even an increase with time. Overall, test specimens from Quarry B shown more resistance in the point load test.

1-D compression tests were carried out to examine the mechanical behavior of the crushed limestone soils. Tests were realized in crushed limestone soils at zero days as received from the quarries and after a submergence of 150 days in fresh and salt water. The results indicate that moisture effects, after 150 days of submergence, were considerable in terms of increased compressibility. This can be seen graphically in Figures 5.15 and 5.16 which shows the effects of 150 days of submergence (in both fresh and salt water) on the CLA materials from quarries A and B, respectively. However, it is important to point out that unfortunately the initial relative densities of all tests were not uniform. Nevertheless, increased compressibility was observed for the tests on aged CLA materials submerged in fresh water for 150 days. These two tests, for both quarries, had higher initial relative densities than the corresponding tests for unaged conditions. The initial coefficient of volume compressibility (m_{vi}) values for the CLA from Quarry A increased 300% and 350% after 150 days of submergence in fresh and salt water, respectively. Similarly, the coefficient of volume compressibility (m_{vi}) values for the CLA from Quarry B increased 350% and 60% after 150 days of submergence in fresh and salt water, respectively. These levels of compressibility increase are not negligible and are considered moderate to high.

Triaxial compression tests were performed on the selected CLA materials. Triaxial compression test specimens were approximately 6 inches in height and 3 inches in diameter. Stress-Strain behavior was evaluated and the peak stress of the soils studied from Quarry A and Quarry B were found to increase with increasing confining pressure. At low pressures, the peak stress showed a little dependency with the confining pressure resulting in similar values for the applied stress. The maximum axial strain permitted for the crushed limestone soils to experience was

20%. In general, triaxial tests specimens experienced failure at approximately 8-16% of the axial strain. The United Stated Army Corps of Engineers suggest a maximum axial strain of 15% but coarse grained materials may require higher stress levels to reach failure.

Mohr circles were drawn using two failure criterion: (1) peak shear strength and (2) 10% of the axial strain, for each specimen. At all times and moisture conditions crushed limestone soils from Quarry B exhibited higher failure envelopes meaning that these soils are more resistant and higher stresses are required to reach failure. The greatest failure envelope was exhibited by the specimens from Quarry B cured for 90 days in salt water. Failure envelopes when grouped together did not show a noticeable or evident pattern. Totally arbitrary results were obtained and no relationship between water submergence and aging can be established. Neither a relationship between uniformity coefficient and shear strength was found.

Higher failure envelopes results in lower values for the internal friction angle. Difference for this value for Quarry A and Quarry B is not significant. Internal friction angle was evaluated by means of triaxial testing using the Φ_{sec} theory and under two different failure criteria: maximum peak strength and 10% of the axial strain. The values for the internal friction angle were found to decrease as the confining pressure increased. Values ranging from 54.13° to 37.77° were found.

The stiffness moduli were found to be stress and strain dependent, which means that it can change as the stress and strain condition change. Also it was found that as the confining pressure increases the stiffness moduli also increases. Results from the moisture effects in the initial stiffness moduli and secant stiffness moduli do not address a specific behavior or similar pattern of results. For example: for the CLA materials from Quarry A submerged in fresh water the initial stiffness moduli and secant moduli reaches its higher value when tested at time zero but for the CLA materials from Quarry B the pattern is different.

The CLA materials subjected to Modified Proctor Test experienced very high particle breakage factor. This behavior was the expected given the compaction effort that was applied to the materials. For the 1-D Compression test the particle breakage factor was very low, almost negligible. Values reported for the triaxial compression test were very similar and ranged from 0 to 0.37 and 0 to 0.41 for Quarry A and B, respectively.

6.3. Conclusions

From the series of tests performed to characterize the crushed limestone soils we can conclude that for both of the quarries the soils presented the same gradation coefficient, specific gravity, and similar minimum and maximum unit weight. A noticeable difference between porosity and water absorption was found.

X-ray diffraction revealed a predominance of carbonate materials such as calcite and magnesium calcite for both of the selected crushed limestone soils. X-ray diffractograms were almost identical for these soils. The calcium carbonate ($CaCO_3$) content was determined quantitatively through Thermo-gravimetric analysis and was found to be in the range of 93-97%

Slake durability test revealed that the crushed limestone soils are durable and when subjected to this test the retained pieces in the drum remained virtually unchanged. Slake durability index varied from 98-99% which indicated a rock of very high durability. Moisture changes and aging did not affect the durability of the crushed limestone.

Limestone rock samples tested in the point load test at zero days did not presented significant differences. The limestone rock samples from Quarry A tested after 90 days of submergence in fresh and salt water tended to decrease its peak load value, its point load index, and estimated compressive strength except for the limestone rock samples submerged 90 days in salt water that apparently gained resistance. For the limestone rock samples of Quarry B no pattern was observed.

For the Los Angeles abrasion test moisture conditions did affect the results. CLA materials tested as received from the quarry loose less material than the CLA materials submerged in fresh and salt water after 90 and 150 days. Similar results were found in the 1-D compression tests that reveal that the moisture condition produced greater deformation of the specimens.

Stress-Strain behavior of the crushed limestone soils from Quarry A and Quarry B reveal that the peak stress tend to increase as the confining pressure increases. Moisture conditions did not directly affect the result of the geotechnical properties measured in the triaxial compression testing. No pattern was observed and not necessarily specimens tested as received from the quarries presented higher shear strength than the specimens tested after 150 days of submergence in fresh and salt water. No relationship was found between the uniformity coefficient and shear strength. The internal friction angle showed dependency on the confining pressure. As the confining pressure increased the value for this angle decreased. But again, moisture changes did not revealed any pattern on these values. These analyses suggest that the selected crushed limestone soils for this study: one from the North Karst Landform and the other from the South Karst Landform are durable rocks and resistant to moisture and aging conditions.

6.4. Recommendations for future work

Recommendations for further research into the moisture effects on short term mechanical properties of Puerto Rico crushed limestone soils are as follows:

- Since no significance difference was found due to moisture changes, a more aggressive environment should be analyzed such as acidic water and wetting and drying cycles. Specimens should be tested after a curing time of at least 365 days for the long-term condition.
- Crushed limestone aggregates instead of being submerged in water for a pre-determined period could be subjected to a transient state in where the volume of water changes over time.
- Since a significant number of membranes were broken during triaxial testing and at some cases double thick membranes were necessary to perform a full test, another type of membrane should be taken into consideration.
- A more detailed crushability analysis should be perform in order to establish correlations between shear strength and particle breakage.
- A more detailed mineralogy characterization should be considered in future investigations.

References

American Society for Testing and Materials. (2004). Test Method D-4644 Standard Test Method for Slake Durability Test of Shales and Similar Weak Rocks. 2004 Edition. American Society for Testing and Materials, West Conshohocken, PA.

American Society for Testing and Materials. (2006). Test Method D-5731 Standard Test Method for Determination of Point Load Strength Index of Rock and Application to Rock Strength Classification. 2006 Edition. American Society for Testing and Materials, West Conshohocken, PA.

American Society for Testing and Materials. (2006). Test Method C-131 Standard Test Method for Resistance to Degradation of Small-Size Coarse Aggregate by Abrasion and Impact in the Los Angeles Machine. 2006 Edition. American Society for Testing and Materials, West Conshohocken, PA.

American Society for Testing and Materials. (1998). Test Method D-2216 Laboratory Determination of Water (Moisture) Content of Soil and Rock by Mass. 1998 Edition. American Society for Testing and Materials, West Conshohocken, PA.

American Society for Testing and Materials. (1998). Test Method D-2488 Standard Practice for Description and Identification of Soils (Visual-Manual Procedure). 1998 Edition. American Society for Testing and Materials, West Conshohocken, PA.

American Society for Testing and Materials. (1998). Test Method C-702 Reducing Samples of Aggregate to Testing Size. 1998 Edition. American Society for Testing and Materials, West Conshohocken, PA.

American Society for Testing and Materials. (2000). Test Method D-4252 Minimum Index Density and Unit Weight of Soils Calculation of Relative Density. American Society for Testing and Materials, West Conshohocken, PA.

American Society for Testing and Materials. (2000). Test Method D-4254 Maximum Index Density and Unit Weight of Soils Calculation of Relative Density. American Society for Testing and Materials, West Conshohocken, PA.

American Society for Testing and Materials. (2004). Test Method D-4767 Standard Test Method for Consolidated Undrained Triaxial Compression Test for Cohesives Soils. American Society for Testing and Materials, West Conshohocken, PA.

American Society for Testing and Materials. Test Method D 1557 – 02 Standard Test Method for Laboratory Compaction Characteristics of Soil Using Modified Effort (56,000 ft-lbf/ft3 (2,700 kN-m/m3)). 2002 Edition. American Society for Testing and Materials, West Conshohocken, PA.

American Society for Testing and Materials. Test Method D 422 – 63 Standard Test Method for Particle-Size Analysis of Soils. 2002 Edition. American Society for Testing and Materials, West Conshohocken, PA.

American Society for Testing and Materials. Test Method D 854 – 02 Standard Test Method for Gravity of Soil Solids by Water Pycnometer. 2002 Edition. American Society for Testing and Materials, West Conshohocken, PA.

American Society for Testing and Materials. Test Method D 2488 – 93 Standard Test Methods for Decription and Identification of Soils (Visual-Manual Procedure). 1993 Edition. American Society for Testing and Materials, West Conshohocken, PA.

Atlantic Minerals Limited (2008). http://www.atlanticminerals.com/Amlprop.htm (last accessed July 21, 2008)

Attewell, P.B. (1970). Geotechnical properties of the great limestone in Northern England (1970). Engineering Geology Vol 5(2), 89-116 p

Barksdale, R. D. (1991) . The Aggregate Handbook (1991). National Stone Association, Washington, D.C, 800pp.

Bolton, M.D, Fragaszy, R.J, and Lee, D.M (1991). Broadening the Specification of Granular Fills, Transportation Research Record 1309, 35-41pp.

Brace, W.F, at al. (1968). Permeability of granite under high pressure. Journal of Geophysical Research Vol.73 2225-2236 pp.

Brewer, J.E., (1996). Corps of Engineers Procedure in the Development of a New Limestone or Dolomite Source (1996). The Ohio Journal of Science 66 (2): 188, March, 1966.

Broch, E and Franklin, J.A. (1972). Point Load Strength Test (1972). International Journal of Rock Mechanics and Mining Sciences. Vol.9 , 669-697p.

Cataño, J. (2006). “Stress-strain Behavior and Dinamic Properties of Cabo Rojo Calcareous Sands,” M.Sc. Thesis, University of Puerto Rico at Mayaguez.

Coduto, D. P. (2001). Foundation Design: Principles and Practices. 2nd Ed.Prentice Hall Inc, NJ.

Das, Braja M. (2002). Principles of Geotechnical Engineering. 5th Ed. Brook/Cole, CA.

Datta, M., Gulhati, S. K., and Rao, G. V. (1982). “Engineering Behavior of Carbonate Soils of India and Some Observations on Classification of Such Soils”. Geotechnical Properties, Behavior and Performance of Calcareous Soils, ASTM Special Technical

Publication 777, 113-140p.
Demars, and Cheney, (1992). Geotechnical Properties, Behavior and Performance of Calcareous Soils (1992). American Society for Testing Materials, Special Technical Publication #777.

Dukatz, E.L. (1995). “Aggregate Properties Related to Pavement Performance,” Journal of the Association of Asphalt Paving Technology, vol. 50

Estudios Tecnicos Inc. (2004). Primer estudio sobre el impacto económico de la Industria de Agregados. 86pp.

Fourmaintraux, D. (1976). Characterization of rocks; laboratory tests, Chapter IV in *La Méchanique des roche applliquée aux ouvrages du genie civil* by Marc Panel et al. Echole Nationale des Ponts et Chaussees, Paris.

Franklin, J.A. and Chandra, R. (1971). “The Slake-Durability Test,” Int. J. Rock Mech. Min. Sci., vol. 9, 325-341

Giusti, E.V. (1978). *Hydrogeology of the Karst of Puerto Rico*, Geological Survey Professional Paper 1012. U.S. Dept. of Interior, Geological Survey, Washington D.C.. Document available Online at http://pr.water.usgs.gov/public/online_pubs/pp_1012/pp1012.pdf (last accesed on July 13, 2008)

Glover, L. and Mattson, P. (1973). Geologic Map of the Rio Descalabrado Cuadrangle, Puerto Rico. US Geological Survey. Miscelaneous Geologic Investigation Series Map I-735.

Goodman, R.E. (1989). Introduction to Rock Mechanics, 2nd Ed, John Wiley and Sons Inc.

Gopal, R. and A.S.R Rao, (2000). Basic and Applied Soil Mechanics. 2nd Ed. New Age International Publishers.

Gunaydin, O. and Kahraman S, (2007). Empirical methods to predict the abrasion resistance of rock aggregates (2007). Bulleting of Engineering Geology and the Environment. Springer Berlin/Heidelberg, Vol. 66, Num. 4, 449-455 p.

Gupta, A.K. (2009), “Effect of Particle Size and Confining Pressure on Breakage and Strength Parameters of Rockfill Materials”, Electronic Journal of Geotechnical Engineering, Vol. 14, Bund. H, pp. 1-12.

Gupta, A. K., (2009). Triaxial Behaviour of Rockfill Materials, Electronic Journal of Goetchnical Engineering, Vol.14, Bund. J, 1-18p.

Hendron, Jr., A.J., Mechanical Properties of Rocks, in *Rock Mechanics in Engineering Practice*, Stagg, K.G. and Zienkiewicz, O.C., Eds., Wiley, New York, 1969, chap 2.

Hyodo, M., Hyde, A. F. L., and Aramaki, N. (1998). Liquefaction of Crushable Soils. Geotechnique, 48(4), 527-543.

Jewell, and Korshid, (1988). Engineering for Calcareous Sediments (1988**).** Balkema, Rotterdam, Vol. 1, General Proceedings, xxx p.

Jewell, and Korshid, (1988). Engineering for Calcareous Sediments (1988). Balkema, Rotterdam, Vol 2 North Rankin “A” Foundation Project State of the Art Reports

Kahraman, S. and Gunaydin, O. (2007). Empirical methods to predict the abrasion resistance of rock aggregates. Bulleting of Engineering Geology and the Environment, Vol. 66 No.4, 449-455 pp.

Kolay, E. and Kayabili, K. (2006). Investigation of the effect of aggregate shape and surface roughness on the slake durability index using the fractal dimension approach. Engineering Geology 86 (2006) pp 271-284

Lugo, A.E. (2004). *El Karso de Puerto Rico – Un Recurso Vital*, Informe Técnico General WO-65, Departamento de Agricultura de los Estados Unidos.

Mineral Data Publishing 2001-2005 Version 1. Document available online at http://www.handbookofmineralogy.org/pdfs/DOLOMITE.pdf

Mitchell, J. K. y Soga, K. (2005). Fundamentals of Soil Behavior. 3ra Ed. John Wiley & Sons, Inc. New York.

Monroe, W.H. (1969).Geologic Map of the Moca and Isabela Cuadrangles, Puerto Rico. US Geological Survey Miscellaneous Investigations Series Map I-565.

Monroe, W.H. (1980). *Some Tropical Landforms of Puerto Rico*, Geological Survey Professional Paper 1159. U.S. Dept. of Interior, Geological Survey, Washington D.C.

Monroe, W.H. (1976). *The Karst Landforms of Puerto Rico*, Geological Survey Professional Paper 899. U.S. Dept. of Interior, Geological Survey, Washington D.C.

Ogbonnaya, I., Kyoji, S. and Fawu, W. (2007). “The influence of grading on the shear strength of loose sands in stress-controlled ring shear tests,” Landslides Journal, Vol 4. No.1, 43-51p.

Romero, R. and Bernal, J. (1998). Strength and Compressibility Characteristics of Puerto Rico’s Limestone Soils. Project number 90084-spr-pr-pl-stp-1(33)-Function 821 (1998).

Seed, H. B., Wong, R. T., Idriss, I. M., and Tokimatsu, K. (1986). “Moduli and Damping Factors for Dynamic Analyses of Cohesionless Soils”. J. Geotech. Engrg., ASCE, 112(11), 1016-1032.

Smith, M.R. and Collis, L. (1993). Aggregates**.** Geological Society Engineering Geology Special Publication No. 9, Sandberg, London. Document available online at http://www.agiweb.org/environment/publications/aggregate.pdf (last acessed on July 13, 2008)

Todor, D.N. (1976). “Thermal Analyses of Minerals.” Abaccus press, Tunbridge Wells, UK.

Thom, N.H. and Brown, S.F. (1985). “The effect of grading and density on the mechanical properties of a crushed dolomitic limestone,” Proc., 14th Australian Road Research Board Conf., Part 7, 94-100

Thom, N.H. and Brown, S.F. (1987). “Effect of Moisture on the Structural Performance of a Crushed-Limestone Road Base,” Transportation Research Record No. 1121, 50-56

Ulusay R.and Hudson J.A. (2007). “The Complete ISRM Suggested Methods for Rock Characterization, Testing and Monitoring: 1974-2006”. Compilation arranged by the ISRM Turkish National Group, Ankara, Turkey, 85-92p.

Verdugo, R y de la Hoz, K. (2006). “Caracterización Geomecánica de Suelos Granulares Gruesos,” Revista Internacional de Desastres Naturales, Accidentes e Infrestructura Civil, Vol 6(2), 199-214p.

Winchell, A.N. (1942). Elements of Mineralogy, Prentice Hall, Englewood Cliffs, NJ.

Appendices

Appendix A.

Suggested Method for Porosity/Density Determination Using Saturation and Buoyancy Techniques

Porosity of the selected crushed limestone soils was evaluated following the suggested procedure by the International Society of Rock Mechanics (2007). This test method is intended to measure porosity of a rock sample in the form of lumps or aggregate of irregular geometry and should be used only on rocks that do not swell or disintegrate when oven dried and immersed in water.

Approximately 500 grams of both crushed limestone soils were collected for the test. The soil samples were saturated by water immersion in a vacuum for a period of at least 1 hour, with periodic agitation to remove trapped air. After the saturation phase, the soil sample was then transferred, under water, to a basket in the immersion bath to determine its saturated submerged mass (M_{sub}). Then, the sample was removed from the immersion bath and surface-dried with a moist cloth. Extra care was taken to ensure the removal of only surface water and to prevent rock fragment loss. The saturated-surface dry mass of the sample was determined (SSD-Mass). Finally soil samples were oven dried to constant mass at a temperature of 105°C (for approximately 24 hours) and allowed to cool at room temperature for 30 minutes before determining the oven-dried sample mass (Dry-Mass). Porosity results are presented in the following Table. Figure A.1 shows the water immersion bath arrangement and Figure A.2 shows the saturation of the sample by water immersion in a vacuum

Table A.1 Porosity results for Quarry A and B crushed limestone soils.

	Quarry A	Quarry B
Initial Mass (g)	500.01	500.01
M_{sub} (g)	302.7	302.4
Sample Basket (g)	440.6	440.6
Sample Container (g)	212.99	458.56
SSD Mass (g)	695.3	956.14
Dry Mass (g)	691.8	941.72
ρ_w (g/cm^3)	1	1
Saturated Surface Dry Mass (M_{sat}, g)	482.31	497.58
Grain Weight (M_s, g)	478.81	483.16
Bulk Volume (V, cm^3)	179.61	195.18
Pore Volume (Vv, cm^3)	3.5	14.42
Porosity (%)	1.95	7.39
Dry density (ρ_d, g/cm^3)	2.67	2.48

Figure A.1 Equipment arrangement for the saturation of the sample by water immersion at the Graduate Soils Laboratory, UPRM.


Figure A.2 Water immersion bath arrangement at the Graduate Soils Laboratory,UPRM.

Appendix B:

Slake Durability Test Results

SLAKE DURABILITY OF SHALES AND SIMILAR WEAK ROCKS
ASTM D 4644

QUARRY A SPECIMEN 5/16" –
SUBMERGED IN FRESH WATER – Feb/23/09
TIME – 0 DAYS

0.046	Natural Moisture Content, %
1216.44	Mass of drum, grams
1670.46	Mass of drum plus oven dried specimen before the first cycle, grams
1668.39	Mass of drum plus oven dried specimen retained after the second cycle, grams

Type I Retained pieces remain virtually unchanged

99.54 Slake Durability Index (%)

Figure B.1. Specimen before SDT

Figure B.2. Specimen after SDT

SLAKE DURABILITY OF SHALES AND SIMILAR WEAK ROCKS
ASTM D 4644

QUARRY B SPECIMEN 3/8" –
SUBMERGED IN FRESH WATER – Feb/27/09
TIME – 0 DAYS

2.43	Natural Moisture Content, %
1217.05	Mass of drum, grams
1657.02	Mass of drum plus oven dried specimen before the first cycle, grams
1650.67	Mass of drum plus oven dried specimen retained after the second cycle, grams

Type I   Retained pieces remain virtually unchanged

98.55   Slake Durability Index (%)

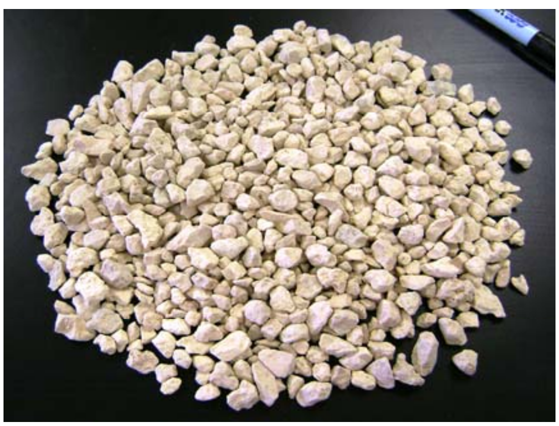

Figure B.3. Specimen before SDT

Figure B.4. Specimen after SDT

SLAKE DURABILITY OF SHALES AND SIMILAR WEAK ROCKS
ASTM D 4644

QUARRY A SPECIMEN 5/16" –
SUBMERGED IN FRESH WATER – June/23/09
TIME – 90 DAYS, CURED IN FRESH WATER

0.12	Natural Moisture Content, %
1216.59	Mass of drum, grams
1686.09	Mass of drum plus oven dried specimen before the first cycle, grams
1684.57	Mass of drum plus oven dried specimen retained after the second cycle, grams

Type I Retained pieces remain virtually unchanged

99.67 Slake Durability Index (%)

Figure B.5. Specimen before SDT

Figure B.6. Specimen after SDT

SLAKE DURABILITY OF SHALES AND SIMILAR WEAK ROCKS
ASTM D 4644

QUARRY A SPECIMEN 5/16" –
SUBMERGED IN FRESH WATER – July/06/09
TIME – 90 DAYS, CURED IN SALT WATER

0.14	Natural Moisture Content, %
1217.29	Mass of drum, grams
1686.58	Mass of drum plus oven dried specimen before the first cycle, grams
1684.19	Mass of drum plus oven dried specimen retained after the second cycle, grams

Type I Retained pieces remain virtually unchanged

99.49 Slake Durability Index (%)


Figure B.7. Specimen before SDT


Figure B.8. Specimen after SDT

SLAKE DURABILITY OF SHALES AND SIMILAR WEAK ROCKS
ASTM D 4644

QUARRY B SPECIMEN 3/8" –
SUBMERGED IN FRESH WATER – June/23/09
TIME – 90 DAYS, CURED IN FRESH WATER

0.21	Natural Moisture Content, %
1217.33	Mass of drum, grams
1686.43	Mass of drum plus oven dried specimen before the first cycle, grams
1682.70	Mass of drum plus oven dried specimen retained after the second cycle, grams

Type I	Retained pieces remain virtually unchanged

99.20	**Slake Durability Index (%)**

Figure B.9. Specimen before SDT

Figure B.10. Specimen after SDT

SLAKE DURABILITY OF SHALES AND SIMILAR WEAK ROCKS
ASTM D 4644

QUARRY B SPECIMEN 3/8" –
SUBMERGED IN FRESH WATER – July/06/09
TIME – 90 DAYS, CURED IN SALT WATER

0.30	Natural Moisture Content, %
1216.49	Mass of drum, grams
1684.92	Mass of drum plus oven dried specimen before the first cycle, grams
1678.90	Mass of drum plus oven dried specimen retained after the second cycle, grams

Type I Retained pieces remain virtually unchanged

98.71 Slake Durability Index (%)

Figure B.11. Specimen before SDT

Figure B.12. Specimen after SDT

SLAKE DURABILITY OF SHALES AND SIMILAR WEAK ROCKS
ASTM D 4644

QUARRY A SPECIMEN 5/16” –
SUBMERGED IN FRESH WATER – Aug/25/09
TIME – 150 DAYS, CURED IN FRESH WATER

0.07	Natural Moisture Content, %
1217.18	Mass of drum, grams
1676.88	Mass of drum plus oven dried specimen before the first cycle, grams
1675.37	Mass of drum plus oven dried specimen retained after the second cycle, grams

Type I	Retained pieces remain virtually unchanged

99.67	**Slake Durability Index (%)**

SLAKE DURABILITY OF SHALES AND SIMILAR WEAK ROCKS
ASTM D 4644

QUARRY A SPECIMEN 5/16" –
SUBMERGED IN FRESH WATER – Aug/25/09
TIME – 150 DAYS, CURED IN SALT WATER

0.20	Natural Moisture Content, %
1216.50	Mass of drum, grams
1675.49	Mass of drum plus oven dried specimen before the first cycle, grams
1673.41	Mass of drum plus oven dried specimen retained after the second cycle, grams

Type I	Retained pieces remain virtually unchanged

99.55	**Slake Durability Index (%)**

SLAKE DURABILITY OF SHALES AND SIMILAR WEAK ROCKS
ASTM D 4644

QUARRY B SPECIMEN 3/8" –
SUBMERGED IN FRESH WATER – Aug/10/09
TIME – 150 DAYS, CURED IN FRESH WATER

0.34	Natural Moisture Content, %
1217.25	Mass of drum, grams
1685.50	Mass of drum plus oven dried specimen before the first cycle, grams
1680.32	Mass of drum plus oven dried specimen retained after the second cycle, grams

Type I	Retained pieces remain virtually unchanged

98.89	**Slake Durability Index (%)**


Figure B.14. Specimen before SDT


Figure B.15. Specimen after SDT

SLAKE DURABILITY OF SHALES AND SIMILAR WEAK ROCKS
ASTM D 4644

QUARRY B SPECIMEN 3/8" –
SUBMERGED IN FRESH WATER – Aug/10/09
TIME – 150 DAYS, CURED IN SALT WATER

1.24	Natural Moisture Content, %
1216.54	Mass of drum, grams
1680.70	Mass of drum plus oven dried specimen before the first cycle, grams
1675.47	Mass of drum plus oven dried specimen retained after the second cycle, grams

Type I Retained pieces remain virtually unchanged

98.87 Slake Durability Index (%)


Figure B.16. Specimen before SDT


Figure B.17. Specimen after SDT

Appendix C:

Point Load Test Results

STANDARD TEST METHOD FOR DETERMINATION OF THE POINT LOAD STRENGHT INDEX OF ROCK AND APPLICATION TO ROCK STRENGTH CLASSIFICATION – ASTM D 5731-95

Quarry: **A**
Simple Condition: As received
Date: March.04.09

Specimen ID:	*A*
L prom (mm):	83.49667
D prom (mm):	52.76333
W prom (mm):	58.99667
Peak Load (KN):	13.64
Water Content (%):	0.076
I_s (MPa):	3.44
I_{s50} (MPa):	3.82

Figure C.1. Specimen A before, during, and after Point Load Test.

STANDARD TEST METHOD FOR DETERMINATION OF THE POINT LOAD STRENGHT INDEX OF ROCK AND APPLICATION TO ROCK STRENGTH CLASSIFICATION – ASTM D 5731-95

Quarry: **B**
Simple Condition: As received
Date: March.09.09

Specimen ID:	*A*
L prom (mm):	75.69
D prom (mm):	48.50
W prom (mm):	54.21
Peak Load (KN):	15.87
Water Content (%):	0.13
I_s (MPa):	4.74
I_{s50} (MPa):	5.06

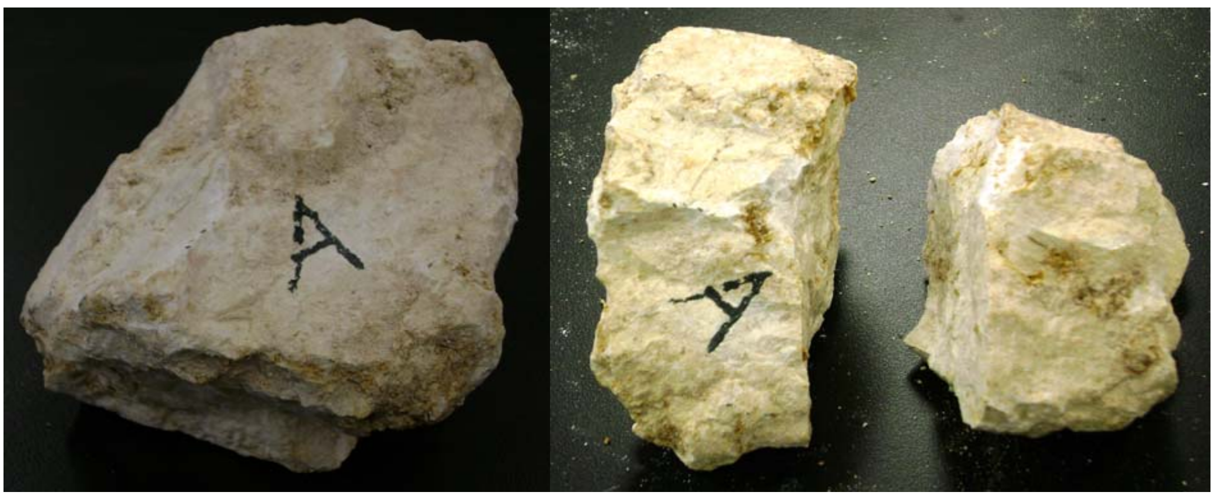

Figure C.2. Specimen A before and after Point Load Test.

STANDARD TEST METHOD FOR DETERMINATION OF THE POINT LOAD STRENGHT INDEX OF ROCK AND APPLICATION TO ROCK STRENGTH CLASSIFICATION – ASTM D 5731-95

Quarry: **A**
Sample Condition: Submerged – Fresh Water
Submersion Time: 90 days
Date: July 7 2009

Specimen ID:	*A*
L prom (mm):	71.48
W prom (mm):	47.23
D prom (mm):	58.77
Peak Load (KN):	10.5
Water Content (%):	0.05
I_s (MPa):	2.97
I_{s50} (MPa):	3.21

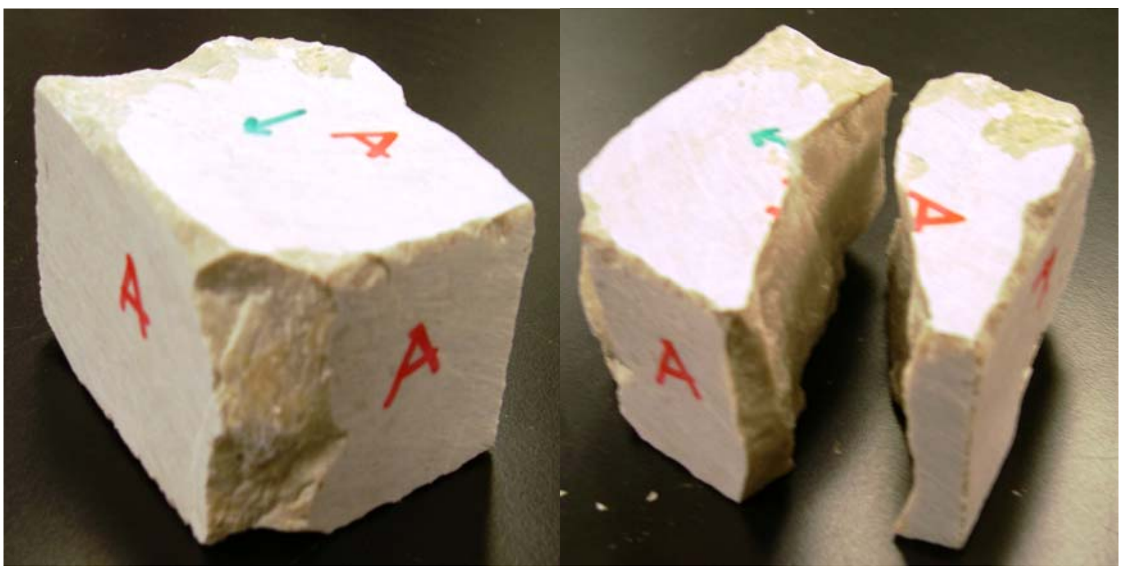

Figure C.3. Specimen A before and after Point Load Test.

STANDARD TEST METHOD FOR DETERMINATION OF THE POINT LOAD STRENGHT INDEX OF ROCK AND APPLICATION TO ROCK STRENGTH CLASSIFICATION – ASTM D 5731-95

Quarry: **A**
Sample Condition: Submerged – Salt Water
Submersion Time: 90 days
Date: July 7 2009

Specimen ID:	*A*
L prom (mm):	74.19
W prom (mm):	56.05
D prom (mm):	66.97
Peak Load (KN):	12.77
Water Content (%):	0.076
I_s (MPa):	2.67
I_{s50} (MPa):	3.09

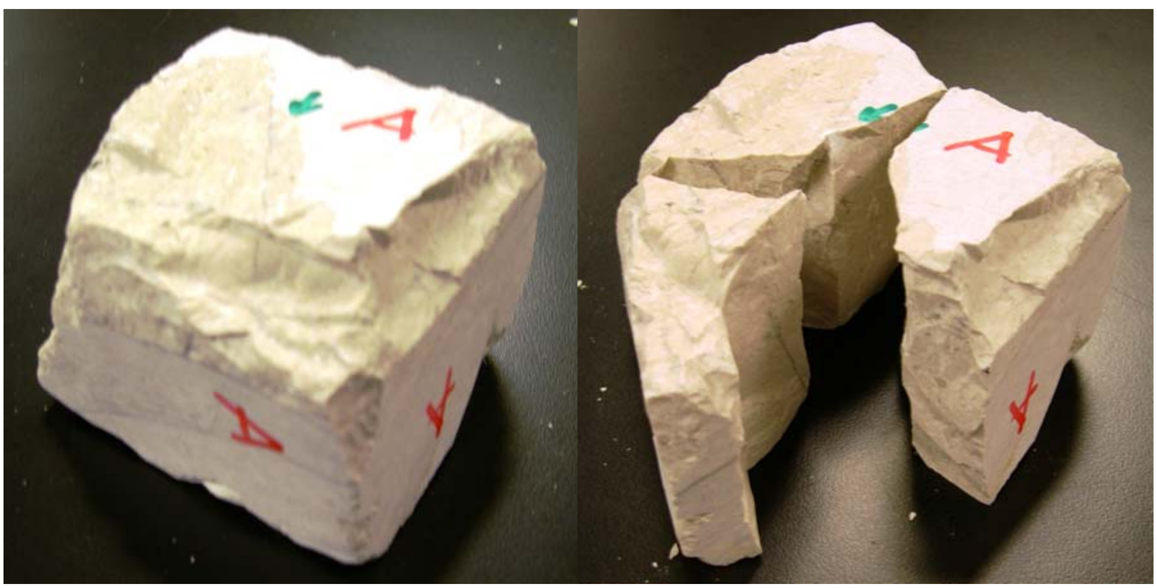

Figure C.4. Specimen A before and after Point Load Test.

STANDARD TEST METHOD FOR DETERMINATION OF THE POINT LOAD STRENGHT INDEX OF ROCK AND APPLICATION TO ROCK STRENGTH CLASSIFICATION – ASTM D 5731-95

Quarry: **B**
Sample Condition: Submerged – Fresh Water
Submersion Time: 90 days
Date: July 7 2009

Specimen ID:	*A*
L prom (mm):	70.16
W prom (mm):	45.56
D prom (mm):	52.79
Peak Load (KN):	9.65
Water Content (%):	0.04
I_s (MPa):	3.15
I_{s50} (MPa):	3.30

Figure C.5. Specimen A before and after Point Load Test.

STANDARD TEST METHOD FOR DETERMINATION OF THE POINT LOAD STRENGHT INDEX OF ROCK AND APPLICATION TO ROCK STRENGTH CLASSIFICATION – ASTM D 5731-95

Quarry: **B**
Sample Condition: Submerged – Salt Water
Submersion Time: 90 days
Date: July 7 2009

Specimen ID:	*A*
L prom (mm):	79.03
W prom (mm):	43.99
D prom (mm):	60.99
Peak Load (KN):	7.16
Water Content (%):	0.05
I_s (MPa):	2.09
I_{s50} (MPa):	2.25

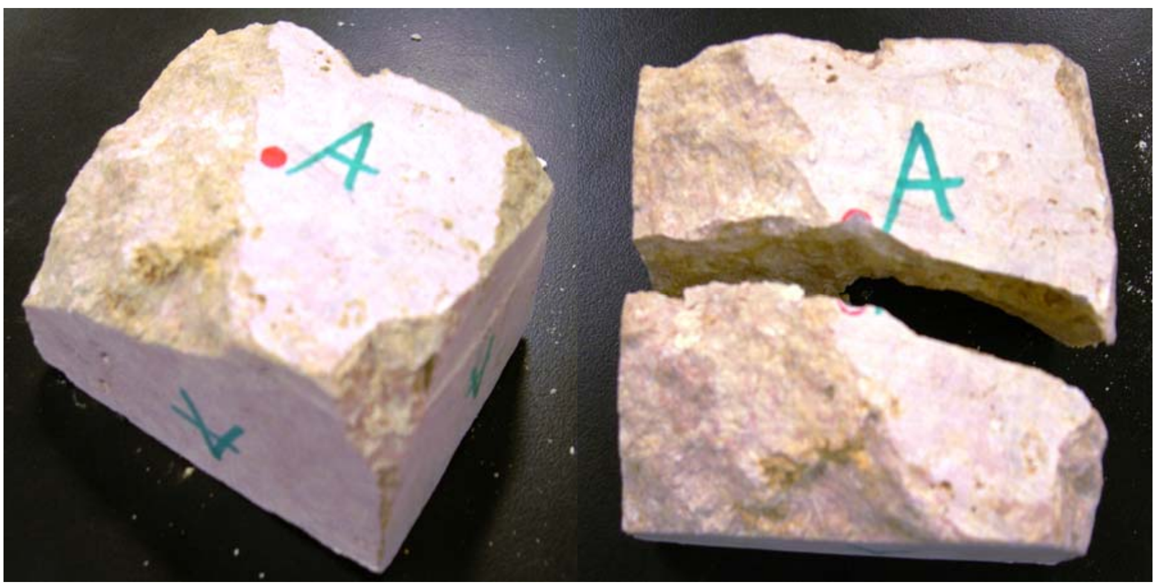

Figure C.6. Specimen A before and after Point Load Test.

STANDARD TEST METHOD FOR DETERMINATION OF THE POINT LOAD STRENGHT INDEX OF ROCK AND APPLICATION TO ROCK STRENGTH CLASSIFICATION – ASTM D 5731-95

Quarry: **A**
Sample Condition: Submerged – Fresh Water
Submersion Time: 150 days
Date: August 7 2009

Specimen ID:	*A*
L prom (mm):	62.21
W prom (mm):	51.08
D prom (mm):	57.04
Peak Load (KN):	13.86
Water Content (%):	0.14
I_s (MPa):	3.73
I_{s50} (MPa):	4.08

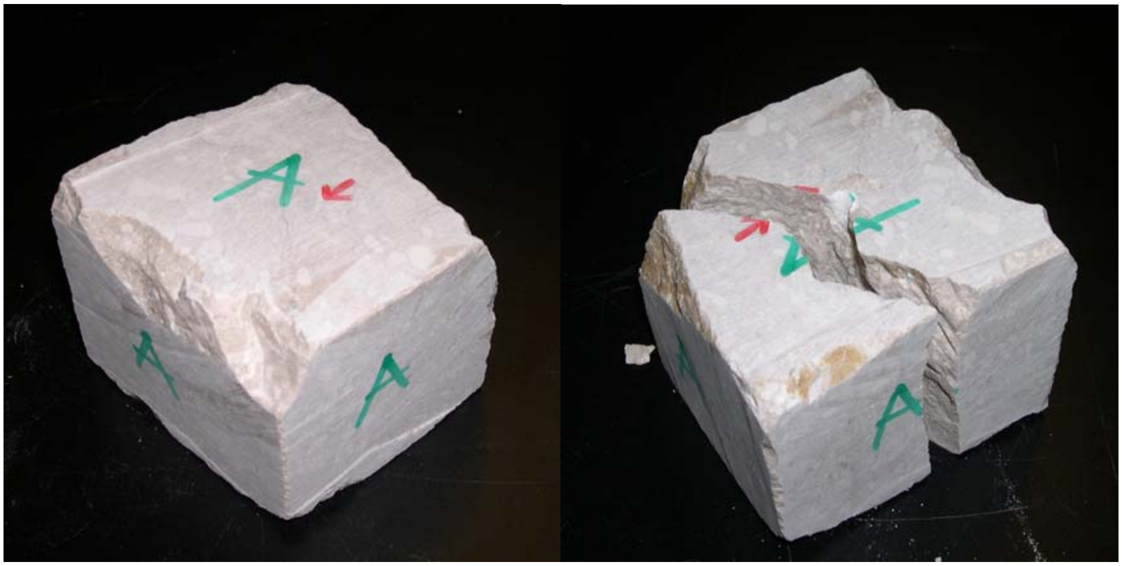

Figure C.7. Specimen A before and after Point Load Test

STANDARD TEST METHOD FOR DETERMINATION OF THE POINT LOAD STRENGHT INDEX OF ROCK AND APPLICATION TO ROCK STRENGTH CLASSIFICATION – ASTM D 5731-95

Quarry: **A**
Sample Condition: Submerged – Salt Water
Submersion Time: 150 days
Date: August 7 2009

Specimen ID:	*A*
L prom (mm):	51.60
W prom (mm):	45.48
D prom (mm):	51.83
Peak Load (KN):	2.92
Water Content (%):	0.15
I_s (MPa):	0.97
I_{s50} (MPa):	1.01

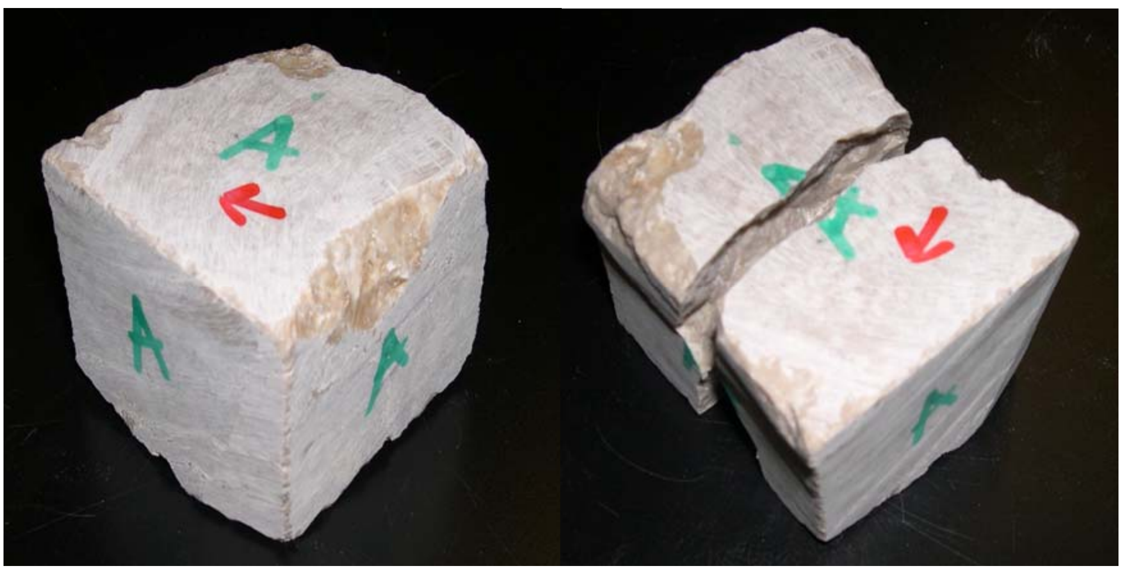

Figure C.8. Specimen A before and after Point Load Test.

STANDARD TEST METHOD FOR DETERMINATION OF THE POINT LOAD STRENGHT INDEX OF ROCK AND APPLICATION TO ROCK STRENGTH CLASSIFICATION – ASTM D 5731-95

Quarry: **B**
Sample Condition: Submerged – Fresh Water
Submersion Time: 150 days
Date: August 7 2009

Specimen ID:	*A*
L prom (mm):	70.42
W prom (mm):	43.25
D prom (mm):	55.00
Peak Load (KN):	10.69
Water Content (%):	0.45
I_s (MPa):	3.53
I_{s50} (MPa):	3.69

Figure C.9. Specimen A before and after Point Load Test

STANDARD TEST METHOD FOR DETERMINATION OF THE POINT LOAD STRENGHT INDEX OF ROCK AND APPLICATION TO ROCK STRENGTH CLASSIFICATION – ASTM D 5731-95

Quarry: **B**
Sample Condition: Submerged – Salt Water
Submersion Time: 150 days
Date: August 7 2009

Specimen ID:	*A*
L prom (mm):	72.41
W prom (mm):	37.47
D prom (mm):	65.58
Peak Load (KN):	12.24
Water Content (%):	0.84
I_s (MPa):	3.91
I_{s50} (MPa):	4.11

Figure C.10. Specimen A before and after Point Load Test.